THE BRANCHED ENTNER-DOUDOROFF PATHWAY IN HYPERTHERMOPHILIC ARCHAEA

Inaugural-Dissertation

zur

Erlangung des Doktorgrades

Dr. rer. nat.

des Fachbereichs

Biologie und Geographie

an der

Universität Duisburg-Essen

vorgelegt von

HATIM AHMED

aus Hannover

Juni 2006

Die dieser Arbeit zugrundeliegenden Experimente wurden am Institut für Biologie in der Abteilung Mikrobiologie I der Universität Duisburg-Essen, Campus Essen, durchgeführt.

1. Gutachter: HD. Dr. Bettina Siebers

2. Gutachter: Prof. Dr. Peter Bayer

Vorsitzender des Prüfungsausschusses: Prof. Dr. Reinhard Hensel

Tag der mündlichen Prüfung: 25.10.2006

بسم الله الرحمن الرحيم

يَعْلَمُ مَا بَيْنَ أَيْدِيهِمْ وَمَا خَلْفَهُمْ وَلاَ يُحِيطُونَ بِشَيْءٍ مِنْ عِلْمِهِ إِلاَّ بِمَا شَاءَ. ﴿٢٥٥﴾

سورة البقرة

He knows what lies before them and what is after them, and they comprehend not anything of His knowledge save such as He wills.

Surat al-Baqara: 255

TABLE OF CONTENTS

1. INTRODUCTION 1

2. MATERIALS AND METHODS 10

2.1 CHEMICALS AND PLASMIDS 10
2.2 INSTRUMENTS 10
2.3 STRAINS AND GROWTH CONDITIONS 12
2.4 MOLECULAR BIOLOGICAL METHODS WITH DNA 16
2.4.1 Genomic DNA preparation 16
2.4.2 Isolation of plasmid DNA from *E. coli* 17
2.4.3 DNA precipitation 18
2.4.4 Quantification of DNA 18
2.4.5 Agarose gel electrophoresis for DNA 18
2.4.6 Purification of DNA fragments 19
2.4.7 Polymerase chain reaction (PCR) 19
2.4.8 Amplification of genomic DNA and plasmid DNA by PCR 20
2.4.9 Enzymatic manipulation of DNA 20
2.4.9.1 Restriction of DNA 20
2.4.9.2 5`-Dephosphorylation of the linearized vector DNA 20
2.4.9.3 Ligation of vector DNA and insert 21
2.4.10 Transformation 21
2.4.10.1 Preparation of competent *E. coli* cells 21
2.4.10.2 Transformation of the competent *E. coli* cells 22
2.4.11 Sequencing 22
2.4.11.1 Automated DNA sequencing 22
2.4.11.2 Computer assisted analysis of the nucleotide sequence 22
2.5 MOLECULAR BIOLOGICAL METHODS WITH RNA 23
2.5.1 Handling of solutions, glassware and equipments 23
2.5.2 Isolation of total RNA from *T. tenax* and *S. solfataricus* 23
2.5.3 Quantification of RNA 24
2.5.4 Agarose/Formaldehyde gel electrophoresis of RNA 24
2.5.5 Capillary transfer of RNA to a nylon membrane (Northern Blot) 25
2.5.6 Hybridization of RNA with Digoxigenin-labelled RNA probes 26
2.5.6.1 Synthesis of DIG-Labelled specific antisense mRNA probes by *in vitro* transcription 26
2.5.6.2 Hybridization of immobilized RNA with DIG-labelled specific antisense mRNA probes 27
2.5.6.3 Detection of RNA-RNA hybrid by immunological detection 27
2.5.7 Primer extension analysis 28
2.6 BIOCHEMICAL METHODS 29
2.6.1 Heterologous expression of the *T. tenax* and the *S. solfataricus* ED proteins in *E. coli* 29

2.6.2 Preparative protein purification 29
2.6.3 Enzyme assays 30
2.6.3.1 2-keto-3-deoxy-6-(phospho)gluconate (KD(P)G) aldolase 30
2.6.3.2 Gluconate dehydratase (GAD) 31
2.6.3.3 2-keto-3-deoxygluconate (KDG) kinase 31
2.6.3.4 Non-phosphorylating glyceraldehyde-3-phosphate dehydrogenase GAPN 32
2.6.3.5 Kinetic parameters 33
2.6.4 Biocatalytic synthesis of KDG 34
2.6.5 *In vitro* assays with crude extracts 34
2.6.6 ^{14}C-Labelling experiments and Thin Layer Chromatography (TLC) 34
2.6.7 *In vitro* reconstruction of the ED pathway 35
2.6.8 Analytical protein methods 35
2.6.8.1 Protein quantification 35
2.6.8.2 SDS-Polyacrylamide gel electrophoresis (SDS-PAGE) 35
2.6.8.3 Molecular mass determination 37

3. RESULTS 38

3.1 SEQUENCE ANALYSIS AND GENE CONTEXT 39
3.2 PRIMER EXTENSION ANALYSIS 43
3.2.1 Northern Blot analysis 43
3.3 HETEROLOGOUS EXPRESSION OF THE *T. TENAX* AND *S. SOLFATARICUS* ED PROTEINS IN *E. COLI* 46
3.4 ENZYMES ENRICHMENT AND PURIFICATION 47
3.5 BIOCHEMICAL CHARACTERIZATION 49
3.5.1 Catalytic and kinetic parameters 49
3.5.1.1 Glucose dehydrogenase 49
3.5.1.2 KD(P)G aldolase 49
3.5.1.3 Gluconate dehydratase 53
3.5.1.4 KDG kinase 54
3.5.1.5 Non-phosphorylating glyceraldehyde-3-phosphate dehydrogenase (GAPN) from *S. solfataricus* 57
3.6 CRUDE EXTRACTS STUDIES 61
3.7 *IN VITRO* RECONSTRUCTION OF THE ED PATHWAY IN *T. TENAX* 62

4. DISCUSSION 64

4.1 THE ED GENE CLUSTER-COMPARATIVE GENOMICS 64
4.2 ED GENE ORGANIZATION AND TRANSCRIPT ANALYSIS OF *T. TENAX* AND *S.SOLFATARICUS* 66
4.3 ENZYME CHARACTERIZATION 67
4.3.1 Heterologous expression of the *T. tenax* and *S. solfataricus* ED proteins in *E. coli* 67
4.3.2 KD(P)G aldolase of *T. tenax* and *S. solfataricus* 67
4.3.3 Gluconate dehydratase of *T. tenax* and *S. solfataricus* 70

4.3.4 KDG kinase of *T. tenax* and *S. solfataricus* 71
4.3.5 Non-phosphorylating glyceraldehyde-3-phosphate dehydrogenase (GAPN) of *S. solfataricus* 73
4.4 THE BRANCHED ED PATHWAY IN *T. TENAX* AND *S. SOLFATARICUS*..... 76
4.5 PHYSIOLOGICAL IMPLICATIONS..... 79
5. SUMMARY..... 83
6. LITERATURE..... 86
ABBREVIATIONS LIST..... 98

FIGURES LIST

FIGURE 1: UNIVERSAL PHYLOGENETIC TREE BASED ON rRNA SEQUENCES. 1
FIGURE 2: GLUCOSE CATABOLISM VIA THE DIFFERENT ENTNER-DOUDOROFF (ED) PATHWAYS. .. 6
FIGURE 3: ELECTRON MICROGRAPH OF *THERMOPROTEUS TENAX* KRA1. 8
FIGURE 4: ELECTRON MICROGRAPH OF *SULFOLOBUS SOLFATARICUS*. 9
FIGURE 5: ENTNER-DOUDOROFF GENE CLUSTERS IN ARCHAEA IDENTIFIED BY CONSERVED GENOME CONTEXT ANALYSIS. 38
FIGURE 6: NUCLEOTIDE SEQUENCE OF THE ED GENE CLUSTER IN *T. TENAX* AND *S. SOLFATARICUS*. 42
FIGURE 7: IDENTIFICATION OF PUTATIVE PROMOTER STRUCTURES OF THE ED GENES OF *T. TENAX* AND *S. SOLFATARICUS*. 42
FIGURE 8: MAPPING OF TRANSCRIPTION START SITES OF THE *gad* GENE AND THE *kdgA-kdgK-gaa* OPERON OF *T. TENAX* AND OF THE *gapN* GENE AND THE *gad-kdgA-kdgK* OPERON OF *S. SOLFATARICUS*. 43
FIGURE 9: NUCLEOTIDE SEQUENCES OF ANTISENSE mRNA PROBES. 45
FIGURE 10: NORTHERN BLOT ANALYSIS OF THE *kdgA-kdgK-gaa* OPERON. 46
FIGURE 11: SDS-PAGE OF RECOMBINANT EXPRESSION OF *S. SOLFATARICUS* GAD AND KDG KINASE. 47
FIGURE 12: SDS-PAGE OF RECOMBINANT EXPRESSION AND PURIFICATION OF *T. TENAX* AND *S. SOLFATARICUS* ED PROTEINS. 49
FIGURE 13: KD(P)G ALDOLASE ACTIVITY OF *T. TENAX* (A) AND *S. SOLFATARICUS* (B). 51
FIGURE 14: DETECTION OF ^{14}C-LABELLED KDG AND KDPG VIA THIN LAYER CHROMATOGRAPHY AND AUTORADIOGRAPHY. 52
FIGURE 15: GLUCONATE DEHYDRATASE (GAD) ACTIVITY OF *T. TENAX*. 54
FIGURE 16: KDG KINASE (KDGK) ACTIVITY OF *T. TENAX*. 55
FIGURE 17: KDG KINASE (KDGK) ACTIVITY OF *S. SOLFATARICUS*. 56
FIGURE 18: GAPN ACTIVITY OF *S. SOLFATARICUS*. 57
FIGURE 19: GAPN ACTIVITY OF *S. SOLFATARICUS*. 58
FIGURE 20: INFLUENCE OF GLUCOSE 1-PHOSPHATE ON GAPN ACTIVITY OF *S. SOLFATARICUS*. .. 59
FIGURE 21: RECONSTRUCTION OF THE ED PATHWAY *IN VITRO*. 63
FIGURE 22: THE CENTRAL CARBOHYDRATE METABOLISM IN *T. TENAX* AND *S. SOLFATARICUS*. ... 81

TABLES LIST

TABLE 1: PRIMER SETS, PLASMIDS, STRAINS AND HOSTS..... 15
TABLE 2: INFLUENCE OF ALLOSTERIC EFFECTORS ON THE *S. SOLFATARICUS* GAPN ACTIVITY. ... 60
TABLE 3: SPECIFIC ACTIVITIES OF ED ENZYMES IN CRUDE EXTRACT OF *T. TENAX*..... 62
TABLE 4: COMPARATIVE KINETIC, MACROMOLECULAR, STRUCTURAL AND EFFECTOR PROPERTIES OF THE GAPN FROM *T. TENAX* AND *S. SOLFATARICUS*. 74
TABLE 5: BRANCHED ED PATHWAY IN ARCHAEA… 82

1. INTRODUCTION

For over 50 years, scientists were confident with the notion that there were two basic kinds of living organisms, eubacteria and eukaryotes [STANIER, 1970; STANIER & VAN NIEL, 1941; STANIER & VAN NIEL, 1962]. In the late 1970s, this fundamental belief was shattered by the revelations of Woese and co workers that life consisted of three distinct groups of organisms [FOX et al., 1977; WOESE & FOX, 1977]. In 1990, on the basis of cluster dendograms of data based on oligonucleotide catalogs of small subunit rRNA, Woese and co workers [WOESE et al., 1990] strongly advocated the replacement of the bipartite view of life with a new tripartite scheme based on three domains: the *Bacteria* (eubacteria), *Archaea* (archaebacteria) and *Eucarya* (eukaryotes) (Fig 1).

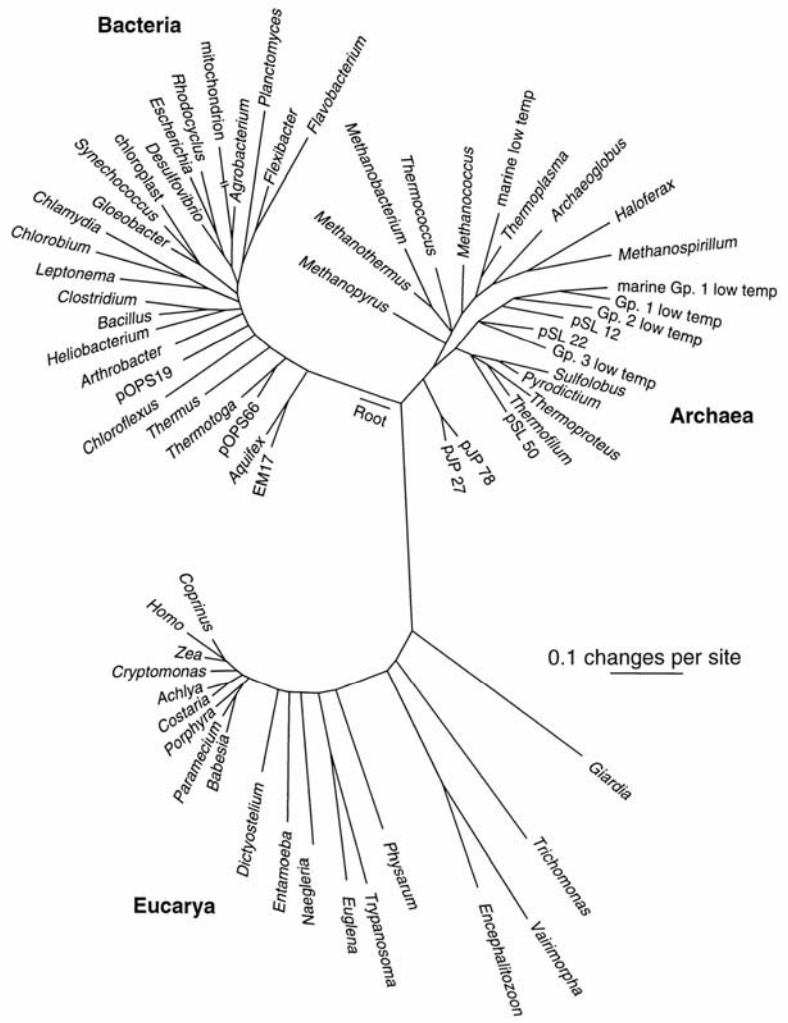

FIGURE 1: UNIVERSAL PHYLOGENETIC TREE BASED ON rRNA SEQUENCES.
16S rRNA sequences representative of all known phylogenetic domains were aligned according to Pace [PACE, 1997]. The tree shows a modification of the original tree from Woese and Fox [WOESE & FOX, 1977]. The scale bar corresponds to 0.1 changes per nucleotide.

For about 15 years of classical biochemical and molecular biological research and after the 'genomic era' revolution with large-scale genomic comparison an increases in our understanding of similarities and differences at the nucleotide level as well as in structure among the Archaea and the other two domains of life is gained. Although Archaea share several features with Bacteria such as being unicellular, lack of nuclear membrane and organelles, the presence of large circular DNA plasmids and the organization of genes in operon structures, the two prokaryotic kingdoms have also been found to differ in many aspects of their cell composition and molecular biology. For example, the presence of pseudomurein in some archaeal species instead of the peptidoglycan (murein) in the bacterial cell walls [WOESE et al., 1978], while most other Archaea, consist of a paracrystalline surface layer (S-layer). On the other hand, Archaea show many other features otherwise found only in Eucarya. All processes involved in information processing (e.g. systems involved in translation, transcription, chromatin packing and modulation (histones) [GAVIN et al., 2002], DNA repair [WHITE, 2003], protein turnover [BAUMEISTER & LUPAS, 1997] and RNA degradation [EVGUENIEVA-HACKENBURG et al., 2003; KOONIN et al., 2001]) resembles eukaryal systems. For example the basal transcription initiation machinery shows similarity to the eucaryal RNA polymerase II transcription apparatus [FORTERRE & ELIE, 1993], i.e. the TATA box, the initiator element (INR) and the transcription factor IIB recognition element (BRE) promoter elements. Contrary to that, there are specific features that in general can be said to be archaeal, for example, the archaeal membrane consists of ether linkages between glycerol and their hydrophobic side chains instead of ester linkages that bond the fatty acids to glycerol in Bacteria and Eukarya. In addition, Archaea lack fatty acids. Instead, their side chains are composed of repeating units of five-carbon hydrocarbon isoprene.

Within Archaea, four phyla are found: Crenarchaeota, Euryarchaeota, Korarchaeota and Nanoarchaeota [HUBER et al., 2002]. Most investigated so far are the crenarchaeal and euryarchaeal species. The Crenarchaeota branch generally consists of hyperthermophiles or thermoacidophiles. One hallmark of the Archaea is their remarkable specialization, and isolates have been recovered almost exclusively from

extreme environments and specialized niches. More recently a mesophilic member of the division Crenarchaeota was cultivated from plant roots [SIMON et al., 2005; BUCKLEY et al., 1998]. The Euryarchaeota spans a boarder ecological range and includes hyperthermophiles found at super-heated, active volcanic sea floors, often in chimney-like structures called "black smokers", methanogens which can generally be found in anoxic swamp and lake sediments, and in mammalian gastrointestinal tracts, halophiles found in hyper saline environments and even thermophilic methanogens [BELLY & BROCK, 1972; SCHLEPER et al., 1995]. The Korarchaeota, which branch deep in the archaeal tree, have been identified with sequenced-based techniques applied on environmental samples but no members were isolate. The Nanoarchaeota represent a unique kingdom of Archaea that harbors tiny parasitic cells with the smallest genomes of all known prokaryotes. The first species of the Nanoarchaeota branch *Nanoarchaeum equitans* was reported in 2002 by Huber and colleagues [HUBER et al., 2002].

However, with the availability of sequence-based techniques, it became evident that archaeal species are ubiquitous [PACE, 1997], and not restricted to extreme environments like habitats with extreme high pressure, low or high pH values, under high salt concentrations or at extreme high temperature. The strong interest to these organisms has been evoked during the past 20 years and many studies have focused not only on understanding their molecular mechanisms of adaptation to extreme physico-chemical conditions but also on the potential biotechnological applications.

Current studies of hyperthermophilic Archaea allow new insights into the nature of presumably ancient metabolic pathways. Polysaccharides are a major source of carbon in the three domains of life. Their utilization generally involves extracellcular hydrolysis, uptake of oligosaccharides by specific transporters and their intracellular hydrolysis to generate hexoses (e.g. glucose, galactose, mannose and fructose). Subsequently, these monosaccharides are being oxidized via a well-conserved set of central metabolic pathways.

Two pathways are involved in the degradation of glucose into pyruvate. The Embden-Meyerhof (EMP) pathway (glycolysis) is the general route for glucose

degradation in Eukarya and Bacteria. Some Bacteria use an alternative pathway for glucose degradation, i.e. the Entner-Doudoroff (ED) pathway. In addition, Bacteria and Eukarya utilize the classical oxidative pentose phosphate (PP) pathway which serves mainly to generate NADPH and tetrose and pentose sugars and therefore maybe considered as a supplementary pathway to the main two catabolic routes.

Comparative studies of the glucose degradation in thermophilic and hyperthermophilic Archaea have revealed a large number of variations of the classical bacterial and eukaryal routes; the EMP pathway and the ED pathway [ROMINUS & MORGAN, 2002; VERHEES et al., 2004; VERHEES et al., 2003; SIEBERS et al., 2004; SIEBERS & SCHÖNHEIT, 2005]. In addition, modified pathways were identified for the generation of pentose sugars [VERHEES et al., 2004; VERHEES et al., 2003]. Whereas the ED-like pathway seems to be restricted to the aerobic Archaea (e.g. *Sulfolobus solfataricus* [DE ROSA et al., 1984] and *Thermoplasma acidophilum* [BUDGEN & DANSON, 1986]), the archaeal modified EMP pathways are found in most anaerobic Archaea (e.g. *Pyrococcus furiosus*, *Thermococcus sp.*, *Desulfurococcus amylolyticus* and *Archaeoglobus fulgidus*) [VERHEES et al., 2004; VERHEES et al., 2003; SIEBERS et al., 2004]. The presence of both modified pathways has so far only been demonstrated in the anaerobe *Thermoproteus tenax* [SIEBERS et al., 2004; SIEBERS & HENSEL, 1993; SELIG & SCHÖNHEIT, 1994; SIEBERS et al., 1997; SELIG et al., 1997].

The classical ED pathway [ENTNER & DOUDOROFF, 1952] involves (i) the initial phosphorylation of glucose to glucose 6-phosphate either by a glucokinase or by the action of a phosphoenolpyruvate-dependent phosphotransferase system (PTS), (ii) the oxidation to 6-phosphogluconate by glucose-6-phosphate dehydrogenase and phosphogluconolactonase, (iii) the dehydration to 2-keto-3-deoxy-6-phophogluconate (KDPG) by 6-phosphogluconate dehydratase, and (iv) the cleavage of the characteristic KDPG intermediate by KDPG aldolase yielding glyceraldehyde 3-phosphate (GAP) and pyruvate. GAP is further metabolized via the lower, common shunt of the EMP pathway yielding a second molecule of pyruvate (Fig 2). The net ATP yield of ED pathway is 1 mol ATP/mol glucose.

Whereas the classical ED pathway seems to be restricted to Bacteria, modifications have been identified in all three domains of life: the Eukarya, Bacteria and Archaea [CONWAY, 1992]. One of the modified versions of the ED pathway that is generally referred to as the semi-phosphorylative ED pathway which was first discovered in the bacterium *Rhodobacter sphaeroides* [SZYMONA & DOUDOROFF, 1958], which concerns (i) the oxidation of glucose to gluconate via glucose dehydrogenase, (ii) the conversion of gluconate by a specific gluconate dehydratase to 2-keto-3-deoxygluconate (KDG), (iii) the subsequent phosphorylation by KDG kinase to form 2-keto-3-deoxy-6-phosphogluconate (KDPG), and (iv) the cleavage by KDPG aldolase (Fig 2).

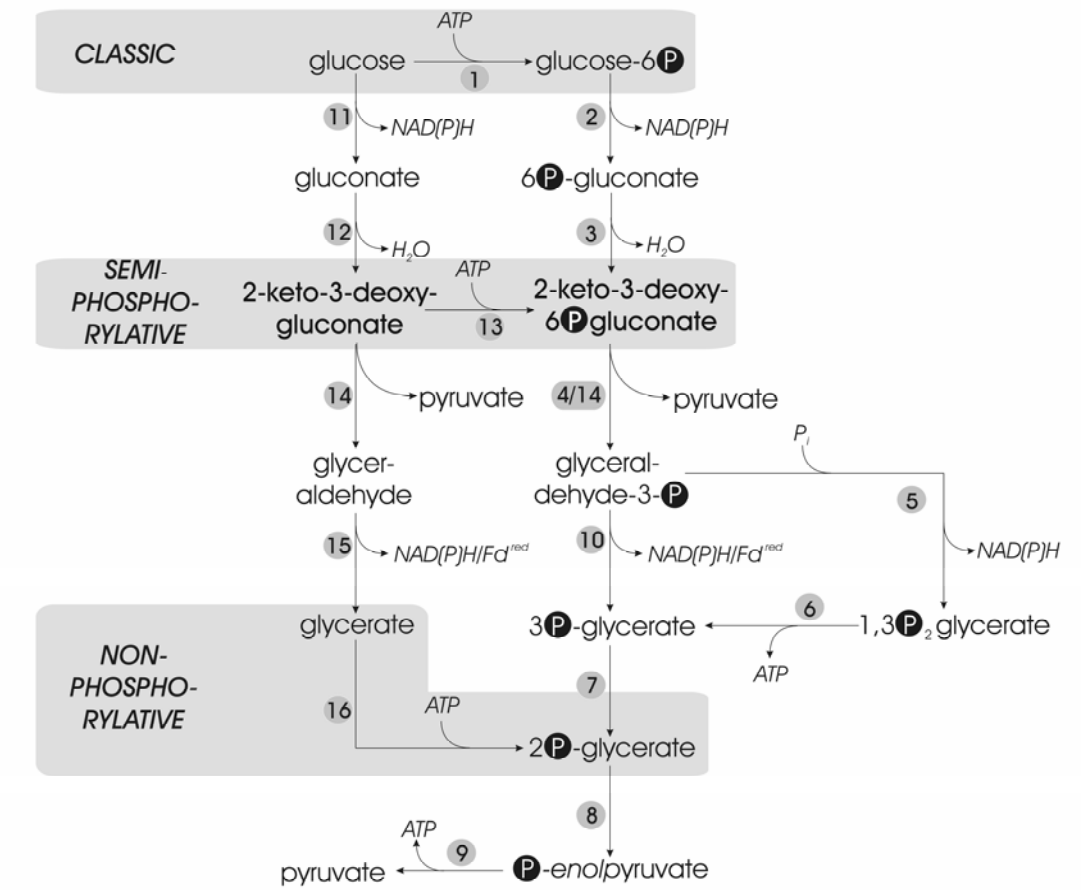

FIGURE 2: GLUCOSE CATABOLISM VIA THE DIFFERENT ENTNER-DOUDOROFF (ED) PATHWAYS.
Overview of the classical and modifications of the ED pathway, each with the characteristic phosphorylation level indicated. Non-phosphorylated intermediates are depicted on the left, and phosphorylated intermediates on the right. The key phosphorylation reactions for the different ED versions are highlighted in grey boxes (glucokinase/hexokinase for the classical ED, KDG kinase for the semi-phosphorylative ED and glycerate kinase for the non-phosphorylative ED). Key to enzymes: 1: glucokinase/hexokinase; 2: glucose-6-phosphate dehydrogenase; 3: 6-phosphogluconate dehydratase; 4: 2-keto-3-deoxy-6-phosphogluconate (KDPG) aldolase; 5: glyceraldehyde-3-phosphate (GAP) dehydrogenase; 6: 3-phosphoglycerate kinase; 7: phosphoglycerate mutase; 8: enolase; 9: pyruvate kinase; 10: non-phosphorylating GAP dehydrogenase (GAPN)/GAP oxidoreductase; 11: glucose dehydrogenase; 12: gluconate dehydratase (GAD); 13: 2-keto-3-deoxygluconate (KDG) kinase; 14: KD(P)G aldolase; 15: aldehyde dehydrogenase/aldehyde oxidoreductase; 16: glycerate kinase.

The semi-phosphorylative ED pathway has been shown to operate in several species of *Clostridium* [ANDREESEN & GOTTSCHALK, 1969], as well as the halophilic archaea *Halobacterium saccharovorum* and *H. halobium* [TOMLINSON et al., 1974].

Another variant pathway, the so-called non-phosphorylative ED pathway, has been reported for the hyperthermophilic Archaea *S. solfataricus* [DE ROSA et al., 1984], *S. acidocaldaricus* [SELIG et al., 1997], *T. tenax* [SIEBERS et al., 2004; SIEBERS & HENSEL, 1993;

SELIG & SCHÖNHEIT, 1994; SIEBERS et al., 1997; SELIG et al., 1997], the thermophilic archaeon *T. acidophilum* [BUDGEN & DANSON, 1986] and several species of the fungal genus *Aspergillus* [ELZAINY et al., 1973]. In contrast to the semi-phosphorylative ED modification, KDG (rather than KDPG) has been reported to be subjected to aldol-cleavage by the KDG aldolase, forming pyruvate and glyceraldehyde. Glyceraldehyde is further oxidized to form glycerate, either by an $NAD(P)^+$-dependent glyceraldehyde dehydrogenase [BUDGEN & DANSON, 1986] or by a ferredoxin-dependent glyceraldehyde oxidoreductase [SELIG & SCHÖNHEIT, 1994; MUKUND & ADAMS, 1991; SCHICHO et al., 1993; KARDINAHL et al., 1999]; Glycerate is phosphorylated to 2-phosphoglycerate by glycerate kinase [BUDGEN & DANSON, 1986]. 2-Phosphoglycerate enters the lower shunt of the EMP pathway and forms a second molecule of pyruvate via the enolase and pyruvate kinase reaction (Fig 2).

Reconstruction of the central carbohydrate metabolism by the use of genomic and biochemical data combined with comparative genome approaches suggested the presence of the semi-phosphorylative ED pathway in both *T. tenax* [SIEBERS et al., 2004] and *S. solfataricus* [AHMED at al, 2005; SIEBERS & SCHÖNHEIT, 2005]. *Thermoproteus tenax* is a sulfur-dependent anaerobe which grows optimally around 90°C, pH 5 [ZILLIG et al., 1981] (Fig 3) and was shown to grow both chemolithoautotrophically (CO_2, H_2) and chemoorganoheterotrophically on different carbon sources (e.g. glucose, starch). *T. tenax* uses two different pathways for glucose catabolism, the modified EMP and the non-phosphorylative ED pathway, as deduced from detected enzyme activities in crude extracts, and from the identification of characteristic intermediates in ^{14}C labelling experiments and *in vivo* ^{13}C NMR studies [SIEBERS et al., 2004; SIEBERS & HENSEL, 1993; SELIG & SCHÖNHEIT, 1994; SIEBERS et al., 1997; SELIG et al., 1997; DÖRR et al., 2003].

The variants of the EMP pathway in *T. tenax* is characterized by (i) a hexokinase with reduced allosteric potential, (ii) a non-allosteric, reversible PPi-dependent phosphofructokinase, (iii) three different GAP (glyceraldehyde 3-phosphate)-converting enzymes, a classical, phosphorylating GAPDH (glyceraldehyde-3-phosphate dehydrogenase), GAPN (a non-phosphorylating, highly allosteric GAPDH) and GAPOR (a

ferredoxin-dependent glyceraldehyde-3-phosphate oxidoreductase), and (iv) three enzymes for phosphoenolpyruvate and pyruvate interconversion, a catabolic pyruvate kinase with low allosteric potential, an anabolic PEPS (phosphoenolpyruvate synthetase) and a reversible PPDK (pyruvate phosphate dikinase) [SIEBERS et al., 2004].

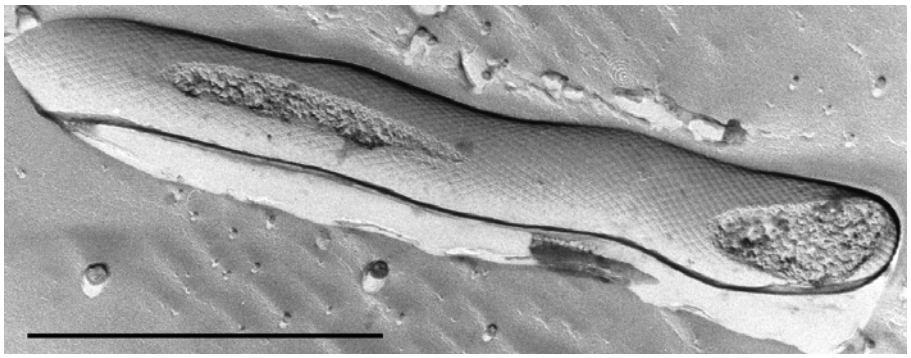

FIGURE 3: ELECTRON MICROGRAPH OF *THERMOPROTEUS TENAX* KRA1.
Photo by PD Dr. Reinhard Rachel, Universität Regensburg.

Sulfolobus solfataricus grows optimally at 80-85°C and pH 2-4 (Fig 4). Aerobic heterotrophic growth is reported on several carbon sources such as starch, glucose, arabinose, fructose and peptide-containing substrates like peptone, tryptone and yeast extract [GROGAN, 1989]. The non-phosphorylative ED pathway was proposed as pathway for glucose catabolism on the basis of ^{14}C-labelling studies and identification of the characteristic intermediates (KDG, GA) [DE ROSA et al., 1984], as well as characterization of key enzyme activities [DE ROSA et al., 1984; BUCHANAN et al., 1999; LAMBLE et al., 2003]. The glucose dehydrogenase and KDG aldolase of *S. solfataricus* have been studied in detail [LAMBLE et al., 2003; THEODOSSIS et al., 2004; MILBURN et al., 2006] indicating that this pathway is promiscuous and represents an equivalent route for glucose and galactose catabolism in this organism. In addition to a glucose dehydrogenase which exhibits high activity with glucose and galactose, the KDG aldolase was shown to lack facial selectivity in catalyzing the cleavage of KDG as well as 2-keto-3-deoxygalactonate (KDGal), both yielding glyceraldehyde and pyruvate

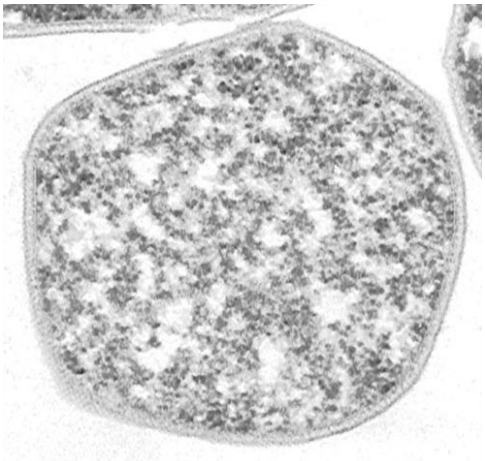

FIGURE 4: ELECTRON MICROGRAPH OF *SULFOLOBUS SOLFATARICUS*.
Image provided by D. Janckovik and W. Zillig.

In the current view about the ED pathway in Archaea, it is assumed that a semi-phosphorylative version is operative in Haloarchaea, whereas a non-phosphorylative version is present in hyperthermophilic and thermophilic Archaea. The aforementioned available biochemical data on *T. tenax* and *S. solfataricus* do not disagree with this assumption. However, in our ongoing attempts to reconstruct the archaeal central carbohydrate metabolizing pathways, a comparative genomics approach has revealed ED gene clusters that are conserved in *T. tenax* [SIEBERS et al., 2004], *S.* so*lfataricus*, *S. tokodaii* and *Halobacterium* sp. NRC, suggesting the presence of the semi-phosphorylative pathway in these organisms. Qualitative analysis of the corresponding gene products of *T. tenax* and *S. solfataricus* were performed in order to confirm the presence of the semi- as well as the non-phosphorylative ED pathway and to extend our current understanding of central carbohydrate metabolism in hyperthermophilic Archaea. This study provides novel insights on the operation of the modified "branched" ED pathways in hyperthermophilic Archaea.

2. MATERIALS AND METHODS

2.1 CHEMICALS AND PLASMIDS

All chemicals and enzymes were purchased from Amersham Pharmacia Biotech Europe GmbH, Applied Biosystems, ARK Scientific, Bio-Rad Laboratories GmbH, Biometra, Difco Laboratories, Fermentas Life Science, Gerbu Biotechnik GmbH, Life Technologies, MBI Fermentas GmbH, Merck, QIAGEN, Roche Diagnostics GmbH, Roth GmbH, Schleicher & Schuell, SERVA Electrophoresis GmbH, Sigma-Aldrich, Tropix and VWR International in analytical grade. ^{14}C-labelled glucose and pyruvate were obtained from Amersham Life Technologies. For heterologous expression the pET vector system (pET-15b, pET-24a, pET-24d) (Novagen) was used. For *in vitro* transcription the pSPT19 (Böhringer Mannheim) vector was used (Table 1)

2.2 INSTRUMENTS

Chemiluminescent detector for gel documentation	Detector: ChemiDoc Gel Documentation System (Bio-Rad Laboratories GmbH, München) Video copy processor: Mitsubishi P91W
Protein chromatography	BioLogic DuoFlow Pathfinder 20 system (Bio- Rad Laboratories GmbH, München) System: F10 work station, MX-1 mixer, 3-Tray rack, AVR7-3 sample inject valve, QuadTec UV/Vis detector with 3 mm PEEK flow cell, system cable 25 (RS-232), BioFrac fraction collector
Chromatography column	HiLoad 26/60 Superdex 200 prep grade
Autoclave	Webeco Modell H (Webeco GmbH, Bad Schwartau) Zirbus LVSA 40/60 (ZIRBUS technology GmbH, Bad Grund / Harz)
Agarose gel electrophoreses	Agagel Mini (Biometra GmbH, Göttingen); self-made by the fine mechanics dept. (University of Duisburg-Essen) Power supply: Consort E143 (MS Laborgeräte)

SDS-PAGE (polyacrylamide gel electrophoresis)	Minigel-Twin (Biometra GmbH, Göttingen); self-made by the fine mechanics dept. (University of Duisburg-Essen) Power supply: Consort E835 (MS Laborgeräte)
Fermenter	Biostat® 100 L Fermenteranlage (Sartorius BBI Systems GmbH, Melsungen) Heat exchanger: Integra T10000 460 / 60HZ 3P Lauda
Cell Disruption	French Press (SLM Aminco Instruments Inc., Spora, Büttelborn)
Incubators	RFI-125 Inkubator (Infors AG, Bottmigen,Basel, Swizerland); Minitron Infros HT, Bottmingen
Photometer	Philips 8720, thermostatisierbares UV/VIS Photo spectrometer (Philips Analytical, Cambridge, England); Eppendorf 1101M, thermostatisierbares UV/VIS Photo spectrometer (Eppendorf AG, Hamburg); Specord 200 analytikjena Analytik Jena AG, Jena
Aqua bidest water system	Seral Pro 90 CN (Elga-Seral, Ransbach-Baumbach)
Thermocycler	iCycler (Bio-Rad Laboratories GmbH, München)
Vacuum centrifuge	Speedvac Concentrator (Savant, Farmindale, GB)
Centrifuges	Bench centrifuges: Sigma 3K12 (B. Braun AG, Melsungen); Centrikon T 1170 (Kontron Instruments, Neufahrn b. München); Hettich Universal centrifuge 32R; Biofuge pico, Heraens Insteruments Lagre centrifuges: Avanti J-25 (Beckmann, München); Avanti J25 (Beckmann, München) Ultracentrifuges: L8-80 (Beckman Coulter GmbH, Krefeld)
Contamination monitors	Contamat FHT 111M, CA, USA LB 124 Berthold Technologies GmbH Bad Wildbad
Ultraviolet light	Konrad Benda N90, MW312 nm, Wiesloch
Anaerobic tent	Coy lab Inc (Toepffer lab systems, Göppingen)

2.3 STRAINS AND GROWTH CONDITIONS

Thermoproteus tenax Kra1 strain; DSMZ 2078 [ZILLIG et al., 1981]

Sulfolobus solfataricus P1 strain; DSMZ 1617 [ZILLIG et al., 1980]

Escherichia coli K12 DH5α strain; DSMZ 6897 [HANAHAN, 1983]

Escherichia coli BL21(DE3); Novagen [STUDIER & MOFFATT, 1986]

Escherichia coli BL21-CodonPlus(DE3)-RIL; Stratagene [CARSTENS & WAESCHE, 1999]

Escherichia coli JM109(DE3); Promega [YANISCH-PERRON et al., 1985]

Mass cultures of *Thermoproteus tenax* Kra1 (DSM 2078) were grown at 86°C in an enamelled 100-l fermenter (Braun Biotic International, Melsungen, Germany) in a basic medium according to Brock, [BROCK et al., 1972] containing:

1.3 g/liter $(NH_4)_2SO_4$, 0.28 g/liter KH_2PO_4, 0.25 g/liter $MgSO_4$ x 7 H_2O, 0.07 g/liter $CaCl_2$ x 2 H_2O, 0.02 g/liter $FeSO_4$ x 7H_2O, 1.8 mg/liter $MnCl_2$ x 4 H_2O, 4.5 mg/liter $Na_2B_4O_7$ x10 H_2O, 0.22 mg/liter $ZnSO_4$ x 7 H_2O, 0.05 mg/liter $CuCl_2$ x 2 H_2O, 0.03 mg/liter Na_2MoO_4 x 2 H_2O, 0.03 mg/liter $VOSO_4$ x 5 H_2O, 0.01 mg/liter $CoSO_4$ x 7 H_2O, 1 mg/liter resazurin. Additionally, 2.5 g elemental sulfur and 0.02 g yeast extract per liter were added. For heterotrophic growth, 1 g glucose and 0.01 g yeast extract per liter medium were added.

Anaerobic growth conditions were established by the addition of Na_2S x 7–9 H_2O. For autotrophic growth conditions, cultures were continuously gassed with 80% H_2/20% CO_2 [v/v] and for heterotrophic growth conditions with 80% H_2/20% N_2 [v/v] at a flow rate of 1 l/min and stirred at 250 rpm. Cells were harvested at different growth phases. After cooling down to 10°C by a plate heat exchanger, sulfur was removed by two fold passage through a folded filter (Schleicher & Schuell) and the cells were concentrated by cross-flow filtration in a Pellicon Acryl system (Millipore). Cells were then stored at –80°C. Cells were counted by using a Neubauer chamber. Under autotrophic growth conditions, cells were harvested at a cell density of 3-4 x 10^8, while under heterotrophic growth conditions cells were harvested at a cell density of around 1 x 10^8.

Cultivation of *Sulfolobus solfataricus* P2 (DSM1617) was carried out in the laboratory of Microbiology (Wageningen University, The Netherlands). Briefly, cells were grown aerobically in a rotary shaker (100 rpm) at 80°C in chemically defined medium containing: 2.5 g/liter $(NH_4)_2SO_4$, 3.1 g/liter KH_2PO_4, 203.3 mg/liter, $MgCl_2$ x 6 H_2O, 70.8 mg/liter $Ca(NO_3)_2$ x 4 H_2O, 2 mg/liter $FeSO_4$ x 7 H_2O, 1.8 mg/liter $MnCl_2$ x 4 H_2O, 4.5 mg/liter Na_2B4O_7 x 2 H2O, 0.22 mg/liter $ZnSO_4$ x 7 H_2O, 0.06 mg/liter $CuCl_2$ x 2 H_2O, 0.03 mg/liter Na_2MoO_4 x 2 H_2O, 0.03 mg/liter $VOSO_4$ x 2 H_2O and 0.01 mg/liter $CoCl_2$ x 6 H_2O. The medium was supplemented with Wollin vitamins, and 0.3% of carbon source as indicated. The Wollin vitamin stock (100X) contained per liter: 2 mg D-biotin, 2 mg folic acid, 10 mg pyridoxine-HCl, 10 mg riboflavin, 5 mg thiamine-HCl, 5 mg nicotinic acid, 5 mg DL-Ca-pantothenate, 0.1 mg vitamin B12, 5 mg *p*-aminobenzoic acid and 5 mg lipoic acid. The pH of the culture media was adjusted at room temperature to pH 3.5 with 0.1 M H_2SO_4. Cell growth was monitored by measuring the turbidity at 600 nm.

Escherichia coli K12 strain DH5α, Bl21(DE3), BL21-CodonPlus(DE3)-RIL and JM109(DE3) were grown aerobically in 2–400 ml batch cultures in reaction tubes or erlenmeyer flasks at 37°C with aeration by gyratory shaking (180 rpm). Mass culture volumes (up to 5–15 liters) were aerated by gassing compressed air through a bacterial tight filter with a 50 l/min flow rate. Cultures were grown on Luria-Bertani (LB-) medium (1% [w/v] peptone (Difco Laboratories), 0.5% [w/v] yeast extract (Difco Laboratories), 1% [w/v] NaCl, pH 7). For solid medium plates, 1.5% [w/v] agar-agar (Difco Laboratories) was added. Antibiotics (Sigma-Aldrich) were added according to the encoded plasmid resistance in the following concentrations: ampicillin 100 µg/ml, kanamycin 50 µg/ml, chloramphenicol 34 µg/ml. Growth was monitored spectrophotometrically at 578 nm.

E. coli DH5α was used for the cloning and storage using plasmid derived vectors. *E. coli* BL21(DE3), BL21-CodonPlus(DE3)-RIL and JM109(DE3) strains were used for the heterologous expression of recombinant *T. tenax* and *S. solfataricus* proteins. 1% of a preculture was inoculated into liquid LB-medium containing the appropriate antibiotic and incubated at 37°C in a rotary shaker. Protein expression was induced at OD_{578} = 0.6–0.8 by the addition of 1 mM Isopropyl-beta-D-thiogalactopyranoside (IPTG) (Gerbu

Biotechnic GmbH) and incubation continued for 3–4 hours. Afterwards cells were chilled on ice and harvested by centrifugation (6 000 x *g*, 15 min, 4°C) and finally stored at –80°C.

TABLE 1: PRIMER SETS, PLASMIDS, STRAINS AND HOSTS.

The introduced mutations are shown in boldface and the restriction sites are underlined. f: forward primer; rev: reverse primer.

Gene	Primer	Sequence (5'→3')	Plasmid	Host
Ttx gdh	GDH-*Bsp*H1-f	TAGAGGCT**C**ATGAGGGCTG	pET-15b	BL21 (DE3) CodonPlus
	GDH-*Bam*H1-rev	ACTACCGTG**GATC**CACAAC		
Ttx gad	GAD-*Nco*I-f	TTTGGCCAGCGC**C**ATGGCCTCATCG	pET-15b	BL21-CodonPlus(DE3)-RIL
	GAD-*Xho*I-rev	AAATGCCGGC**C**TCGA**G**GGAATGGGA		
Ttx kdgA	KDGA-*Nco*I-f	AGGGCGCCCCGAGTACTATC**C**ATGGAGA	pET-15b	BL21-CodonPlus(DE3)-RIL
	KDGA-*Xho*I-rev	GGGGCTCCCCT**C**G**A**GCTACCAGGC		
	KDGA-pSPT19-*Eco*RI-f[2]	5′-TAGCGCTGGCC**G**AAT**T**CGCCGAGTCGAG-3′	pSPT19	DH5α
	KDGA-pSPT19-*Bam*HI-rev[2]	5′-ATAGTTGGCCGAGGA**TC**CCACGACTCCG-3′		
Ttx kdgK	KDGK-*Nde*I-f	GAGCCAGCTGAG**CA**TATGATAAGCCTGG	pET-24a	BL21-CodonPlus(DE3)-RIL
	KDGK-*Eco*RI-rev3	TTGCCCAGAAT**TC**CGCTCCTC		
	KDGK-pSPT19-*Eco*RI-f[2]	5′-ACAGGAAGGGGA**ATT**CCGGCAGCAG-3′	pSPT19	DH5α
	KDGK-pSPT19-*Bam*HI-rev[2]	5′-TATGCCTCCTCG**GGATCC**CTCACTCCGA-3′		
Sso gad[3]	BG1069 (*Nco*I-f)	GCGCGCCATGGCGAGAATCAGAGAAATAGAACCAATAG	pET-24d	BL21-CodonPlus(DE3)-RIL
	BG1070 (*Bam*HI-rev)	GCGCGGGATCCTCAAACACCATAATTCTTCCAGGTTCCC		
Sso kdgA[3]	BG1067 (*Nco*I-f)	GCGCGCCATGGCGCCAGAAATCATAACTCCAATCATAACC	pET-24d	BL21-CodonPlus(DE3)-RIL
	BG1068 (*Bam*HI-rev)	GCGCGGGATCCCTATTCTTTCAATATTTTAAGCTCTAC		
Sso kdgK[3]	BG1071 (*Nco*I-f)	GCGCGCCATGGTTGATGTAATAGCTTTGGGAGAGCC	pET-24d	JM109(DE3)
	BG1072 (*Nco*I-mut-f)[1]	CTGGGGCTGGTGACGC**A**ATGGCAGGGACATTTGTTTCC		
	BG1073 (*Nco*I-mut-rev)[1]	GGAAACAAATGTCCCTGCCAT**T**GCGTCACCAGCCCCAG		
	BG1074 (*Eco*RI-rev)	GCGCGGAATTCTTACGTTTTAAACTCATTTAAAAATC		
Sso gapN	BG1451 (*Nco*I-f)	GCGCGCCATGGAGAAAACATCAGTGTTG	pET-24d	JM109(DE3)
	BG1452 (*Bam*HI-rev)	GCGCGGGATCCTTACAAGTATTCCCAAATACCTTTCCC		
Tm eda[4]			pET-28b	BL21-CodonPlus(DE3)-RIL

[1] For the cloning of *S. solfataricus kdgK* an internal *Nco*I site was disrupted by site-directed mutagenesis, without changing the coding region. The mutated base is indicated in bold.

[2] Primers used for the synthesis of DIG-Labelled specific antisense mRNA probes by *in vitro* transcription.

[3] The *S. solfataricus* genes were cloned by A. C. M. Geerling and T. Ettema in the laboratory of Microbiology (Wageningen University, The Netherlands).

[4] The expression plasmid was provided by Carol A. Fierke (University of Michigan, Ann Arbor, MI, USA)

2.4 MOLECULAR BIOLOGICAL METHODS WITH DNA

2.4.1 Genomic DNA preparation

Genomic DNA from *T. tenax* was isolated using DNAzol (Invitrogen) according to the manufacturer's instructions, with slight modifications. The method is based on the use of a novel guanidine-detergent lysing solution that hydrolyzes RNA and promotes the selective precipitation of DNA from the cell lysate [CHOMCZYNSKI et al., 1993] [MACKEY et al., 1996]

T. tenax cells (0.3 g wet weight) were suspended in 2 ml DNAzol reagent and incubated for 15 minutes at room temperature. Sample was homogenized by using a hand held glass-teflon homogenizer and then incubated for 5–10 minutes at room temperature. The homogenate was sedimented by centrifugation (10 000 x *g*, 10 min, RT). Centrifugation was repeated until all visible traces of sulphur compounds were removed and the viscous supernatant was then transferred to a fresh tube. DNA was precipitated by adding 0.5 ml of 100% ethanol per 1 ml of DNAzol, mixing by inverting the tube 5–8 times and incubating the sample at room temperature for 1–3 minutes. DNA was sedimented by centrifugation (10 000 x *g*, 10 min, RT). The supernatant was decanted and DNA was washed twice with 1.0 ml 70% ethanol and then centrifuged again. The remaining ethanol was completely removed under vacuum (speed vac) and the pelleted DNA was then resolved in 200 µl A. bidest for 30 minutes at room temperature. The quality of purified DNA was checked by restriction digestion and subsequent agarose gel electrophoresis.

The isolation of genomic DNA from *Sulfolobus solfataricus* was performed by T. Ettema in the laboratory of Microbiology (Wageningen University, The Netherlands). 30–50 ml culture centrifuged using a swinging-bucket rotor at 6000 x *g* for 10 minutes. Sedimented cells were resuspended in 800 µl TNE solution (100 mM Tris-HCl pH 8.0, 50 mM NaCl, 50 mM EDTA, pH 8.0) and then incubated for 10 minutes at room temperature. 100 µl of 10% SDS and 100 µl of 10% Sarkosyl was added and mixed by inverting the tube 5–6 times after adding 10 µl RNase (10 mg/ml in TE buffer). The sample was incubated for 15 minutes at room temperature. 50 µl Proteinase K (20 mg/ml in 10

mM Tris-HCl, pH 8.0) was added and afterwards incubated in awater bath at 55°C for 1 hour. 1 ml TE-saturated Phenol solution (10 mM Tris-HCl pH 8.0, 1 mM EDTA, pH 8.0) was added, mixed gently (but thoroughly), centrifuged (10 000 x *g*, 10 min, RT) and the upper aqueous layer was collected. The homogenate was extracted 2 times with phenol:chloroform:indole-3-acetic acid (IAA) (25:24:1) followed with 1 time extraction with chloroform:IAA (24:1). Then an equal volume of isopropanol was added to the aqueous phase and mixed by inverting the tube several times. Genomic DNA was spun down (10 000 x g, 10–15 min, RT). The pellet was washed twice with 70% ethanol, dried completely under vacuum and then dissolved in 100 µl TE buffer.

2.4.2 Isolation of plasmid DNA from *E. coli*

Plasmid DNA used for restriction and cloning was isolated by the alkaline lysis method according to Birnboim & Doly [BIRNBOIM & DOLY, 1979]. Thereby, 1–2 ml overnight culture was centrifuged (12 000 x *g*, 5 min, 4°C) and the cell pellet was resuspended in 200 µl buffer 1 (50 mM Tris, 10 mM EDTA, pH 8, 100 µg/ml RNase A) followed by incubation on ice for 30 minutes. Cell lysis was achieved by the addition of 300 µl buffer 2 (0.2 M NaOH, 1% SDS) and incubation for 5 minutes at room temperature. Genomic DNA was precipitated by the addition of 300 µl buffer 3 (3 M K-Acetate, pH 4.8) and incubation on ice for 20 minutes. Precipitated genomic DNA and cell debris was removed by centrifugation (20 000 x *g*, 15 min, 4°C). Plasmid DNA was precipitated by 0.7 volumes isopropanol (10 min, RT), centrifugation (20 000 x *g*, 15 min, 4°C) and washing in 1.0 ml 70% ethanol. The pellet was completely dried under vacuum (speed vac) and then resuspended in 50 µl A. bidest.

Boiling-PCR was used for a rapid qualitative analysis of recombinant *E. coli* clones by PCR-amplification. The colonies were picked with a sterilized pipette tip, part of the cells was streaked on an LB agar plate and the rest was resuspended in 50 µl 10 mM Tris-HCl, pH 7.0, cells were lysed by incubation at 94°C for 5 minutes, centrifuged (14 000 x *g*, 1 min, RT) and finally 5 µl of the supernatant was used as a DNA-template for the PCR (25 µl reaction assay)

Plasmid DNA preparations used for quantitative and qualitative analysis were prepared by the QIAfilter Plasmid Midi Kit (QIAGEN) following the manufacturer's instructions.

2.4.3 DNA precipitation

Ethanol or isopropanol was used to precipitate DNA [SAMBROOK et al., 1989]. Typically, 0.7 volumes of isopropanol were added to the DNA sample and precipitation was performed by incubation at –20°C for 30 minutes. Precipitated DNA was centrifuged (20 000 x *g*, 15 min, 4°C) and the pellet was washed with ice cold 70% ethanol. After a second centrifugation, the supernatant was discarded, and the DNA pellet was dried under vacuum (speed vac) and then rinsed with an adequate volume of A. bidest.

2.4.4 Quantification of DNA

DNA concentrations were measured by ultraviolet absorbance spectrophotometry. Absorbance was measured at 260 nm using Specord 200 (Analytic Jena) spectrophotometer in combination with WinASPECT Spectralanalysis-Software. At 260 nm, an absorbance (A_{260}) of 1.0 corresponds to 50 µg of dsDNA per ml [SAMBROOK et al., 1989].

The purity of DNA was determined at 260 nm and 280 nm wavelength. For a pure DNA sample the ratio of the absorbance (A_{260}/A_{280}) was 1.8. Ratios less than 1.8 indicated that the preparation was contaminated, either with protein or with phenol.

2.4.5 Agarose gel electrophoresis for DNA

Agarose gel electrophoresis [SAMBROOK et al., 1989] was employed to monitor the progression of a restriction enzyme digestion, to quickly determine the yield and purity of a DNA isolation or PCR reaction, and to size fractionate DNA molecules, which then could be eluted from the gel. Agarose gels (0.7% and 1.5%) (Life Technologies) were performed in TAE-buffer (40 mM Tris-Acetat, 1 mM EDTA). Ethidium bromide (Sigma-Aldrich) with a concentration of 1 µg/ml was included in the gel matrix to enable

fluorescent visualization of the DNA fragments under UV light. The DNA samples were mixed with loading buffer (6 times: 0.2% Bromophenolblue, 0.2% xylencyanol FF, 60% glycerol and 60 mM EDTA) and loaded into the sample wells. Electrophoresis was usually performed at 60–100 mA for 0.5–1 hour at room temperature, depending on the gel size. Size marker (GeneRuler™ 1kb DNA ladder, MBI Fermentas) was co-electrophoresed with DNA samples. After electrophoresis, the gel was placed on a UV light chamber and a picture was taken by using the ChemiDoc-Gel Documentation System (BioRad).

2.4.6 Purification of DNA fragments

Extraction and purification of DNA fragments from agarose gels and of PCR fragments were achieved by using the QIAquick Gel Extraction and QIAquick PCR Purification Kit (QIAGEN), respectively, following the manufacturer's instructions.

2.4.7 Polymerase chain reaction (PCR)

PCR is an *in vitro* method for the enzymatic synthesis of defined DNA sequences. The reaction uses two oligonucleotide primers that hybridize to opposite strands and flank the target DNA sequence that is to be amplified. The elongation of the primers is catalyzed by a heat-stable DNA polymerase [MULLIS et al., 1986].

The PCR standard method includes three main steps:

Denaturation: Initial heating of the PCR mixture for 2 minutes at 94–95°C denatures double-stranded genomic DNA complex into two single strands.

Primer annealing: Annealing of the oligonucleotide primers to the complementary DNA sequence.

Primer extension: The synthesis of new double stranded DNA molecules at the region marked by the primers. DNA polymerase (ex. *Taq*-polymerase, *Pwo*-polymerase) synthesizes exclusively in the 5' to 3' direction.

The cycling protocol consisted of 25–30 cycles. Annealing temperature has to be optimized empirically. The approximately melting temperature (T_m) for primers shorter than 25 nucleotides was calculated using the following formula [THEIN & WALLACE, 1986]:

$$Tm = (\%\ AT) \times 2 + (\%\ GC) \times 4$$

The identified open reading frames (ORFs) of the ED cluster from *T. tenax* were amplified using *T. tenax* genomic DNA as template. The following annealing temperature was used for the different amplified genes; 58°C *gdh*, 61.5°C *gad*; 65.9°C *kdgA*, 60.7°C *kdgK*. Mutagenic primer sets were used to introduce a restriction sites (Table 1). Cloning of the *S. solfataricus* genes was carried out (A. Geerling and T. Ettema in the laboratory of Microbiology, Wageningen University, The Netherlands).

2.4.8 Amplification of genomic DNA and plasmid DNA by PCR

For PCR amplification, 50–100 ng genomic DNA template, 1 µM each of forward and reverse primers (ARK Scientific), 1.5 mM $MgCl_2$, 200 µM dNTPs (Life Technologies) 1 x reaction buffer (MBI Fermentas) and 1 unit of DNA polymerase (*Taq* or *Pwo* polymerase) (MBI Fermentas or Roche Diagnostics, respectively) was used. The PCR reaction was performed using a thermocycler iCycler (BioRad).

2.4.9 Enzymatic manipulation of DNA

2.4.9.1 Restriction of DNA

Digestion with restriction enzymes was performed by incubating the double-stranded DNA molecules with an appropriate amount of restriction enzyme, in its respective buffer. Restriction assays for genomic DNA and plasmid DNA was performed with up to 5 µg DNA, 2–3 units of restriction endonuclease (MBI Fermentas GmbH, New England Biolab GmbH) and 1 x restriction buffer (New England Biolab GmbH). The restriction reaction was performed at 37°C for 1 hour according to manufacturer's instructions.

2.4.9.2 5`-Dephosphorylation of the linearized vector DNA

In order to avoid the self-ligation of restricted vector DNA, the 5'phosphate group was eliminated by treatment with calf intestinal alkaline phosphatase (CIP) (Promega), by which 0.05 units of CIP/pmol DNA was added to the restriction reaction and incubated at 37°C for 1 hour.

2.4.9.3 Ligation of vector DNA and insert

DNA ligation was performed by incubating the restricted DNA inserts with the restricted linearized dephosphorylated vector in the presence of T4 DNA ligase [PAN et al., 1994] [BANKIER et al. 1987]. DNA ligase catalyses the formation of a phosphodiester bond between the 3' hydroxyl of one nucleotide and the 5' phosphate of another nucleotide.

For ligation, equimolar amounts of restricted plasmid DNA and insert at the ratio of 1:3 were used. DNA (8 µl total volume) was incubated at 45°C for 5 minutes and chilled on ice. 1 µl of 10 x reaction buffer (400 mM Tris-HCl, 100 mM $MgCl_2$, 100 mM DTT, 5 mM ATP, pH 7.8) and 1 µl T4 DNA ligase (1 weiss-unit/µl) (MBI Fermentas) were added to a final volume of 10 µl. Ligation was carried out overnight at 4°C or for 2 hours at 16°C and subsequently T4 DNA Ligase was inactivated by incubation at 70°C for 10 minutes. Ligated DNA was stored at –20°C.

2.4.10 Transformation

2.4.10.1 Preparation of competent *E. coli* cells

Competent cells from *E. coli* DH5α, BL21(DE3), BL21-CodonPlus(DE3) strains were prepared by using the rubidium chloride/calcium chloride method [PROMEGA TECHNICAL MANUAL, 1994].

Therefore, 20 ml LB-medium was inoculated with 0.2 ml overnight culture, incubated at 37°C in a rotary shaker till OD_{578} reaches 0.3–0.5. The cell suspension was then centrifuged (1 730 x *g*, 10 min, 4°C). The following procedures were all carried out on ice. Cell pellet was gently resuspended in 10 ml ice cold solution A (10 mM MOPS, 10 mM RbCl, pH 7.0), centrifuged (10 min, 1 730 x *g*, 4°C) then cell pellet was gently resuspended in 10 ml ice cold solution B (100 mM MOPS, 50 mM $CaCl_2$, 10 mM RbCl, pH 6.5), and incubated on ice for 30 minutes. After the final centrifugation (700 x *g*, 15 min, 4°C), the pelleted cells were resuspended in 2 ml ice cold solution B and stored on ice.

2.4.10.2 Transformation of the competent *E. coli* cells

150 µl competent *E. coli* cells were gently mixed with plasmid DNA and incubated on ice for 60 minutes. Transformation was achieved by heat shock at 42°C for 45 seconds and subsequent storage on ice for 2 minutes. Cells were transformed to 800 µl LB-medium and incubated at 37°C for about 1 hour in a rotary shaker. 100 µl of transformed cells were plated on LB agar plates containing the respective antibiotics. The remaining 850 µl were centrifuged, pelleted cells were resuspended in about 100 µl LB-medium and plated. After incubation of LB agar plates containing the respective antibiotics at 37°C overnight, colonies were screened for positive clones carrying the recombinant plasmid DNA by boiling PCR or restriction digestion of isolated plasmid DNA (see 2.4.2).

2.4.11 Sequencing

2.4.11.1 Automated DNA sequencing

Automated DNA sequencing [SANGER et al., 1977] was done at Seqlab Company (Göttingen), GATC Biotech AG (Konstanz) and in the DNA Sequencer Service at the Medical Faculty, University Clinic of Essen.

2.4.11.2 Computer assisted analysis of the nucleotide sequence

The sequence chromatogram was visualized by using CHROMAS sofware. Sequence analysis was undertaken using GENMON 4.4 software (German Research Center for Biotechnology, Braunschweig). Calculating DNA and protein sequence similarity and homology searches were performed with Basic Local Alignment Search Tool (BLAST) at The National Center for Biotechnology Information (NCBI; http://www.ncbi.nlm.nih.gov/BLAST) [ALTSCHUL et al., 1990; ALTSCHUL et al., 1997]. For DNA and protein sequence alignments, the Multiple Sequence Alignment Parameters (Clustal W 1.7) was used [THOMPSON et al., 1994].

2.5 MOLECULAR BIOLOGICAL METHODS WITH RNA

2.5.1 Handling of solutions, glassware and equipments

To minimize degradation of RNA by RNases, gloves were worn and changed regularly when handling samples and reagents. All buffers and solutions were treated with 0.1% diethyl pyrocarbonate (DEPC), shaken vigorously to distribute the DEPC throughout the solution, left at room temperature overnight and then autoclaved for 20 minutes to remove any remaining DEPC. Glassware was heat sterilized by incubation at 200°C for at least 2 hours before use. Non-disposable plasticware was treated with 3% H_2O_2 or RNase Away (Roth GmbH). RNase-free solutions, reagents, and consumables, such as pipette tips, were separated and used only for RNA work.

2.5.2 Isolation of total RNA from *T. tenax* and *S. solfataricus*

Total RNA was isolated from *T. tenax* and *S. solfataricus* by using TRIzol reagent (Life Technologies) and RNeasy kit (QIAGEN), respectively, according to the manufacturer's instructions. The classic RNA isolation procedures by using TRIZOL reagent are based on a mono-phasic solution of phenol and guanidine isothiocyanate, followed by organic extraction and alcohol precipitation of the RNA as described by Chomczynski [CHOMCZYNSKI et al., 1993].

Briefly, 0.1 g cells from mid-log glucose and CO_2 grown *T. tenax* cultures (3.5–4 x 10^7 cells/ml) were suspended in 1 ml TRIzol reagent and lysed by incubation for 5 minutes at room temperature. Each sample was homogenized by using a hand held glass-teflon homogenizer and then stored for 5–10 minutes at room temperature. 200 µl chloroform was added to the homogenate, shaken vigorously for 15 seconds and then incubated for 2–3 minutes at room temperature. After incubation, the sample was centrifuged (12 000 x *g*, 15 min, 4°C) and the upper aqueous phase (approx. 400 µl) was transferred to a fresh tube. RNA was precipitated from the aqueous phase by mixing with 500 µl isopropanol, stored at room temperature for 10 minutes and centrifugation (12 000 x *g*, 10 min, 4°C). The supernatant was decanted and RNA was washed with 100 µl 70% ethanol, centrifuged (7 500 x *g*, 5 min, 4°C) and then stored in 100% ethanol at –80°C.

For *S. solfataricus* total RNA was isolated by T. Ettema (laboratory of Microbiology, Wageningen University, The Netherlands) from mid-log cultures (A_{600} = 0.5) grown on D-glucose, D-arabinose and tryptone using the RNeasy kit (QIAGEN). 50 ml of culture was washed in 1 ml of medium and resuspended in 100 µl of TE (10 mM Tris-HCl, 1 mM EDTA, pH 8.0). After addition of 5 µl of 10% Triton X-100, the RNA was further purified according to the manufacturer's prescriptions, except that genomic DNA was sheared through a 0.45 mm needle before the sample was applied onto a spin column. Columns were eluted twice with 50 µl of water.

2.5.3 Quantification of RNA

The concentration of RNA was determined by measuring the absorbance at 260 nm (A_{260}) in Specord 200 (Analytik Jena) spectrophotometer in combination with WinASPECT Spectralanalysis-Software. An absorbance at (A_{260}) of 1.0 unit corresponds to 40 µg of RNA per ml [SAMBROOK et al., 1989].

The ratio between absorbance values at 260 nm and 280 nm wavelengths gave an estimate of RNA purity. With a pure sample of RNA the ratio of the absorbance at (A_{260}/A_{280}) was around 2.0.

2.5.4 Agarose/Formaldehyde gel electrophoresis of RNA

The first successful method for electrophoretic analysis of the full size range of RNA molecules was described by Staynov [STAYNOV et al., 1972], by which RNA is denatured by formaldehyde and separated by Agarose gel electrophoresis in order to assess the overall quality of an RNA preparation.

For 1–1.2% MOPS/Formaldehyde gels, 1–1.2 g agarose were added to 73.8 ml DEPC treated water and 10 ml 10 x MOPS buffer (10 x: 200 mM morpholine propane sulfonic acid (MOPS), 50 mM sodium-acetate, 10 mM EDTA, pH 7.0) and microwaved for 2 minutes. After cooling down till 60°C, 16.2 ml of 37% formaldehyde was added. The agarose-formaldehyde gel was poured into the tray of the electrophoresis chamber, and

when the gel was solidified the electrophoresis chamber was filled with 1x MOPS buffer to cover the gel.

The RNA probe and the RNA marker (RNA Ladder High Range, Fermentas Life Science) were mixed with 3 times volumes of fresh prepared formaldehyde loading dye (250 µl deionised formamid, 83 µl formaldehyde (37%), 50 µl 10 x MOPS buffer, 2.5 µl bromophenol blue (2%) and 14.5 µl DEPC treated water), then incubated at 65°C for 10 minutes and afterwards incubated on ice. 10 µg RNA and 5 ng RNA marker were loaded on the gel. Electrophoresis was usually performed at 75–100 V for 2–3 hours in a 32 cm electrodes distance electrophoresis chamber.

2.5.5 Capillary transfer of RNA to a nylon membrane (Northern Blot)

Once separated by denaturing agarose gel electrophoresis, the RNA was transferred to a positively charged nylon membrane (0.45 µm pore size) (Roche Diagnostics) and then immobilized for subsequent hybridization.

Therefore, the gel was placed in an RNase-free dish and equilibrated in 20 x SSC buffer (3 M NaCl, 0.3 M Na-Citrate, pH 7.0) (2 times 15 min). A piece of nylon membrane was cut to the exact dimensions of the agarose gel, raised in DEPC treated water for about 1 minute and then soaked in sufficient 20 x SCC buffer until the start of the transfer. 3 pieces of Whatman filter paper (GB004) (Schleicher & Schuell) were soaked as well in 20 x SSC buffer. The transfer apparatus was built as follows (from bottom to top):

- Stack of paper towels based on a glass plate
- 1 piece of dry Whatman filter paper
- 2 pieces of wet Whatman filter paper
- Nylon membrane
- Agarose gel, turned upside down
- 2 pieces of wet Whatman paper

A glass plate was laid on the stack and 2 kg weight was placed on top to hold everything in place. The transfer was performed overnight at 4°C.

Once the RNA was transferred, the membrane was washed with DEPC treated water in order to remove salts, wrapped in transparent plastic foil and the RNA was crosslinked by UV radiation (UV transilluminator, λ = 254 nm, 3 min) in order to fix the RNA to the membrane. Afterwards, the blot was stained by shaking for approximately 1 minute in staining solution (50 mg metheylene blue, 6.6 ml 3 M sodium-acetate, pH 5.2, 1 ml 100% acetic acid, ad 50 ml with DEPC treated water), and afterwards destained by washing 3–4 times with DEPC treated water.

2.5.6 Hybridization of RNA with Digoxigenin-labelled RNA probes

Northern Blot analysis were carried out in order to analyze the cotranscription of genes

2.5.6.1 Synthesis of DIG-Labelled specific antisense mRNA probes by *in vitro* transcription

Digoxigenin-labelled antisense mRNA was obtained by *in vitro* transcription from the T7 promoter of the pSPT 19 vector (Roche Diagnostics) using the DIG RNA Labelling Kit (SP6/T7) (Roche Diagnostics) following the manufacturer's instructions.

For that purpose, part of the coding DNA region (~ 360 bp) of the gene to be analyzed (*kdgA* and *kdgK*) was amplified by PCR using mutagenic primer sets (Table 1) and then cloned into a polylinker site of the pSPT19 transcription vector which contains T7 RNA polymerase [DUNN & STUDIER, 1983; KASSAVETIS et al., 1982]. The "runoff" transcript synthesis was achieved by using a restriction enzyme (*Eco*RI) that creates a 5'-overhang which linearizes the template prior to transcription. The protocol incorporates one modified nucleotide (DIG-UTP) at approximately every 20–25th position in the transcript. Starting with 1 µg linear DNA template approximately 10 µg of full-length labelled RNA transcript can be produced. Finally after precipitation with ethanol, probes were washed by 70% ethanol, resuspended in 50 µl DEPC treated water and stored at –80°C.

2.5.6.2 Hybridization of immobilized RNA with DIG-labelled specific antisense mRNA probes

Prehybridization and hybridization of the RNA blots was carried out by using the DIG Easy Hyb solution (Roche Diagnostics). For that purpose, an appropriate volume of DIG Easy Hyb solution (approximately 20 ml/100 cm^2) was pre-heated, and afterwards the RNA blot was incubated in the solution for 2 hours at 68°C with gentle agitation. For hybridization, the DIG-labelled specific antisense mRNA probe was first denaturated by boiling for 10 minutes, rapidly cooled in an ice/ethanol bath and then added to the DIG Easy Hyb solution with a final concentration of 50–100 ng/ml hybridization solution. The prehybridization solution was poured off and the mRNA probe/DIG Easy Hyb mixture was added immediately to the membrane. Incubation was carried out overnight at 68°C with gentle agitation.

After hybridization, unhybridized probe was removed by washing with several buffer changes. 2 times 5 minutes at room temperature in low stringency buffer (2 x SSC, 0.1% SDS) to remove the hybridization solution and unhybridized probe, and then 2 times 15 minutes at 68°C in high stringency buffer (0.1 x SSC, 0.1% SDS) to remove partially hybridized molecules.

2.5.6.3 Detection of RNA-RNA hybrid by immunological detection

The probe-RNA hybrid was identified with an alkaline phosphatase-conjugated anti-DIG antibody by a chemiluminescent reaction. The detection of the alkaline phosphatase activity was carried out by the alkaline phosphatase substrate CDP-*Star* (Tropix) [BOEHRINGER MANNHEIM MANUAL, 1995].

Thereby, the RNA blot was washed for 5 minutes at room temperature in buffer 1 (0.1 M maleic acid, 3 M NaCl, pH 8.0). The membrane was then blocked by adding 2% blocking reagent (Roche Diagnostics) to the same buffer (buffer 2) and incubated for 1 hour at room temperature with shaking. The probe-RNA hybrid was localized by the addition of anti-digoxigenin-AP (Roche Diagnostics), with a final dilution of 1:20 000, to buffer 2 and incubation for 30 minutes at room temperature. The unbound antibody was

washed off with buffer 1 (4 times 10 min). The blot was equilibrated for 5 minutes at room temperature in the detection buffer (buffer 3) (0.1 M NaCl, 0.1 M Tris-HCl, pH 9.5).

The chemiluminescent reaction was carried out in a transparent development foil. The membrane (RNA side facing up) was placed on the foil and covered with CDP-*Star* (30-40 µl/cm^2). After applying the substrate, the blot was wrapped and the substrate was spread evenly over the membrane. The chemiluminescent signals were detected with the ChemiDoc Gel Documentation System (Bio-Rad), with an exposition time from 10 seconds to 10 minutes.

2.5.7 Primer extension analysis

The primer extension reaction was used to determine the start site(s) of RNA transcription for particular genes. It is done by annealing a specific end-labelled oligonucleotide primer that is complementary to a region towards the 5' end of the transcript, and transcribing the target RNA into cDNA by a reverse transcriptase. The size of the labelled single-stranded DNA is then determined on a sequencing gel relative to a sequence ladder [SAMBROOK et al., 1989].

Briefly, primer extension analysis was carried out by T. Ettema in the laboratory of Microbiology, Wageningen University, The Netherlands. The transcription start sites were mapped for the transcripts of *gad* and the *kdgA-kdgK-gaa* operon of *T. tenax* and for *gapN* and the *gad-kdgA-kdgK* operon of *S. solfataricus*, respectively. Primer extension analysis was performed using the following radiolabeled antisense oligonucleotides 5'-CGTCGGAGGTCACCACTC-3' for the *T. tenax gad* gene; 5'-CGCAACGAAGACTACGTCGACTCCC-3' for the *T. tenax kdgA* gene; 5'-CCATTTTCCGTAATGACCCTTGTGAC-3', for the *S. solfataricus gad* gene and 5'-CTGATCCACTGACCCGATAGATAGG-3' for the *S. solfataricus gapN* gene. For the primer extension reaction, 30 µg of total RNA and 2.5 ng of radiolabeled oligonucleotide were resuspended in 2 × AMV-RT buffer (Promega) in a final volume of 25 µl. Samples were heated to 70°C for 10 minutes and slowly cooled down to room temperature. $MgCl_2$, dNTPs, RNasin, and AMV-RT (Promega) were added to a concentration of 5 mM, 0.4

mM, 0.8 units/µl, and 0.4 units/µl, respectively, in a final volume of 50 µl. The samples were incubated at 42°C for 30 minutes, extracted with phenol/chloroform, precipitated with ethanol and resuspended in formamide loading buffer. The primer extension product was analyzed on an 8% denaturing sequencing gel along with a sequence ladder that was generated using the same radiolabeled oligonucleotides.

2.6 BIOCHEMICAL METHODS

2.6.1 Heterologous expression of the *T. tenax* and the *S. solfataricus* ED proteins in *E. coli*

For expression of the *gdh* (glucose dehydrogenase, AJ621346), *gad* (gluconate dehydratase, AJ621281), *kdgA* (KD(P)G aldolase, AJ621282) and *kdgK* (KDG kinase, AJ 621283) from *T. tenax* and the *gad* (SSO3198), *kdgA* (SSO3197), *kdgK* (SSO3195) and *gapN* (non-phosphorylating glyceraldehyde-3-phosphate dehydrogenase (GAPDH), SSO3194) from *S. solfataricus* the genes were cloned into the pET vector system using the restriction sites introduced by PCR mutagenesis (Table 1). Cloning of the *S. solfataricus* genes was carried out by A. Geerling and T. Ettema in the laboratory of Microbiology, Wageningen University, The Netherlands. PCR mutagenesis was performed using *Pwo* or *Taq* polymerase and genomic DNA from *T. tenax* or *S. solfataricus* as template. The sequences of the cloned genes were verified by dideoxy sequencing and expression of the recombinant enzymes in *E. coli* BL21 (DE3), BL21 (DE3) CodonPlus, and JM109 (DE3) was performed as discussed previously (see 2.3).

2.6.2 Preparative protein purification

Recombinant *E. coli* cells (7.5 g wet weight) were suspended in 15 ml of 100 mM HEPES/KOH (pH 7.0, 70°C) containing 7.5 mM dithiothreitol (buffer A) and passed three times through a French pressure cell at 150 MPa. Cell debris and unbroken cells were removed by centrifugation (60 000 x *g*, 30 min at 4°C). For enrichment the resulting crude extracts were diluted 1:1 with buffer A, and subjected to a heat precipitation for 30 minutes at different temperatures. Extracts containing recombinant *T. tenax* and *S.*

solfataricus protein were incubated at the following temperatures: *T. tenax* and *S. solfataricus* KD(P)G aldolase and *T. tenax* GAD at 85°C, *T. tenax* GDH and KDG kinase at 80°C. Extracts containing recombinant *S. solfataricus* GAPN were incubated at 70°C (20 min), and *S. solfataricus* GAD and KDG kinase at 65°C (20 min).

After heat precipitation the samples were cleared by centrifugation (60 000 x *g*, 30 min at 4°C). GAD and KDG kinase of *S. solfataricus* were dialyzed overnight against 50 mM HEPES/KOH (pH 7.0, 70°C), 7.5 mM dithiothreitol (2-liter volume, 4°C) and directly used for enzymatic assays. GAD, KD(P)G aldolase, KDG kinase of *T. tenax* and KD(P)G aldolase and GAPN of *S. solfataricus* were dialyzed overnight (50 mM HEPES/KOH (pH 7.0, 70°C), 7.5 mM dithiothreitol, 300 mM KCl and alternatively for GAD 200 mM KCl) and subjected to gel filtration on HiLoad 26/60 Superdex 200 prep grade pre-equilibrated in the respective buffer. Fractions containing the homogeneous enzyme fraction were pooled and used for enzymatic assays.

2.6.3 Enzyme assays

2.6.3.1 2-keto-3-deoxy-6-(phospho)gluconate (KD(P)G) aldolase

KD(P)G Aldolase activity of *T. tenax* and *S. solfataricus* were measured at 70°C using a modification of the TBA (Thiobarbituric acid) assay .

Thereby, the KD(P)G aldolase assay was performed in 100 mM HEPES/KOH (pH 7.0, 70°C). 5 mM pyruvate, and 2 mM D,L-glyceraldehyde or D,L-glyceraldehyde 3-phosphate (GAP) were added as substrates for the enzyme (6 or 12 µg of *T. tenax* and of *S. solfataricus* protein after gel filtration, respectively; total volume 1 ml). The reaction was incubated in a water bath at 70°C. After 0, 2, 5, 7 and 10 minutes incubation, 100 µl probe was withdrawn in ice and the reaction was stopped by the addition of 10 µl of 12% (w/v) trichloroacetic acid. Precipitated proteins were removed by centrifugation (20 000 x *g*, 15 min at 4°C) and 10 µl of the supernatants were then oxidized by the addition of 125 µl of 25 mM periodic acid/0.25 M H_2SO_4 and incubated at room temperature for 20 minutes. Oxidation was terminated by the addition of 250 µl of 2% (w/v) sodium arsenite in 0.5 M HCl. 1 ml of 0.3% (w/v) TBA was then added and the chromophore was developed by

heating at 100°C for 10 minutes. A sample of the solution was then removed and the colour was intensified by adding to an equal volume of DMSO. The absorbance was read at 549 nm ($\varepsilon_{chromophore}$ = 67.8 x 10^3 $M^{-1}cm^{-1}$). Several controls were performed by omitting either one or both substrates, enzyme or by using heat precipitated cell extract of BL21-CodonPlus(DE3)-RIL pET-15b without insert.

2.6.3.2 Gluconate dehydratase (GAD)

GAD activity (30 and 60 µg of *T. tenax* protein after gel filtration; 840 µg of *S. solfataricus* protein after heat precipitation; total volume 1 ml) was assayed in the presence of 10 mM D-gluconate and D-galactonate by using the TBA assay as described previously (see 2.6.3.1).Several controls were performed by omitting either substrates or enzymes or by using heat precipitated cell extract of BL21-CodonPlus(DE3)-RIL pET-15b without insert.

D-galactonate (10 mM) was prepared from D-galactonate γ-lactone (Sigma-Aldrich) by incubation in 1 M NaOH for 1 hour (4 M stock solution) and subsequent dilution in 50 mM HEPES/KOH (pH 7.0, 70°C) as described previously [LAMBLE et al., 2004].

2.6.3.3 2-keto-3-deoxygluconate (KDG) kinase

The activity of the *T. tenax* and *S. solfataricus* KDG kinase was determined at 70°C and 60°C, respectively, using two different assays. The phosphorylation of KDG by ATP was followed by coupling the formation of KDPG to the reduction of NAD^+ via KD(P)G aldolase and GAPN of *T. tenax* . The standard assay was performed in 100 mM HEPES/KOH (pH 7.0, 70°C) in the presence of KDG kinase (1.5 and 3 µg of *T. tenax* protein after gel filtration; 40 and 80 µg of *S. solfataricus* protein after heat precipitation), 2 mM ATP, 2 mM $MgCl_2$, 10 mM NAD^+, KD(P)G aldolase (3 µg of *T. tenax* enzyme after gel filtration) and GAPN (25 µg of *T. tenax* enzyme, protein fraction after heat precipitation). The reaction was started by addition of KDG kinase. Enzymatic activities were measured by monitoring the increase in absorption at 340 nm ($\varepsilon_{NADH,\ 70°C}$ = 5.8 mM^{-1} cm^{-1}).

In addition the activity of the *T. tenax* and *S. solfataricus* KDG kinase was determined using a discontinuous assay. The phosphorylation of KDG by ATP at 70°C and 60°C, respectively, was followed by coupling the formation of ADP to the oxidation of NADH via pyruvate kinase (rabbit muscle, EC 2.7.1.40) and L-lactate dehydrogenase (rabbit muscle, EC 1.1.1.27). KDG was formed by coupling the reaction to the dehydration of gluconate using gluconate dehydratase from *T. tenax*. The standard assay (1 ml total volume) was performed in 150 mM HEPES/KOH (pH 7.5, 70°C) in the presence of KDG kinase (150 µg of *T. tenax* or 100 µg of *S. solfataricus* protein), 10 mM ATP, 10 mM $MgCl_2$, and gluconate dehydratase (42 µg of *T. tenax* protein). The reaction was started by the addition of 10 mM gluconate. The indicator reaction (1 ml total volume) was performed at room temperature in 150 mM HEPES/KOH (pH 7.5, RT), 3 mM $MgCl_2$, 5 mM phosphoenolpyruvate, 0.5 mM NADH, 25 units of pyruvate kinase, and 90 units of L-lactate dehydrogenase. The indicator reaction was started by addition of 25 µl aliquots from the standard assay. Enzymatic activities were measured by monitoring the increase in absorption at 366 nm ($\varepsilon_{NADH} = 3.4\ mM^{-1}\ cm^{-1}$).

2.6.3.4 Non-phosphorylating glyceraldehyde-3-phosphate dehydrogenase GAPN

GAPN activity from *S. solfataricus* was determined as described previously [FABRY & HENSEL, 1987] in a continuous assay at 70°C. The standard assay for the oxidative reaction was performed in the presence of 90 mM HEPES/KOH, 160 mM KCl (pH 7.0, 70°C; total volume 1 ml), 5 mM DL-GAP, and 2 mM $NADP^+$. The reaction was started by the addition of DL-GAP and the enzyme concentration used was 6 µg of protein after gel filtration/ml assay volume. Enzymatic activities were measured by monitoring the increase in absorption at 340 nm ($\varepsilon_{NADPH,\ 70°C} = 5.7\ mM^{-1}\ cm^{-1}$).

For effector studies, activity was determined in the presence of half-saturating concentrations of $NADP^+$ (100 µM) and DL-GAP (500 µM).

2.6.3.5 Kinetic parameters

Enzyme activity was measured photometrically by determining the velocity of the reaction *v*. One unit of enzyme activity is defined as the enzyme activity catalyzing the conversion of 1 µmol substrate in 1 minute. Therefore, the specific activity is given as the number of units per mg protein according to the following formula:

$$\text{Specific activity (U/mg protein)} = \frac{\Delta E/\text{min} * V_{Total}}{\varepsilon * d * C * V_{Protein}}$$

ΔE/min:	Extension change per unit minute
V_{Total}:	Total volume of the assay (ml)
$V_{Protein}$:	Volume of protein (ml)
ε:	Extinction coefficient
d:	Cuvette thickness (cm)
C:	Protein content (mg protein/ml)

The kinetics parameters (K_M and v_{max}) were determined through the relationship between initial velocity and substrate concentration following the Michealis-Menten equation:

$$v = \frac{v_{max} * [S]}{K_M + [S]}$$

where S is a concentration of substrate, v is the initial velocity of reaction, v_{max} is the saturation velocity and K_M is Michaelis-Menten constant.

For the Michaelis-Menten model three different linearization models were available: Lineweaver-Burk plot (1/v versus 1/S), Eadie-Hostee plot (v versus v/S) and Hanes plot (S/v versus S). K_M and v_{max}, were determined by the linear transformation according to Hanes [HANES, 1932]:

$$\frac{[S]}{v} = [S] * \frac{1}{v_{max}} + \frac{K_M}{v_{max}}$$

The intercept in Hanes plot is K_M / v_{max} and the slope is 1/ v_{max}.

Calculation of the kinetic parameters (K_M and v_{max}) was performed by iterative curve-fitting (Hill equation) using the program Origin (Microcal Software Inc.).

2.6.4 Biocatalytic synthesis of KDG

KDG was synthesized via the KD(P)G aldolase from *T. tenax* as described previously . Briefly, 1 g of D,L-glyceraldehyde and 2.2 g of pyruvate were mixed in 100 ml water containing 6.6 mg of enzyme and the reaction mixture was incubated for 8 hours at 70°C. Protein was removed by acetone precipitation and the reaction mix was separated by Dowex 1 X 8 anion exchange chromatography (Sigma-Aldrich) using a linear 0.0–0.2 M HCl gradient. Fractions containing KDG without glyceraldehyde and pyruvate were identified using the TBA assay, the lactate dehydrogenase assay and thin layer chromatography (TLC). Alternatively, KDG was formed by coupling the reaction to the dehydration of gluconate using gluconate dehydratase from *T. tenax*.

2.6.5 *In vitro* assays with crude extracts

Crude extracts of *T. tenax* and *S. solfataricus* cells grown on glucose were prepared as reported for the recombinant *E. coli* cells (see 2.6.3). After centrifugation the protein solution was dialyzed overnight against 50 mM HEPES/KOH (pH 7.0, 70°C), 7.5 mM dithiothreitol (2-liter volume, 4°C) and directly used for enzymatic assays. Activities in crude extracts (450 or 900 µg of protein; total volume 1 ml) were determined as described for the recombinant proteins (see 2.6.3).

2.6.6 ^{14}C-Labelling experiments and Thin Layer Chromatography (TLC)

KD(P)G aldolase activity from *T. tenax* and *S. solfataricus* was followed by incubation of dialyzed fractions after heat precipitation (*T. tenax* 16 µg and *S. solfataricus* 11 µg of protein) in 100 mM HEPES/KOH (pH 7.0, 70°C) in the presence of 0.3 µCi [2-^{14}C] pyruvate, 50 mM pyruvate and either 20 mM GA or GAP (total volume 30 µl). A sample was withdrawn before and after incubation at 70°C (30 min) and analyzed by TLC plates

(silica gel G-60) without fluorescence indicator (VWR International) developed in butan-1-ol/acetic acid/water (v/v/v = 3/1/1)) and autoradiography (Agfa X-ray 90 films).

Intermediates were identified by their R_f-values determined previously [SIEBERS & HENSEL, 1993] and by the formation of KDG and KDPG using the characterized KDPG aldolase (EDA) of *Thermotoga maritima* . The expression plasmid (pTM-*eda*) was kindly provided by Carol A Fierke (University of Michigan, Ann Arbor, MI, USA). The enzyme of *T. maritima* was enriched by heat precipitation (30 min, 75°C) from the expression host (BL21-CodonPlus(DE3)-RIL).

2.6.7 *In vitro* reconstruction of the ED pathway

For the *in vitro* reconstruction of the ED pathway, the labelled intermediates were followed after addition of the different ED enzymes (GDH (*T. tenax* 13 µg of protein), GAD (*T. tenax* 11 µg of protein), KD(P)G aldolase (*T. tenax* 23 µg of protein), KDG kinase (*T. tenax* 35 µg of protein). The assay was performed in the presence of 0.3 µCi [U-^{14}C] glucose, 100 mM HEPES/KOH (pH 7.0, 70°C), 10 mM glucose, and 5 mM $NADP^+$. 10 mM ATP and 10 mM Mg^{2+} were added in the presence of KDG kinase. Samples (30 µl total volume) were incubated for 10, 30 and 60 minutes at 70°C and the labelling was followed by TLC as described previously (see 2.6.6).

2.6.8 Analytical protein methods

2.6.8.1 Protein quantification

Protein concentration was determined using the Bio-Rad Protein Assay based on the method of Bradford [BRADFORD, 1976], following the manufacturer's instructions with bovine serum albumin (BSA) as standard (2–10 µg/ml).

2.6.8.2 SDS-Polyacrylamide gel electrophoresis (SDS-PAGE)

For protein analysis and separation, SDS polyacrylamide gel electrophoresis was used according to Laemmli [LAEMMLI, 1970], Proteins react and denaturate in the presence of sodium dodecylsulfate (SDS) and form negatively charged complexes. The negatively

charged proteins are finally separated on the bases of differences in charges and sizes by electrophoresis through the polyacrylamide gel. The percentage of acrylamide is based on the molecular weight range of proteins to be separated. For proteins with a molecular weight range 20–300 kDa, 10–12% SDS-polyacrylamide gels were used.

Therefore, the stacking gel with 4.0% w/v acrylamide-bisacrylamide (30%), 125 mM Tris (pH 6.8, RT), 0.1% w/v SDS, 0.45% w/v APS (100 mg/ml), 0.15% v/v TEMED, and separation gel with 10% w/v Acrylamide-Bisacrylamide (30%), 375 mM Tris (pH 8.8, RT), 0.1% w/v SDS, 0.67% w/v APS (100 mg/ml), 0.067% v/v TEMED were prepared. Separating gel ingredients were mixed and then poured in the gel casting chamber. The separation gel was covered with n-butanol, and allowed to polymerize for 20 min. After n-butanol was removed, gel surfaces were washed with A. bidest and dried with Whatman paper before pouring the stacking gel solution. Directly after pouring the stacking gel, a comb which was removed after polymerization of the stacking gel for approximately 20 minutes comb was removed and gels were stored at 4°C before usage.

The protein sample was mixed with 2–5 x loading buffer (final concentration: 62.5 mM Tris-HCl, pH 6.8, 10% glycerin, 2% SDS, 5% β-mercaptoethanol, 0.005% bromphenol blue) and then heated for 2–3 minutes at 94°C. Gels were run in Minigel-Twin-Chamber (Biometra) at 10–18 mA. The electrophoresis buffer (anode and cathode buffer) consisted of 25 mM Tris-HCl, 190 mM glycine and 0.1% v/v SDS (pH 8.3). As standard, DALTON MARK VII-L Standard Mixture (SDS-7) (Sigma-Aldrich) was used with a molecular weight range of 14.2–66.0 kDa (standards: α-Lactalbumin albumin bovine milk 14.2 kDa, Trypsin Inhibitor, soybean 20.1 kDa, trypsinogen, bovine pancreas 24.0 kDa, carbonic anhydrase, bovine 29.0 kDa, glyceraldehyde-3-phosphate dehydrogenase, rabbit muscle 36.0 kDa, egg 45.0 kDa and albumin, bovine 66.0 kDa). Proteins were visualized by gel staining (40% methanol, 10% acetic acid and 0.25% coomassie brilliant blue R-250) and destaining (5% methanol and 7.5% acetic acid) [WEBER & OSBORN, 1969]. SDS gels were analyzed using the Chemi Doc System (BioRad) in combination with the Quantity One Software Package (BioRad).

2.6.8.3 Molecular mass determination

The native molecular mass was determined by gel filtration chromatography using a HiLoad 26/60 Superdex 200 prep grade column (Amersham Biosciences) connected with FPLC-BioLogic DuoFlow Pathfinder 20 system (Bio-Rad Laboratories) and pre-equilibrated with HEPES buffer (50 mM HEPES/KOH, 7.5 mM dithiothreitol, 300 mM KCl, pH 7.0, 70°C). As standard calibration proteins ferritin (horse spleen, MW 443.000 1 mg), alcohol dehydrogenase (yeast, MW 148.000 1.25 mg), D-lactate dehydrogenase (*Lactobacillus leichmanii*, MW 78.000 0.118 mg) and cytochrome C (bovine heart, MW 15.500 2 mg) (Sigma-Aldrich) were used and the activity was followed photometrically:

Ferritin:	Absorption at 217 nm
Alcohol dehydrogenase:	Enzyme activity, continuous assay at 366 nm (RT) in 0.1 M Tris-HCl, pH 7.0; 0.4 mM NADH; 2 mM acetaldehyde
D-Lactate dehydrogenase:	Enzyme activity, continuous assay at 366 nm (RT) in 0.1 M Tris-HCl, pH 7.0; 0.4 mM NADH; 2 mM pyruvate
Cytochrome C:	Absorption at 416 nm

3. RESULTS

On the basis of biochemical studies using crude extracts as well as characterization of key enzymes it has been proposed that hyperthermophilic Archaea utilize the non-phosphorylative ED pathway for glucose degradation [SIEBERS et at., 2004; DE ROSA et al., 1984; BUDGEN & DANSON, 1986; SIEBERS & HENSEL, 1993; SELIG & SCHÖNHEIT, 1994; SIEBERS et al., 1997; SELIG et al., 1997]. However, using a comparative genomics approach a conserved ED cluster was detected in the genomes of *T. tenax* [SIEBERS et at., 2004], *S. solfataricus*, and *S. tokodaii S. acidocaldarius* that resembles the cluster present in *Halobacterium* sp. NRC1 (Fig 5). According to the functional organization candidates for: i) a putative gluconate dehydratase (*gad* gene), ii) a 2-keto-3-deoxy-gluconate aldolase (*kdgA* gene), iii) a sugar (KDG) kinase and iv) in *S. solfataricus* a non-phosphorylating glyceraldehyde-3-phosphate dehydrogenase (GAPN, *gapN* gene) were predicted.

FIGURE 5: ENTNER-DOUDOROFF GENE CLUSTERS IN ARCHAEA IDENTIFIED BY CONSERVED GENOME CONTEXT ANALYSIS.

Schematical representation of the conserved gene clusters in archaeal genomes comprising key genes of the semi-phosphorylative ED pathway. The genes are indicated by their systematic gene name, except for *T. tenax* the accession number is displayed, and orthologous genes are shaded in the same greyscale. Genes are not drawn to scale.

3.1 SEQUENCE ANALYSIS AND GENE CONTEXT

In *T. tenax* and *S. solfataricus*, an ED gene cluster was predicted which comprises genes encoding gluconate dehydratase (GAD, *gad* gene), 2-keto-3-deoxy-6-(phospho)gluconate aldolase (KD(P)G aldolase, *kdgA* gene), 2-keto-3-deoxy-6-gluconate kinase (KDG kinase, *kdgK* gene) and glucan-1,4-α-glucosidase (*gaa* gene) in addition to a non-phosphorylating glyceraldehyde-3-phosphate dehydrogenase (GAPN, *gapN* gene) in the *S. solfataricus* genome.

As shown in Figure 6, the ED gene cluster of *T. tenax* is organized in a divergon structure in which the *gad* gene is separated from the rest of the *kdgA-kdgK-gaa* gene cluster by 67 basepairs. The three genes (*kdgA*, *kdgK*, *gaa*) of *T. tenax* overlap by 4 basepairs (the coding regions by 1 bp). In contrast to the *T. tenax* gene cluster, all four genes in *S. solfataricus* are oriented in the same direction and the *gad*, *kdgA*, *kdgK*, and *gapN* genes are separated by 2, 9, and 39 bp, respectively. In *T. tenax* putative promoter structures (TATA box and BRE site) were only identified upstream of the *kdgA* gene indicating that these genes form an operon [SIEBERS et al., 2004], while in *S. solfataricus* putative promoter sequences were only identified in front of the *gad* and *gapN* gene suggesting a polycistronic transcript of the *gad-kdgA-kdgK* genes and a single transcript of the *gapN* gene (Fig 7).

(A)

```
1     AAATGCCGGCGTCAACGGAATGGGAAAAGGGAGCTACGAGATTTCAACGCCAAGTTCCTCTAACGACCCACACCGGCTCCTCTCCCACCG
                                                  *  R  W  T  G  R  V  V  W  V  P  E  E  G  V
91    GGATCTCCGACGGCTCTGCTCTGTATTTTTCCAGAACTCTCTCGTTCACCGCTACGCCTATGCCTGGCCCCCTCGGCACCTCCACGGAGC
      P  I  E  S  P  E  A  R  Y  K  E  L  V  R  E  N  V  A  V  G  I  G  P  G  R  P  V  E  V  S
181   TCTGGGACAGCCGGAAGGGATCGCCTATTAGGTCCCTCTTCCACTGCGGCCAGTAGTCGTAGAAGGACTCCAATCTATACAGAGTGGGCG
      S  Q  S  L  R  F  P  D  G  I  L  D  R  K  W  Q  P  W  Y  D  Y  F  S  E  L  R  Y  L  T  P
271   TTACGGCGGACAGTTGCACCTCCAAGGCGAATTGAACGGGGCCGTAGGCGTTGTGGTAGGAGACCTCGACGCTGAAGGCCTCGGCCAGCG
      T  V  A  S  L  Q  V  E  L  A  F  Q  V  P  G  Y  A  N  H  Y  S  V  E  V  S  F  A  E  A  L
361   CAGCCACCTTCATACTGCCGGTTACTCCGCCTATGTTGCACGCATCGGGCTGGATCACGTCCACGAGGCCCTCCACGAGATACTGGAGAG
      A  A  V  K  M  S  G  T  V  G  G  I  N  C  A  D  P  Q  I  V  D  V  L  G  E  V  L  Y  Q  L
451   CCTCCTTGGCGCTGATGAGCCTCTCACCCATTGCGATCCTCGCGGACGTGAGGGATCTATATTTGCGGTAGCCCTCGATGTCTTCGTGGT
      A  E  K  A  S  I  L  R  E  G  M  A  I  R  A  S  T  L  S  R  Y  K  R  Y  G  E  I  D  E  H
541   GGAGCGGCTCCTCCATGAAGTAGGGTCTGTACGGCTCAAACCTCTTGGCTATCTCCACAGCCGCGTTGGCGTTGAACCTCCCGTGGTGTT
      H  L  P  E  E  M  F  Y  P  R  Y  P  E  F  R  K  A  I  E  V  A  A  N  A  N  F  R  G  H  H
631   CTATTAGGATATCCACGTCGTCGCCTACGGCGTCTCTGACTGCGGCCACTGCCTCCTCAGCGCGTCTGAGCTCCTCAGAGGTTATAGAGT
      E  I  L  I  D  V  D  D  G  V  A  D  R  V  A  A  V  A  E  E  A  R  R  L  E  E  S  T  I  S
721   TGAAGCTGGGACCGAAGGGGTCGAACTTGAGCGCATCGTAGCCCCTCGCGACGACCTCCTTCGCCTTCTCTGCGAAGCACTGGGGGTCTC
      N  F  S  P  G  F  P  D  F  K  L  A  D  Y  G  R  A  V  V  E  K  A  K  E  A  F  C  Q  P  D
811   TACATCCTCCGTACCAACCGTTGGCGTAGACCTTGACTCTGTCCCTCAACTTCCCCCCCAGTAGCTCGTACAACGGGGCCCCCAACTCCC
      R  C  G  G  Y  W  G  N  A  Y  V  K  V  R  D  R  L  K  G  G  L  L  E  Y  L  P  A  G  L  E
901   TCGCCTTTAGGTCCCATAGAGCCATGTCTATCGCGCTCAGGGCCGTCGCGCTCTCGAAGGAGCGGGATAGAAAGAAGTCTTGTCTATACC
      R  A  K  L  D  W  L  A  M  D  I  A  S  L  A  T  A  S  E  F  S  R  S  L  F  F  D  Q  R  Y
991   ACTCGTAGAAAGCCGCCGATATCTCGTGCGGATCCCTCCCCAGAAAGGCTCTGGCAGTCTGCCTTACGGCGGACACCACGGGCAATATCC
      W  E  Y  F  A  A  S  I  E  H  P  D  R  G  L  F  A  R  A  T  Q  R  V  A  S  V  V  P  L  I
1081  TCAAGGTGGGCACCGCTTCGCCGTATGAGACCCTCCCGTCGGAGGTCACCACTCTGACCAGGATTGAGTAGGACGCCCAGCGCGCGTCCG
      R  L  T  P  V  A  E  G  Y  S  V  R  G  D  S  T  V  V  R  V  L  I  S  Y  S  A  W  R  A  D
1171  TCTCTTGTTCATAGAGGACTATGGGCTCTATCTCTTTTATGGTTGCCATATACTGATTGAGCCATCCCTTAATACCTTTTCGTGCTAACT
      T  E  Q  E  Y  L  V  I  P  E  I  E  K  I  T  A  M
1261  TTTTAAGGGCGCCCCGAGTACTATCTATGGAGATTGTGGCGCCAGTCATAACCACCTTTAGGGGCGGGAGGCTGGACCCAGAGCTTTTCG
                                M  E  I  V  A  P  V  I  T  T  F  R  G  G  R  L  D  P  E  L  F  A
```

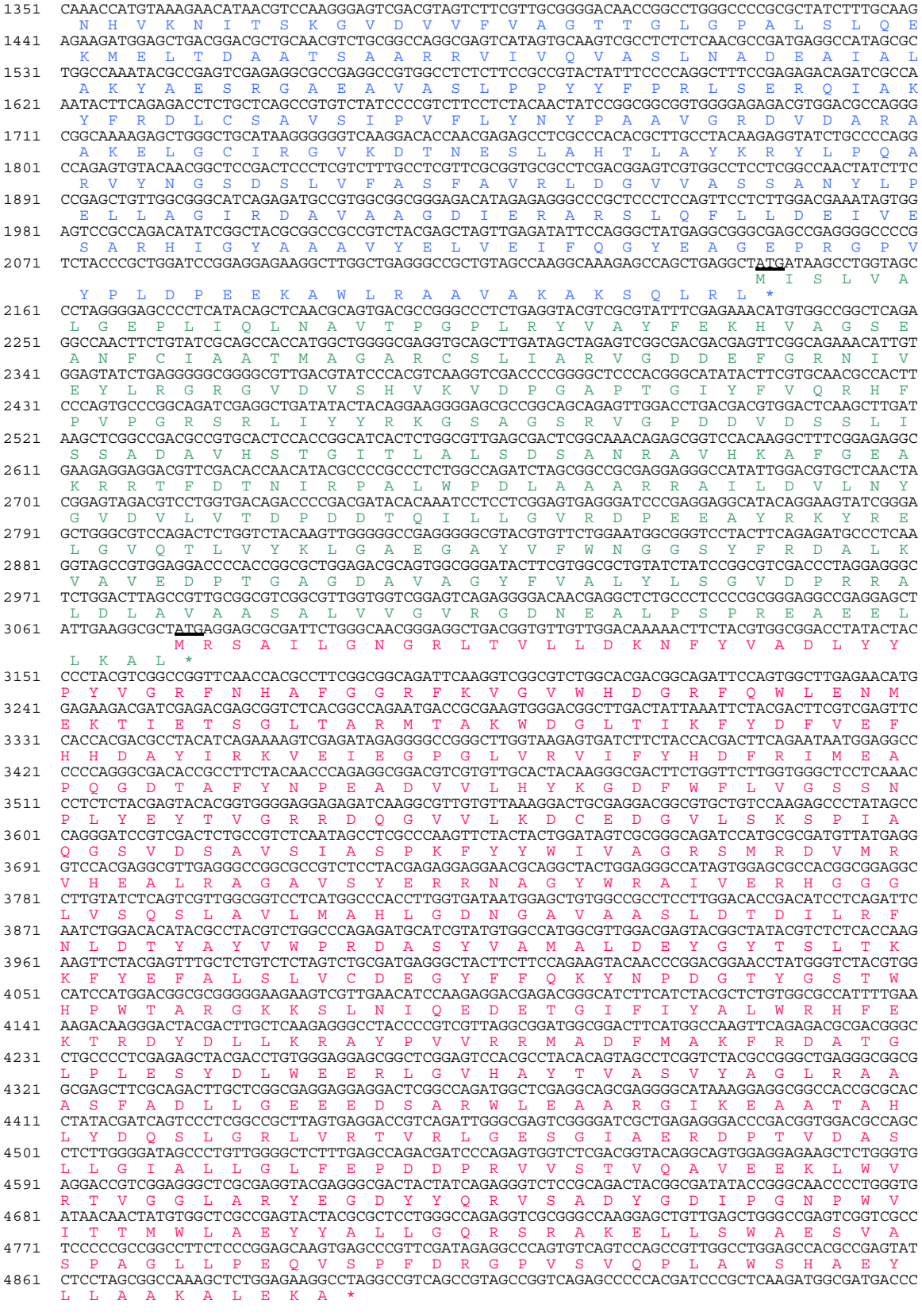

(B)

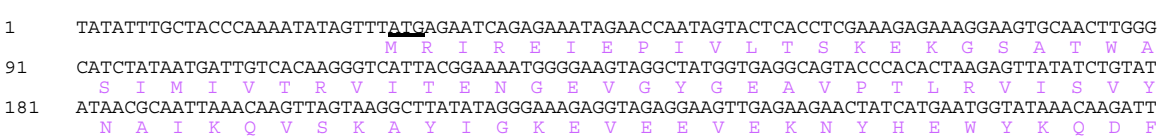

```
        N  K  I  R  K  L  Q  R  F  L  E  V  G  A  I  Y  I  N  D  Y  P  R  H  G  I  G  Y  F  P  F
4501    TGGCGGAAGGAAGGATTCTGGAATTGGCAGAGAGGGGATTGGGTATACAATTCAATATGTAACAGCTTACAAATCAATAGTCTATAATTA
        G  G  R  K  D  S  G  I  G  R  E  G  I  G  Y  T  I  Q  Y  V  T  A  Y  K  S  I  V  Y  N  Y
4591    TAAAGGGAAAGGTATTTGGGAATACTTGTAATTTTTTAATTATAGCTTATAGGGAAGTAAAACATAAATATTAATTAAGTTGGTGTGGTT
        K  G  K  G  I  W  E  Y  L  *
```

FIGURE 6: NUCLEOTIDE SEQUENCE OF THE ED GENE CLUSTER IN *T. TENAX* AND *S. SOLFATARICUS*.
(**A**) The ED gene cluster was identified in the course of the *T. tenax* genome sequencing project and comprises genes coding for a gluconate dehydratase (*gad* gene) (violet), 2-keto-3-deoxy-6-(phospho)gluconate aldolase (*kdgA* gene) (blue), 2-keto-3-deoxy-6-gluconate kinase (*kdgK* gene) (green) and glucan-1,4-α-glucosidase (*gaa* gene) (red). **(B)** In *S. solfataricus,* the ED gene cluster comprises genes coding for a gluconate dehydratase (*gad* gene) (violet), KDG aldolase (*kdgA* gene) (blue), KDG kinase (*kdgK* gene) (green) and GAPN (*gapN* gene) (red). Start codons (bold) are underlined and stop codons are marked as asterisk.

FIGURE 7: IDENTIFICATION OF PUTATIVE PROMOTER STRUCTURES OF THE ED GENES OF *T. TENAX* AND *S. SOLFATARICUS*.
Upstream nucleotide sequences of the *T. tenax* and *S. solfataricus* ED genes. The putative transcription factor B responsive elements (BRE site) (underlined), the TATA box promoter elements (boxed), the start codon (bold) and the mapped transcription start (arrowheads) are marked.

3.2 PRIMER EXTENSION ANALYSIS

For a more accurate assignment of the promoter region, the transcription starts of the *gad* and *kdgA-kdgK-gaa* mRNA from *T. tenax* and the transcription starts of the *gad-kdgA-kdgK* and *gapN* mRNA of *S. solfataricus* were determined by primer extension analysis (Fig 8). No obvious promoter structures in front of internal genes in the ED operon (*kdgK* and *gaa* genes in *T. tenax* and *kdgA* and *kdgK* genes in *S. solfataricus*) were observed

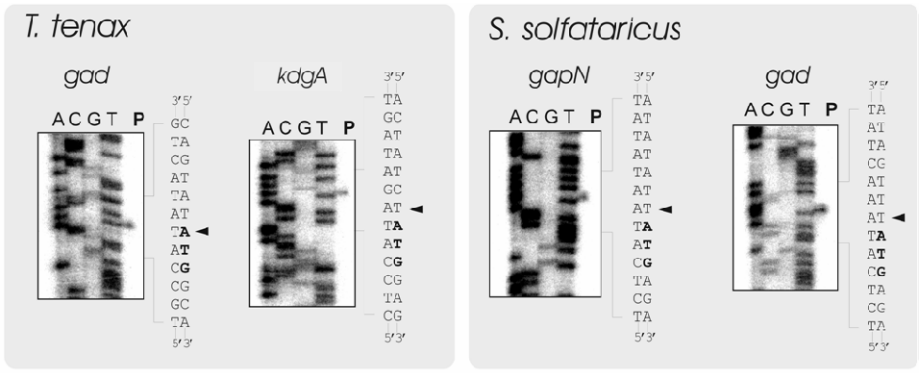

FIGURE 8: MAPPING OF TRANSCRIPTION START SITES OF THE *gad* GENE AND THE *kdgA-kdgK-gaa* OPERON OF *T. TENAX* AND OF THE *gapN* GENE AND THE *gad-kdgA-kdgK* OPERON OF *S. SOLFATARICUS*. The transcripts start sites are indicated (arrowheads) and the start codon is marked bold. The sequence ladder (lanes A, C, G, and T) and the primer extension product (lane P) is shown. cDNA synthesis was performed with 30 µg of total RNA isolated from *T. tenax* and *S. solfataricus* cells grown on glucose.

3.2.1 Northern Blot analysis

To confirm the proposed co-transcription of the ED genes in *T. tenax*, Northern Blot analysis was performed with total RNA isolated from heterotrophically (glucose) grown cells. Specific Digoxigenin-labelled antisense mRNA probes for the *kdgA* and *kdgK* gene were obtained by *in vitro* transcription from the T7 promoter of vector pSPT19.

A part of the *kdgA* gene (362 bp, position: 238-600) and *kdgK* gene (360 bp, position 319-631) was cloned into the *Eco*RI and *Bam*HI restriction sites of the pSPT 19 vector by PCR mutagenesis. The nucleotide sequences of both antisense mRNA probes and the primers set used for PCR mutagenesis (Table 1) for the *kdgA* and *kdgK* gene are shown in (Fig 9).

For both probes one hybridization signal was observed at 3.6 kb (*kdgA-kdgK-gaa*) and 1.8 kb (*kdgA-kdgK*). Additional probe specific signals were identified for the *kdgK*-probe (2.7 kb (*kdgK-gaa*) and 0.9 kb (*kdgK*)) and for the *kdgA*-probe (0.9 kb (*kdgA*)), thus indicating the presence of tri-, bi- and monocistronic transcripts. An additional unspecific signal was observed for the *kdgK*-probe at 0.4 kb (Fig 10). Searching the sequence of the *T. tenax* genome revealed no other gene with similarity to the *kdgK* gene. Therefore, it cannot be rouled out if that is due to degradation.

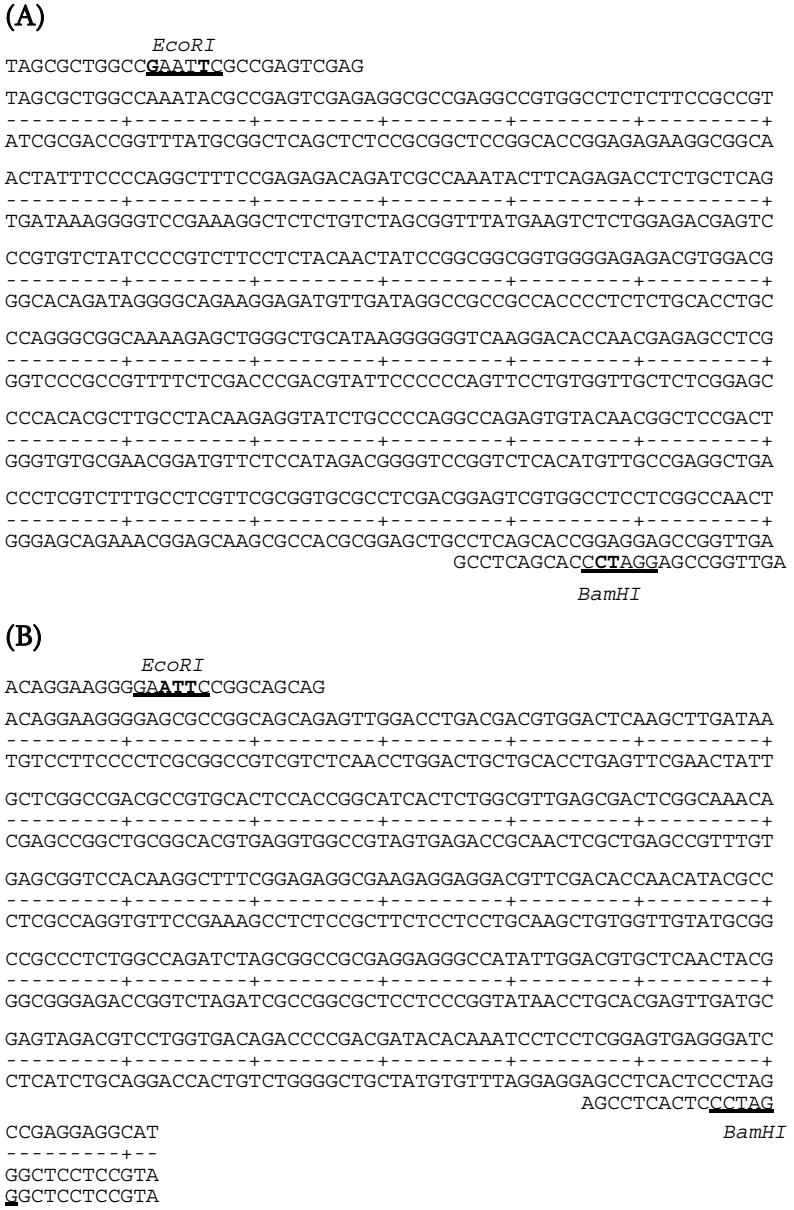

FIGURE 9: NUCLEOTIDE SEQUENCES OF ANTISENSE mRNA PROBES.

The *kdgA* **(A)** and *kdgK* **(B)** digoxigenin-labelled antisense mRNA probes were prepared by *in vitro* transcription from the T7 promoter of the pSPT 19 vector using the DIG RNA Labelling Kit (SP6/T7). The introduced mutations are shown in boldface and the restriction sites are underlined.

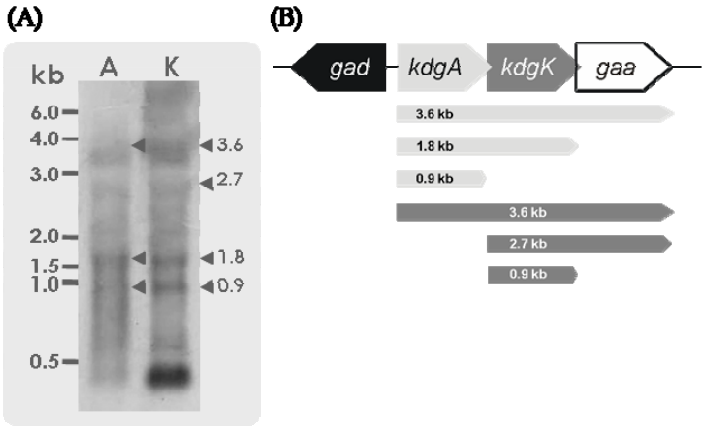

FIGURE 10: NORTHERN BLOT ANALYSIS OF THE *kdgA-kdgK-gaa* OPERON.
(A) Transcript analysis were performed with 5 µg of total RNA from heterotrophically grown cells and digoxigenin-labeled, *kdgA*- **"A"** (KDG aldolase) and *kdgK*-specific antisense mRNAs **"K"** (KDG kinase). The RNA molecular size standard (left) and the derived transcript size (arrows, right) are shown. **(B)** Schematical representation of the identified mono- bi- and tricistronic transcripts using the both *kdgA*- and *kdgK*-specific antisense mRNA probe.

3.3 HETEROLOGOUS EXPRESSION OF THE *T. TENAX* AND *S. SOLFATARICUS* ED PROTEINS IN *E. COLI*

The *gdh*, *gad*, *kdgA*, and *kdgK* genes of *T. tenax* were cloned into the pET expression system and expressed in *E. coli* BL21-CodonPlus(DE3)-RIL (see 2.4.7). The cloning of the *gad*, *kdgA*, *kdgK*, and *gapN* genes of *S. solfataricus* were carried out (A. Geerling and T. Ettema in the laboratory of Microbiology, Wageningen University, The Netherlands) (see 2.4.7).

The identified ED genes in the ED cluster from *T. tenax* (Fig 6A) and *S. solfataricus* (Fig 6B) were amplified by PCR mutagenesis using primer sets (Table 1). In *T. tenax*, genomic DNA was used as a template (parameters: 2 min 94°C; 30 cycle: 45 sec 94°C, 45 sec primer annealing, 1 min 72°C; 7 min 72°C). The following annealing temperature was used for the different amplified genes; 61.5°C *gad*; 65.9°C *kdgA*, 60.7°C *kdgK*. For recombinant expression the amplified *gad* (1200 bp) and *kdgA* (908 bp) genes were cloned into pET-15b and the *kdgK* gene (932 bp) was cloned in pET-24a.

Amplification of the *S. solfataricus* genes was carried out (A. Geerling and T. Ettema in the laboratory of Microbiology, Wageningen University, The Netherlands).

The recombinant enzymes were enriched from crude extracts by heat precipitation at different temperatures. Extracts containing recombinant *T. tenax* and *S. solfataricus* protein were incubated at the following temperatures: *T. tenax* and *S. solfataricus* KD(P)G aldolase and *T. tenax* GAD at 85°C (30 min), *T. tenax* GDH and KDG kinase at 80°C (30 min). Extracts containing recombinant *S. solfataricus* GAPN were incubated at 70°C (30 min), and *S. solfataricus* GAD and KDG kinase at 65°C (30 min).

3.4 ENZYMES ENRICHMENT AND PURIFICATION

Expression of *S. solfataricus* GAD and KDG kinase was rather poor (fig 11), as only little recombinant protein was observed in the soluble fraction. In addition, unlike the native enzyme [LAMBLE et al., 2004; KIM & LEE, 2005], the recombinant *S. solfataricus* GAD appeared to be relatively instable, not allowing the heat precipitation step to be performed above 65°C. Attempts to improve the poor recombinant expression by the use of different expression hosts (BL21 (DE3), BL21-CodonPlus(DE3)-RIL, JM109 (DE3), ROSETTA) and different suspension buffers were not successful.

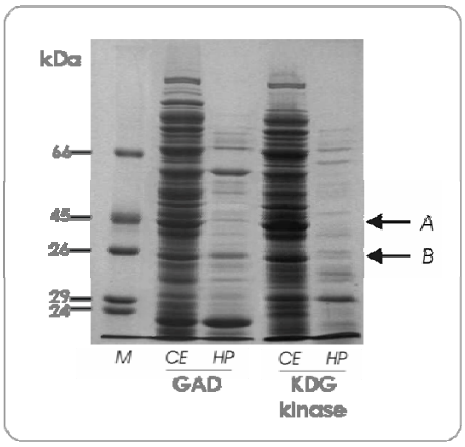

FIGURE 11: SDS-PAGE OF RECOMBINANT EXPRESSION OF *S. SOLFATARICUS* GAD AND KDG KINASE. Arrows indicate the recombinant GAD **(A)** and KDG kinase **(B)**. Lanes containing crude cell extracts (*CE*) and soluble fractions after heat precipitation (*HP*). (*M*) corresponds with the protein marker, Dalton Mark VII-L.

All expressed enzymes with the exception of the *S. solfataricus* GAD and KDG kinase exhibited a good expression and sufficient enrichment was observed from SDS-PAGE (Fig 11 and 12). The molecular masses approximately corresponds to the calculated

mass for *T. tenax* GAD (43/44.033 kDa), *S. solfataricus* GAD (45/44.729 kDa), *T. tenax* KDG kinase (32/33.308 kDa) and *S. solfataricus* KDG kinase (35/34.875 kDa) whereas some deviation was observed for *T. tenax* KD(P)G aldolase (26/30.982 kDa), *S. solfataricus* KD(P)G aldolase (30/33.108 kDa) and *S. solfataricus* GAPN (54/56.927 kDa) (apparent/calculated molecular mass given in parenthesis). However, these differences of 3-5 kDa are in good agreement with generally observed minor deviations.

For further biochemical studies, the recombinant proteins from *T. tenax* and *S. solfataricus* were purified to apparent homogeneity from crude extracts. Cells (7.5 g wet weight) were suspended in 15 ml of 100 mM HEPES/KOH (pH 7.0, 70°C) containing 7.5 mM dithiothreitol and passed through a French pressure cell. Cell debris and unbroken cells were removed by ultracentrifugation in order to gain a cell-free crude extract. The crude extracts were subjected to heat precipitation at different temperatures for 30 minutes (see 3.3). Due to the heat precipitation at 65, 85°C (30min) and the high assay temperature at 70°C, the activity of residual contaminant *E. coli* proteins was very unlikely and was further diminished by analysis of a heat precipitated extract of the expression host with plasmid without insert.

Further purification of the recombinant GAD, KD(P)G aldolase and KDG kinase from *T. tenax* as well as KD(P)G aldolase and GAPN from *S. solfataricus* was achieved by gel filtration. After dialysis overnight (50 mM HEPES/KOH (pH 7.0, 70°C), 7.5 mM dithiothreitol, 300 mM KCl or 200 mM KCl for *T. tenax* GAD due to the inhibition of the enzyme by high salt concentrations), recombinant proteins were subjected to gel filtration on HiLoad 26/60 Superdex 200 prep grade column pre-equilibrated in the respective buffer. For the *T. tenax* GAD two protein bands were enriched after gel filtration, however, both proteins exhibited different elution profiles after gel filtration without salt and the upper band was clearly associated to catalytic GAD activity. Fractions containing the enriched enzyme fractions were pooled and used for enzymatic studies (Fig 12A).

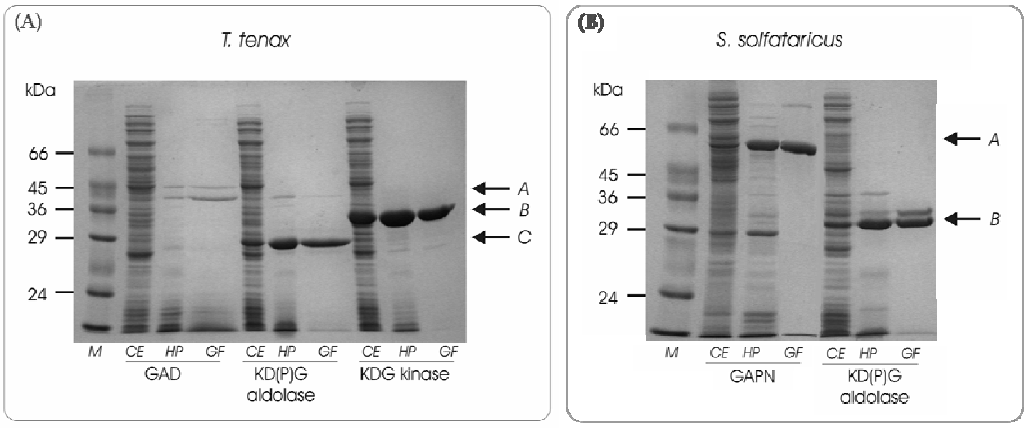

FIGURE 12: SDS-PAGE OF RECOMBINANT EXPRESSION AND PURIFICATION OF *T. TENAX* AND *S. SOLFATARICUS* ED PROTEINS.
(A) SDS-PAGE of recombinant expression and purification of *T. tenax* GAD, KD(P)G aldolase and KDG kinase. Arrows indicate the purified recombinant GAD (A), KDG kinase (B) and KD(P)G aldolase (C). **(B)** SDS-PAGE of recombinant expression and purification of *S. solfataricus* KD(P)G aldolase and GAPN. Arrows indicate the purified recombinant GAPN (A) and KD(P)G aldolase (B). Lanes containing crude cell extracts (*CE*), soluble fractions after heat precipitation (*HP*) and gel filtration (*GF*) were loaded with 20, 10 and 5 µg of protein, respectively. 'M' protein marker, Dalton Mark VII-L (Sigma)).

3.5 BIOCHEMICAL CHARACTERIZATION

3.5.1 Catalytic and kinetic parameters

3.5.1.1 Glucose dehydrogenase

The *T. tenax* glucose dehydrogenase (GDH) catalyzes the oxidation of glucose yielding gluconate. The gene was unequivocally identified by the previously determined N-terminal sequence of the GDH isolated and characterized from *T. tenax* cells [SIEBERS et al., 1997] and confirmed by the activity of the recombinant protein. The enzyme was used for the *in vitro* reconstruction of the pathway.

3.5.1.2 KD(P)G aldolase

In contrast to previous reports for the *S. solfataricus* KDG aldolase [LAMBLE et al., 2003; HENDRY et al., 2000; BUCHANAN et al., 1999], enzymatic characterization revealed a bifunctional enzyme activity. KD(P)G aldolase catalyzes the reversible cleavage of 2-keto-3-deoxygluconate (KDG) as well as 2-keto-3-deoxy-6-phosphogluconate (KDPG) yielding pyruvate and glyceraldehyde (GA) or pyruvate and glyceraldehyde-3-phosphate (GAP), thus representing a true KD(P)G aldolase:

2-keto-3-deoxygluconate (KDG)/ 2-keto-3-deoxy-6-phosphogluconate (KDPG)	⟷	Pyruvate + Glyceraldehyde (GA)/ Pyruvate + Glyceraldehyde-3-phosphate (GAP)

The *T. tenax* and *S. solfataricus* KD(P)G aldolase activity was assayed in the anabolic direction of KDG or KDPG formation from C-3 substrates (condensation reaction) using the discontinuous Thiobarbituric acid (TBA) assay. Activity was observed not only with GA but also with GAP. The time-dependent formation of KDG and KDPG was monitored after incubation for 0, 2, 5, 7 and 10 minutes at 70°C. Only in the presence of the *T. tenax* or *S. solfataricus* enzyme and either pyruvate and GA or pyruvate and GAP as substrate, KDG and KDPG, respectively, formation was observed (Fig 13).

The observed activity was found to be proportional to the amount of recombinant protein, as shown for GA (12.6 ±0.5 mU/ 6 µg, 24.6 ±1.3 mU/ 12 µg) and GAP (66.9 ±2.7 mU/ 6 µg, 141.3 ±6.4 mU/ 12 µg) for *T. tenax* and for GA (13.1 ±1.5 mU/ 6 µg, 23.3 ±1.5 mU/ 12 µg) and GAP (31.8 ±5.1 mU/ 6 µg, 66.7 ±4.3 mU/ 12 µg) for *S. solfataricus*. The negative controls without protein, only one substrate, and cell-free extract of expression host with empty vector revealed no activity (Fig 13).

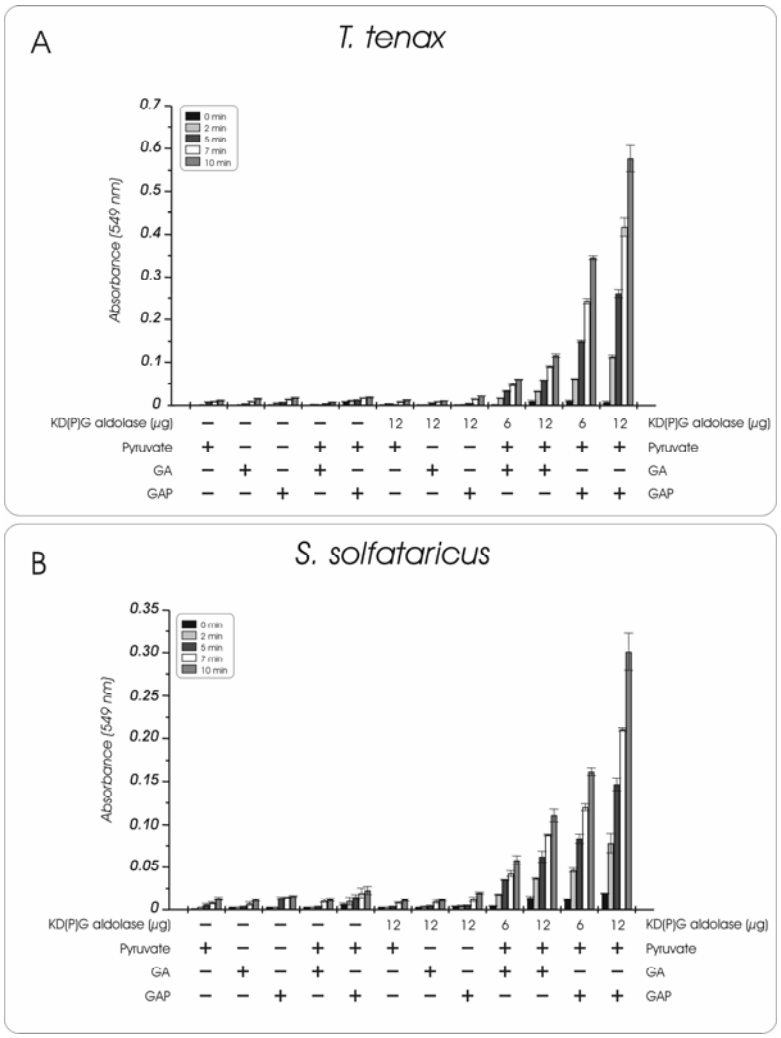

FIGURE 13: KD(P)G ALDOLASE ACTIVITY OF *T. TENAX* (A) AND *S. SOLFATARICUS* (B).
The formation of KDG and KDPG from pyruvate (5 mM) and glyceraldehyde (GA) or glyceraldehyde 3-phosphate (GAP) (2 mM), respectively, was monitored at 70°C using the discontinuous thiobarbituric acid (TBA) assay. The dependence on the amount of protein (6 and 12 µg protein, fraction after gel filtration) and controls with one (GA, GAP, pyruvate) or both (pyruvate and GA or GAP, respectively) substrates without enzyme, and with one substrate (GA, GAP or pyruvate, respectively) in the presence of enzyme are shown. For each sample three independent measurements were performed and the experimental error is given. In the presence of KD(P)G aldolase the formation of KDG from GA and pyruvate as well as KDPG from GAP and pyruvate was observed. The activity with non-phosphorylated and phosphorylated substrates is proportional to the amount of enzyme used in the assay.

In order to confirm these results, enzymes were assayed in the presence of ^{14}C-labelled pyruvate, the products were separated by thin layer chromatography (TLC) and afterwards monitored by autoradiography (Fig 14). In agreement with the aforementioned enzyme assays, the formation of both labelled products was observed: KDG from GA and pyruvate, or KDPG from GAP and pyruvate. No product formation was observed in the

controls without protein, with protein and only one substrate (pyruvate) and with cell-free extract of the host BL21 (DE3) with plasmid pET-15b without insert after heat precipitation. As an additional control the characterized KDPG aldolase (EDA) of the anaerobic, hyperthermophilic bacterium *T. maritima*, which was reported for activity on phosphorylated and non-phosphorylated substrates [GRIFFITHS et al., 2002] was used. In accordance to the *T. tenax* KD(P)G aldolase, KDG and KDPG formation was observed (Fig 14). Different bands of pyruvate were observed which are probably caused by the instability of aqueous solution of pyruvic acid, sodium salt due to intramolecular and intermolecular aldol type condensations as indicated by the manufacturer. The observed change in the pattern of the labelled pyruvate (second spot) was obviously due to the presence of GAP alone, as shown by the controls without KD(P)G aldolase and BL21 (DE3) extract.

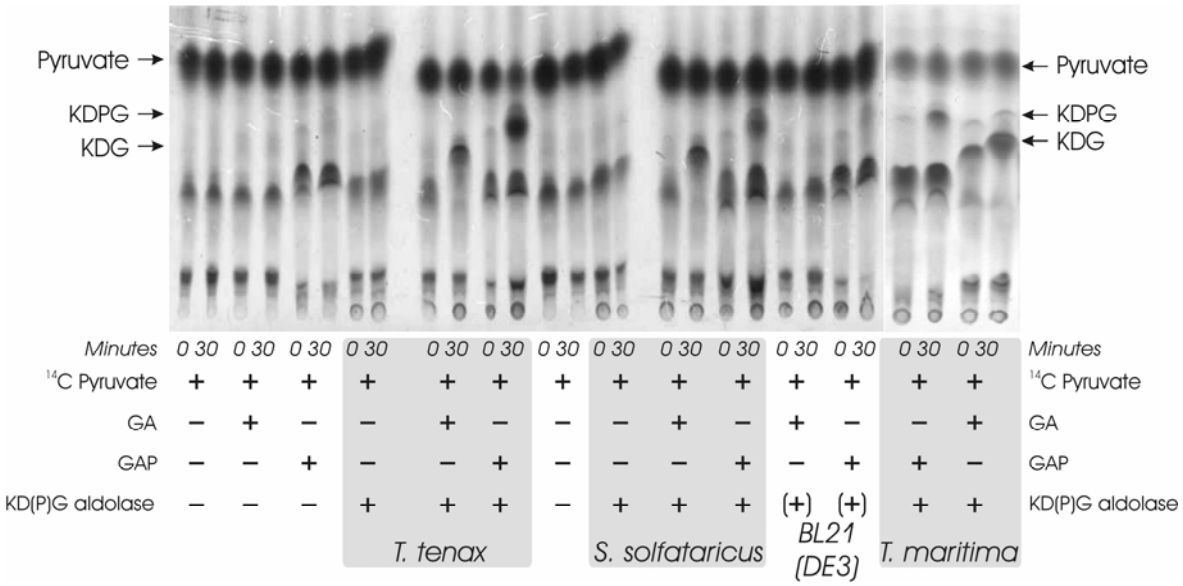

FIGURE 14: DETECTION OF ^{14}C-LABELLED KDG AND KDPG VIA THIN LAYER CHROMATOGRAPHY AND AUTORADIOGRAPHY.

The KD(P)G aldolases of *T. tenax* and *S. solfataricus* (fraction after heat precipitation) were incubated at 70 °C in the presence of labelled pyruvate ([2-^{14}C]pyruvate) and either glyceraldehyde (GA) or glyceraldehydes 3-phosphate (GAP). Control samples containing different combinations of KD(P)G aldolase and substrates are shown as indicated. In addition, control samples of the expression host BL21(DE3) with pET-15b without insert after heat precipitation, indicated as (+), and formation of ^{14}C-labelled KDG and KDPG by the KDPG aldolase (EDA) of *Thermotoga maritima* (fraction after heat precipitation) [GRIFFITHS et al., 2002] are shown. The formation of ^{14}C-labelled KDG and KDPG was followed via thin layer chromatography and visualized using autoradiography. As for the KDPG aldolase of *T. maritima* the formation of both, KDG (from GA and pyruvate) and KDPG (from GAP and pyruvate) is observed in the presence of the KD(P)G aldolase of *T. tenax* or *S. solfataricus*.

3.5.1.3 Gluconate dehydratase

Gluconate dehydratase (GAD) catalyzes the dehydration of gluconate yielding 2-keto-3-deoxygluconate (KDG):

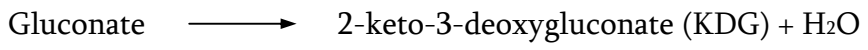

The *T. tenax* GAD was assayed by monitoring KDG formation using the discontinuous TBA assay (70°C). The enriched *T. tenax* enzyme after heat precipitation (0.272 ±0.007 U/mg protein) was shown to exhibit high sensitivity towards salts (KCl). After ion chromatography (Q Sepharose) all activity was lost and after gel filtration in the presence of 200 mM KCl the activity was reduced. The activity of the *T. tenax* enzyme was analyzed in the protein fraction after gel filtration. 30 and 60 µg of *T. tenax* protein (after gel filtration) was used in the assay and the absorbance of the chromophore was followed at 549 nm after 0, 5, 7, 10 and 15 minutes incubation at 70°C. The time-dependent formation of KDG from gluconate was only observed in the presence of enzyme (fraction after gel filtration) and substrate (0.065 ±0.006 U/mg protein at 10 mM gluconate). No activity has been detected with negative controls without protein (gluconate, galactonate), without substrate, as well as with a heat-precipitated cell-free extract of BL21-CodonPlus(DE3) with plasmid pET-15b without insert.

However, considering the reports about pathway promiscuity in *S. solfataricus*, no GAD activity with galactonate as substrate was observed in *T. tenax* crude extracts supporting our studies of the recombinant *T. tenax* enzyme. The specific activity was shown to be proportional to the amount of recombinant protein (2.1 ±0.1 mU/ 30 µg; 3.7 ±0.1 mU/ 60 µg) (Fig 15).

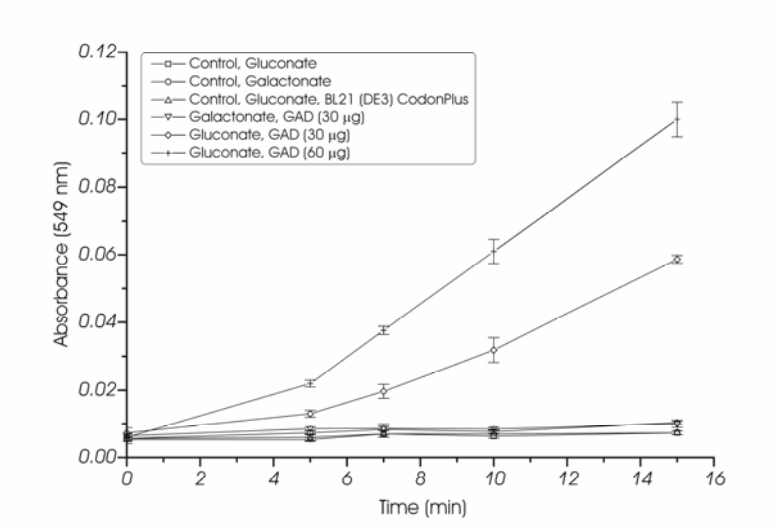

FIGURE 15: GLUCONATE DEHYDRATASE (GAD) ACTIVITY OF *T. TENAX*.
GAD activity (protein fraction after gel filtration) was monitored at 70°C using the discontinuous thiobarbituric acid (TBA) assay. Activity on gluconate (10 mM with 30 and 60 µg protein) as well as galactonate (10 mM with 30 µg protein) and controls without enzyme (10 mM gluconate and galactonate) and heat precipitated extract of BL21-CodonPlus(DE3) with pET-15b without insert are shown. All experiments were performed in triplicate and the standard deviation is given. GAD activity was only observed in the presence of gluconate and the observed activity is proportional to the amount of enzyme.

S. solfataricus GAD was assayed by monitoring KDG formation using the discontinuous TBA assay (70°C) as described for the *T. tenax* GAD. However the high thermal instability of the recombinant *S. solfataricus* GAD allowed for no further characterization of the enzyme.

3.5.1.4 KDG kinase

KDG kinase is the key enzyme of the semi-phosphorylative ED branch, and so far no archaeal enzyme has been characterized to be the first characterized archaeal enzyme. KDG kinase catalyzes the phosphorylation of 2-keto-3-deoxygluconate (KDG) yielding 2-keto-3-deoxy-6-phosphogluconate (KDPG) in the presence of ATP and Mg^{2+}:

$$KDG + ATP/Mg^{2+} \longrightarrow KDPG + ADP$$

Enzyme activity of *T. tenax* and *S. solfataricus* was only observed in the presence of ATP and Mg^{2+}. The phosphorylation of KDG by ATP was followed in a continuous assay by

coupling the formation of KDPG to the reduction of NAD^+ via KD(P)G aldolase and GAPN of *T. tenax*. The KDG kinase activity of *T. tenax* was followed in response to different substrate concentrations, and the enzyme follows Michaelis Menten kinetics for KDG (K_m of 0.178 ±0.011 mM, V_{max} of 43.260 ±0.007 U/mg protein) (Fig 16). The measured enzyme activity of *T. tenax* was directly proportional to the amount of enzyme added to the assay (62.8 ±0.3 mU/ 1.5 µg, 124.0 ±0.4 mU/ 3 µg; at 5 mM KDG) by using the synthesized KDG. Since the expression of the *S. solfataricus* KDG kinase was rather poor the activity was determined directly after heat precipitation in the presence of 3 mM KDG and was shown to be directly proportional to the amount of enzyme added to the assay (4.1 ±0.2 mU/ 40 µg and 8.3 ±1.1 mU/ 80 µg).However, since KDG was synthesized by the KD(P)G aldolase of *T. tenax* (see 2.6.4) and we have no information about the steroselectivity of the *T. tenax* enzyme, we can not rule out contamination by KDGal.

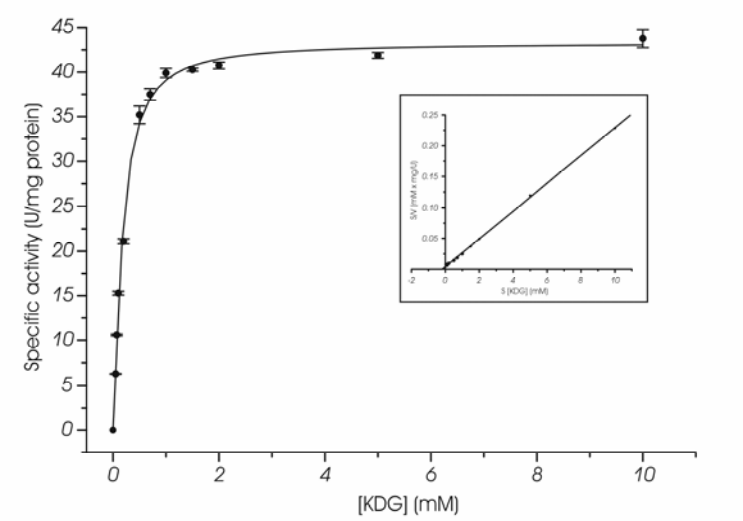

FIGURE 16: KDG KINASE (KDGK) ACTIVITY OF *T. TENAX*.
The KDG kinase activity was determined in a continuous assay at 70°C by monitoring the formation of GAP after KDPG cleavage via KD(P)G aldolase and GAPN of *T. tenax*. The rate dependence on the KDG concentration, determined via the TBA assay, is shown. The enzyme follows Michaelis Menten kinetics for KDG. The insert shows the linear transformation according to Hanes. Three independent assays were performed for each substrate concentration and the standard deviation is given. The rate dependent formation of GAP was only monitored in the presence of KDG, ATP, Mg^{2+}, auxiliary enzymes and the KDG kinase of *T. tenax*.

In order to confirm the activity of the *T. tenax* KDG kinase, the same assay was performed by generating KDG from gluconate by the *T. tenax* GAD during the assay. The measured enzyme activity was directly dependent on the gluconate concentration (6.6

±0.5, 12.2 ±0.6, 14.8 ±0.3 and 22.5 ±0.9 U/mg protein with 1, 1.5, 5 and 10 mM gluconate, respectively).

In addition, the KDG kinase activity was also analyzed using a discontinuous assay by monitoring the formation of ADP from the ATP-dependent phosphorylation of KDG (generated by *T. tenax* GAD) via pyruvate kinase and lactate dehydrogenase. The time-dependent formation of ADP was only observed in the presence of gluconate, GAD and the KDG kinase of *T. tenax*, or *S. solfataricus* whereas no ADP formation was observed with the negative controls (no protein, GAD alone, KDG kinase without GAD, cell free extract with empty vector).

As shown for *S. solfataricus* enzyme (Fig 17) the time-dependent formation of ADP (0, 5, 10, 15 and 30 min at 70°C) was only observed in the presence of gluconate, GAD and the KDG kinase of *S. solfataricus* (0.44 U/mg protein at 10 mM gluconate). No ADP formation was observed for the control BL21(DE3) CodonPlus with pET-15b without insert after heat precipitation.

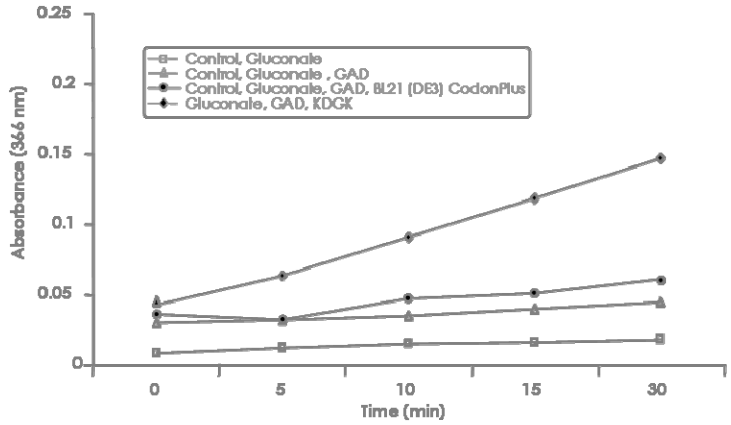

FIGURE 17: KDG KINASE (KDGK) ACTIVITY OF *S. SOLFATARICUS*.
The KDGK activity was determined in a discontinuous assay at 70°C by monitoring the formation of ADP via pyruvate kinase and lactate dehydrogenase. KDG was generated during the assay from gluconate by the gluconate dehydratase of *T. tenax*. Controls without GAD and/or KDGK and BL21(DE3) CodonPlus with pET-15b without insert after heat precipitation are shown.

3.5.1.5 Non-phosphorylating glyceraldehyde-3-phosphate dehydrogenase (GAPN) from *S. solfataricus*

GAPN catalyzes the irreversible, non-phosphorylating oxidation of glyceraldehyde-3-phosphate (GAP) to 3-phosphoglycerate (3-PG):

$$\text{Glyceraldehyde-3-phosphate} + \text{NAD(P)}^+ \longrightarrow \text{3-phosphoglycerate} + \text{NAD(P)H} + \text{H}^+$$

The *S. solfataricus* GAPN activity was determined in a continuous assay at 70°C monitoring the formation of NADPH or NADH at 340 nm. All enzyme properties of GAPN were characterized with enzyme fraction after gel filtration.

The enzyme follows Michaelis Menten kinetics for $NADP^+$ and DL-GAP. For $NADP^+$ a K_m of 0.086 ±0.006 mM and V_{max} of 4.61 ±0.09 U/mg protein (Fig 18A) and for GAP a K_m of 0.511 ±0.035 mM and a V_{max} of 4.62 ±0.09 U/mg protein was determined (Fig 18B). GAP concentrations above 4 mM showed an inhibitory effect on GAPN activity.

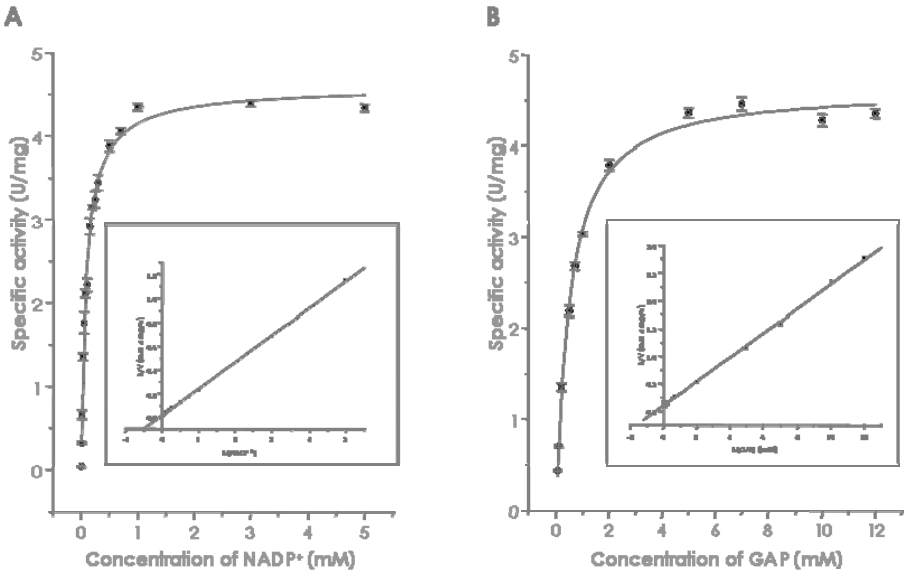

FIGURE 18: GAPN ACTIVITY OF *S. SOLFATARICUS*.
The *S. solfataricus* GAPN activity was determined in a continuous assay at 70°C monitoring the formation of NADPH at 340 nm. The enzyme follows Michaelis Menten kinetics for $NADP^+$ **(A)** and DL-GAP **(B)**. Inserts show the linear transformation according to Hanes. Three independent assays were performed for each substrate concentration and the experimental error is given.

In contrast to the $NADP^+$-dependent reaction, the NAD^+-dependent reaction of *S. solfataricus* GAPN showed a bumpy curve with several pronounced intermediate plateaus (Fig 19). The enzyme exhibited only remote activity with NAD^+ and saturation of the enzyme could not be observed at NAD^+ concentrations up to 50 mM. The highest enzyme activity was observed at 50 mM NAD^+ (0.61 U/mg protein), which is still significantly lower (7–8-fold) than the V_{max} observed using $NADP^+$ as co-factor. In addition, the apparent K_m value for NAD^+ is at least 200-fold higher than for $NADP^+$ (17.38 mM).

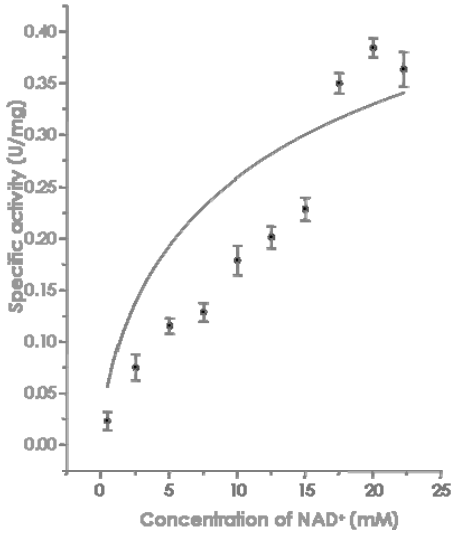

FIGURE 19: GAPN ACTIVITY OF *S. SOLFATARICUS*.
The *S. solfataricus* GAPN activity was determined in a continuous assay at 70°C monitoring the formation of NADH at 340 nm. The NAD^+-dependent reaction of *S. solfataricus* GAPN does not follow classical Michaelis-Menten kinetics and showed a bumpy curve with pronounced intermediate plateaus.

Effector studies were performed in the presence of half saturating concentrations of $NADP^+$ (100 µM) and GAP (500 µM). From the compounds tested (Table 2) glucose 1-phosphate was shown to be most effective, revealing a significant activation of the *S solfataricus* GAPN. The velocity of *S solfataricus* GAPN increased about 4.1-fold by G1P (0.01 mM G1P) whereas no significant change in affinity was observed for the co-substrate $NADP^+$ (K_m of 0.089 ±0.009 mM and a V_{max} of 18,821 ±0.653 U/mg protein) (Fig 20A).

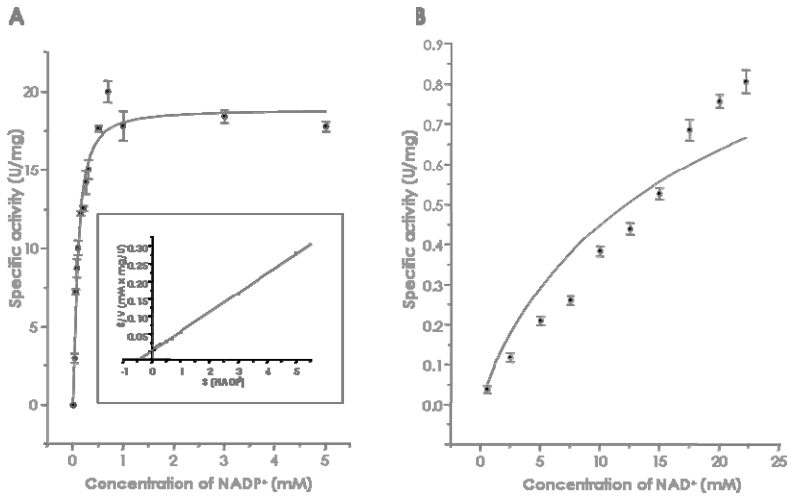

FIGURE 20: INFLUENCE OF GLUCOSE 1-PHOSPHATE ON GAPN ACTIVITY OF *S. SOLFATARICUS*.
The *S. solfataricus* GAPN activity was determined in a continuous assay at 70°C monitoring the formation of NADPH at 340 nm. **(A)** In the presence of $NADP^+$ glucose 1-phophate (G1P 10 µM) resulted in a total increase of the reaction rate (4.1 fold). **(B)** in the presence of NAD^+ glucose 1-phophate (G1P 10 µM) resulted in a total increase of the reaction rate (2–3 fold). Inserts show the linear transformation according to Hanes. Three independent assays were performed for each substrate concentration and the standard deviation is given.

A similar activation of V_{max} (2–3-fold) was observed by the addition of 0.01 mM G1P in the presence of 50 mM NAD^+ as co-factor (1.5 U/mg protein) (Fig 20B). For the other metabolites tested, minor stimulatory effects were observed in the presence of fructose 6-phosphate, AMP and pyruvate. ATP, gluconate and galactonate were found to marginally inhibit the *S solfataricus* GAPN activity, whereas glyceraldehyde and ADP have no effect on GAPN activity at all (Table 2).

TABLE 2: INFLUENCE OF ALLOSTERIC EFFECTORS ON THE *S. SOLFATARICUS* GAPN ACTIVITY.

Effector	Concentration (µM)	Activity (% of control)
control	-	100
G1P	1	133
	5	846
	10	1103
	100	1385
F6P	1	90
	5	110
	10	117
	100	120
AMP	1	95
	5	105
	10	107
	100	117
Pyruvate	1	94
	5	98
	10	99
	100	106
	500	110
	1000	112
ATP	1	73
	5	85
	10	82
	100	87
	500	89
	1000	89
Gluconate	1	104
	5	102
	10	94
	100	92
	500	89
	1000	85
Galactonate	1	95
	5	92
	10	84
	100	83
	500	82
	1000	78

The experiments were performed at 70°C in the presence of half saturating concentrations of $NADP^+$ and GAP. The activity of a control reaction without effector, 0.87 U/mg protein, was set at 100% activity. Additional potential effectors (ADP, pyruvate, glyceraldehydes) did not show a significant effect under the tested conditions.

3.6 CRUDE EXTRACTS STUDIES

In order to prove that the two ED modifications are operative *in vivo*, enzyme assays were performed on crude extracts of *T. tenax* and *S. solfataricus* cells grown on glucose. Crude extract of *T. tenax* and *S. solfataricus* cells were prepared by passing the cells three times through a French pressure cell at 150 MPa. After removing the cell debris and unbroken cells by centrifugation, protein solution was dialyzed overnight against 50 mM HEPES/KOH (pH 7.0, 70°C), 7.5 mM dithiothreitol (2-liter volume, 4°C) and used for enzymatic assays.

In crude extracts of *T. tenax* and *S. solfataricus* The enzyme activities of GAD, KD(P)G aldolase, KDG kinase and GAPN were identified, suggesting the operation of a semi-phosphorylative ED pathway *in vivo* (Table 3). *T. tenax* and *S. solfataricus* GAD were determined by using the discontinuous TBA assay in the presence of either 10 mM gluconate or galactonate. *T. tenax* and *S. solfataricus* KD(P)G aldolase were measured in the presence of both the non-phosphorylative or the phosphorylative substrates (5 mM pyruvate, 2 mM glyceraldehyde or 2 mM glyceraldehyde 3-phosphate, respectively) via the discontinues TBA assay. The KDG kinase from *T. tenax* and *S. solfataricus* were analyzed by coupling the formation of KDPG to the reduction of NAD^+ via KD(P)G aldolase and GAPN from *T. tenax* in the presence of 10 mM KDG and 2 mM ATP/Mg^{2+}. *T. tenax* and *S. solfataricus* GAPN were assayed in a continuous assay by monitoring the reduction of 20 mM $NADP^+$ or 1 mM NAD^+ for *T. tenax* or 2 mM $NADP^+$ or 20 mM NAD^+ for *S. solfataricus* in the presence of 3 mM GAP as substrate.

TABLE 3: SPECIFIC ACTIVITIES OF ED ENZYMES IN CRUDE EXTRACT OF *T. TENAX*.

Enzyme activity	Substrate concentration (mM)	Specific activity (mU/mg)[2]	
		T. tenax	*S. solfataricus*
GAD	10 mM gluconate	10.9 (±0.7)	15.2 (±0.9)
	10mM galactonate	nd	5.7 (±0.6)
KD(P)G aldolase	2 mM glyceraldehyde 5 mM pyruvate	1.4 (±0.1)	1.5 (±0.4)
	2 mM glyceraldehyde 3-phosphate 5 mM pyruvate	1.7 (±0.3)	13.4 (±0.8)
KDG kinase	10 mM KDG, 2 mM ATP	9.1 (±0.5)	8.7 (±0.3)
GAPN	3 mM GAP, 2 mM $NADP^+$	1.13 (±0.04)[1]	32.3 (±0.5)
	3 mM GAP, 1 mM NAD^+	3.5 (±0.1)	nd[1]

[1] Assay was performed in the presence of 20 mM $NADP^+$/NAD^+.
[2] Errors are given from three independent measurements.
(nd) not detected

As a peculiarity for GAD no activity on galactonate was observed in *T. tenax* crude extracts whereas activity on galactonate was observed in *S. solfataricus* crude extract supporting the studies of the recombinant *T. tenax* and *S. solfataricus* enzymes. In addition, KD(P)G aldolase activity was demonstrated with pyruvate and either GA or GAP as substrates, which is in good agreement with the results of the characterization of the recombinant KD(P)G aldolase from *T. tenax and S. solfataricus*. The GAPN activity in the crude extracts from *T. tenax* was (3-fold) higher in the presence of NAD^+, compared to $NADP^+$ as co-substrate (Table 3). The GAPN activity in crude extracts from *S. solfataricus* showed only activity with GAP in the presence of $NADP^+$ as a co-substrate, whereas no activity was determined in the presence of 20 mM NAD^+ (Table 3).

3.7 *IN VITRO* RECONSTRUCTION OF THE ED PATHWAY IN *T. TENAX*

In order to analyze the activities of the different ED enzymes and to confirm their function in the ED pathway [U-^{14}C]glucose was incubated in the presence of different combinations of *T. tenax* ED enzymes (glucose dehydrogenase (GDH), gluconate dehydratase (GAD), KD(P)G aldolase, KDG kinase) and co-substrates ($NADP^+$, ATP, Mg^{2+}). Subsequently, the labelled intermediates which were formed during incubation (10, 20, 30 min at 70°C) were separated by TLC and afterwards detected by autoradiography (Fig 21).

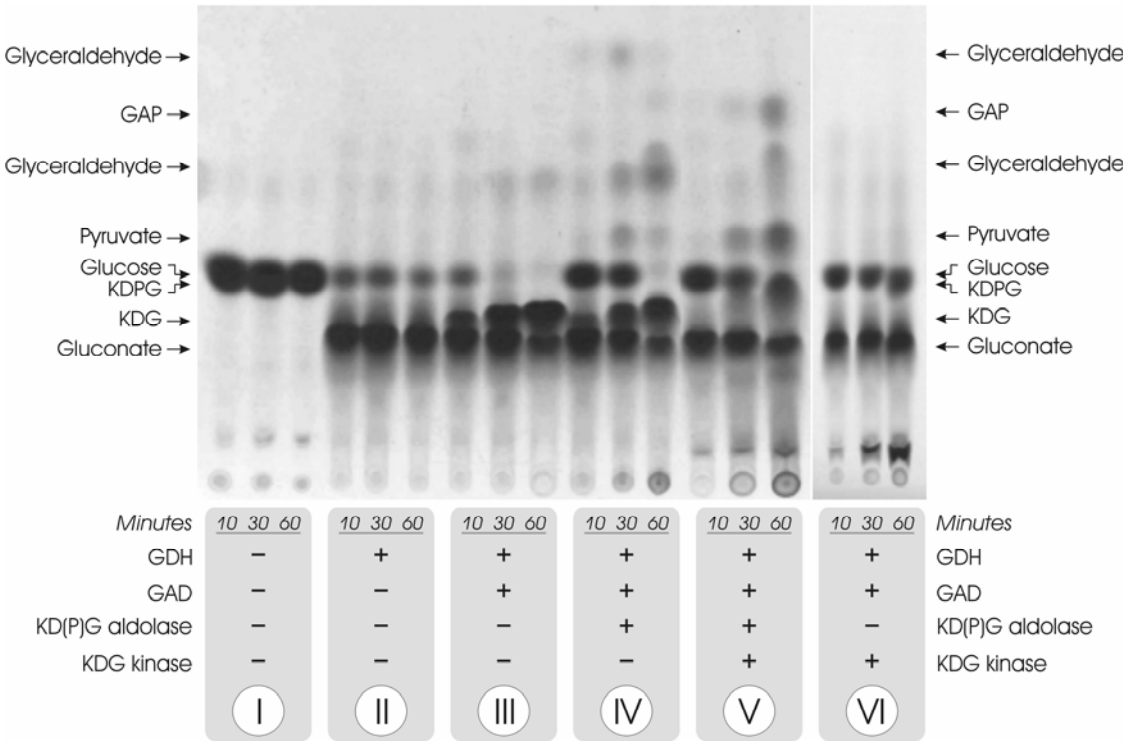

FIGURE 21: RECONSTRUCTION OF THE ED PATHWAY *IN VITRO*.
[U-^{14}C]glucose was incubated in the presence of different combinations of ED enzymes from *T. tenax* (glucose dehydrogenase (GDH), gluconate dehydratase (GAD), KD(P)G aldolase, KDG kinase; protein fractions after heat precipitation) as indicated (10, 30 and 60 min at 70°C, respectively) and the labelled intermediates were separated by thin layer chromatography and visualized using autoradiography. The labelling pattern in the presence of KDG kinase and KD(P)G aldolase (V) indicates the co-existence of both the semi-phosphorylative and the non-phosphorylative ED modification in *T. tenax*.

The step-wise addition of GDH, GAD and KD(P)G aldolase to labelled glucose (I-IV, Fig 21) reveals the characteristic intermediates of the non-phosphorylative ED pathway: gluconate, KDG, pyruvate and glyceraldehyde. However, after the addition of KDG kinase and co-substrates (ATP, Mg^{2+}) KDPG formation was observed in the presence as well as absence of KD(P)G aldolase (V, VI; Fig 21) and KDG disappeared. Further on, in the presence of KD(P)G aldolase formation of GAP was observed, as characteristic intermediate of the semi-phosphorylative ED pathway, in addition to the formation of gluconate, pyruvate and glyceraldehyde. The identification of GA and GAP in this sample indicates that, at least *in vitro*, both the non-phosphorylative and the semi-phosphorylative versions of the ED pathway are active in parallel.

4. DISCUSSION

Comparative studies of carbohydrate metabolism in hyperthermophilic Archaea indicate that sugars are generally metabolized by variants of the Entner-Doudoroff and Embden-Meyerhof-Parnas pathways. Both modifications were demonstrated in *Thermoproteus tenax* [SIEBERS et al., 2004; SIEBERS & HENSEL, 1993; SELIG & SCHÖNHEIT, 1994; SIEBERS et al., 1997; SELIG et al., 1997], whereas in *Sulfolobus solfataricus* glucose was known to be degraded only via the modified ED pathway [DE ROSA et al., 1984]. Initial biochemical studies revealed the utilization of the non-phosphorylative ED pathway in thermophiles and hyperthermophiles [SIEBERS et al., 2004; SIEBERS & HENSEL, 1993; SELIG & SCHÖNHEIT, 1994; SIEBERS et al., 1997; SELIG et al., 1997]. However, using a comparative genomics approach a conserved ED cluster was detected in the genomes of *T. tenax* [SIEBERS et al., 2004], *S. solfataricus*, *S. tokodaii* and *S. acidocaldarius* that resembles the cluster present in *Halobacterium* sp. NRC1 (Fig 5). This conserved functional organization of genes in hyperthermophiles and halophiles suggests the operation of the semi-phosphorylative rather than the previously described non-phosphorylative ED pathway in these organisms.

4.1 THE ED GENE CLUSTER-COMPARATIVE GENOMICS

The ED gene clusters of the hyperthermophilic crenarchaea *T. tenax* and *S. solfataricus* comprise gene homologs coding a novel type gluconate dehydratase (*gad* gene), a bi-functional 2-keto-3-deoxy-(6-phospho)-gluconate aldolase (*kdgA* gene), a 2-keto-3-deoxygluconate kinase (*kdgK* gene). In addition a glucan-1,4-α-glucosidase encoding gene (GAA, *gaa* gene) in *T. tenax* and a non-phosphorylating glyceraldehyde-3-phosphate dehydrogenase (GAPN, *gapN* gene) in *S. solfataricus* was identified in the ED gene cluster.

The *T. tenax* and *S. solfataricus* KD(P)G aldolases exhibit 45% identity and show similarity to predicted dihydrodipicolinate synthases and N-acetylneuraminate lyases in prokaryotes and Eucarya (COG0329). The *T. tenax* and *S. solfataricus* homolog of the enolase superfamily (COG4948) exhibit high similarity to members of the diverse mandelate racemase/muconate lactonizing enzyme family that includes muconate

cycloisomerases, some types of dehydratases and related proteins in all three domains of life [BABBITT et al., 1996]. The enzymes of *T. tenax* and *S. solfataricus* show 59% identity and were probable candidates for the missing gluconate dehydratase (GAD, *gad* gene) activity, because they reside in the ED gene cluster. The conserved clustering of genes encoding putative KDG kinases in addition to *gapN* (in *S. solfataricus* and *S. tokodaii*) was rather surprising, since the modified ED pathway has been reported to proceed via non-phosphorylated intermediates at the C-6 position. This conserved gene clustering did suggest the operation of the semi-phosphorylative pathway in these organisms. Moreover, the high similarity of the thermophilic proteins to the haloarchaeal KDG kinase and KDPG aldolase suggests similar substrate specificity, again indicating the presence of the semi-phosphorylative ED pathway in *T. tenax* and *S. solfataricus*. The *T. tenax* and *S. solfataricus* sugar kinase possess 59% identity and show similarity to putative bacterial and archaeal fructokinases and KDG kinases (COG0524). The GAPN of *S. solfataricus* (NAD^+-dependent aldehyde dehydrogenases, COG1012) shows high similarity (56% identity) to the well characterized enzyme of *T. tenax* [BRUNNER et al., 1998; LORENTZEN et al., 2004]. The glucan-1,4-α-glucosidase (GAA; glucoamylase and related glycosyl hydrolases, COG3387) of *T. tenax* shows high similarity to archaeal (e.g. two enzymes of *S. solfataricus* (SSO2473, 40% identity and SSO0990, 33% identity)), bacterial and eucaryal counterparts and suggests an involvement of the ED enzymes in the hydrolytic degradation of polysaccharides such as glycogen. Homologs of the *gad* and *kdgA* gene (both exhibit 29 % identity to the *T. tenax* enzymes and 31 % identity to the *S. solfataricus gad* and 25 % identity to the *S. solfataricus kdgA*) are also present in the ED cluster of *Halobacterium* sp. NRC1 (*gdh*, *orf-kdgA-gad*), which additionally comprises encoding genes for glucose dehydrogenase (*gdh*, COG1063) and a hypothetical protein. The high similarity to the haloarchaeal enzymes GAD and especially KDG aldolase further supports the presence of the semi-phosphorylative ED pathway in *T. tenax* and *S. solfataricus*, however rising questions about the presence and activity of the KDG aldolase, which is key activity in the non-phosphorylative ED pathway.

In summary, this conserved functional organization of genes in hyperthermophiles and halophiles suggested the presence of the semi-phosphorylative ED pathway —rather than the non-phosphorylative ED pathway as suggested previously— in these organisms.

4.2 ED GENE ORGANIZATION AND TRANSCRIPT ANALYSIS OF *T. TENAX* AND *S. SOLFATARICUS*

In *T. tenax* the genes coding for gluconate dehydratase (GAD), KDG aldolase (KDGA), KDG kinase (KDGK) and glucan-1,4-α-glucosidase (GAA) are organized in a divergon structure in which the *gad* gene is separated from the rest of the *kdgA-kdgK-gaa* gene cluster by 67 basepairs (Fig 6A). The overlap of the three genes (*kdgA*, *kdgK*, *gaa*) of *T. tenax* and the identification of the putative promoter sequence only in front of the upstream of the *kdgA* gene (Fig 7) gave good evidence that these genes form an operon and suggests that posttranscriptional modification rather than differential transcription initiation and termination might be involved as suggested formally [SIEBERS et al., 2004]. In contrast to the ED gene cluster present in *T. tenax*, in *S. solfataricus* all four genes are orientated in the same direction and the presence of the putative promoter sequences only in front of the *gad* and *gapN* gene suggests a polycistronic transcript of the *gad-kdgA-kdgK* genes and a single transcript of the *gapN* gene (Fig 6B and 7).

For a more accurate assignment of promoter structures, the transcription starts of the *gad* and *kdgA-kdgK-gaa* mRNA of *T. tenax* and the *gad-kdgA-kdgK* and *gapN* mRNA of *S. solfataricus* were determined by primer extension analysis. As shown in (Fig 8) No obvious promoter structures in front of internal genes in the ED operon (*kdgK* and *gaa* genes in *T. tenax* and *kdgA* and *kdgK* genes in *S. solfataricus*) were observed and transcription was initiated either at the adenine (A) of the start codon (ATG; *gad* gene) or at the thymidine (T) immediately in front of the start codon ATG (*kdgA-kdgK-gaa* transcript), thus lacking Shine-Dalgarno sequences (SD sequence).

The assignment of crenarchaeal consensus promoter sequences only in front of the first gene of each operon (*T. tenax kdgA*, *S. solfataricus gad*) and in front of the single genes (*T. tenax gad, S. solfataricus gapN*), the absence of Shine-Dalgarno sequences upstream the first gene and subsequent translation via leaderless transcripts is in good

agreement with previous studies in *T. tenax* [SIEBERS et al., 2004; SCHRAMM et al., 2000; SIEBERS et al., 2001] and *S. solfataricus* [TOLSTRUP et al., 2000; CONDO et al., 1999], as well as in another crenarchaeon *Pyrobaculum aerophilum* [SLUPSKA et al., 2001].

The proposed co-transcription of the ED genes in *T. tenax* was confirmed by Northern Blot analysis with total RNA and specific antisense mRNA probes for the *kdgA* and *kdgK* gene revealed the presence of tri-, bi- and monocistronic transcripts (Fig 10).

The coordinate expression of the enzymes for KDPG formation and degradation was previously reported for *Z. mobilis*, *E. coli* and *P. aeruginosa* and seems to be essential, since KDPG is highly toxic for the cell, thus, *E. coli* mutants that accumulate KDPG are lethal. Like in *T. tenax*, several discrete transcripts were also reported for *the Z. mobilis glf-zwf-edd-glk* operon, which codes for a glucose-facilitated diffusion transporter, glucose-6-phosphate dehydrogenase, ED dehydratase and glucokinase. The processing of the polycistronic message in *Z. mobilis* is proposed to appear via endonucleolytic cleavage, as shown by inhibition of transcription with rifampicin, which results in an increase of the abundance of shorter, more stable transcripts at the expense of longer less stable transcripts [CONWAY, 1992].

4.3 ENZYME CHARACTERIZATION

4.3.1 Heterologous expression of the *T. tenax* and *S. solfataricus* ED proteins in *E. coli*

In order to confirm the predicted enzymes activities of the ED genes in *T. tenax* and *S. solfataricus*, the *gdh*, *gad*, *kdgA*, and *kdgK* genes of *T. tenax* and the *gad*, *kdgA*, *kdgK*, and *gapN* genes of *S. solfataricus* (A. Geerling and T. Ettema in the laboratory of Microbiology, Wageningen University, The Netherlands) were cloned. The gene products were expressed, enriched and purified to apparent homogeneity from crude extracts and analysed for their respective activities (Fig 11 and 12).

4.3.2 KD(P)G aldolase of *T. tenax* and *S. solfataricus*

In contrast to previous studies on the *S. solfataricus* KDG aldolase [LAMBLE et al., 2003; HENDRY et al., 2000], the enzymes from both *T. tenax* and *S. solfataricus* were shown to

catalyze the reversible cleavage of KDG forming pyruvate and glyceraldehyde as well as KDPG forming pyruvate and glyceraldehyde-3-phosphate (GAP), thus representing a true KD(P)G aldolase.

The *T. tenax* and *S. solfataricus* KD(P)G aldolase activity was assayed in the anabolic direction of KDG or KDPG formation from C-3 substrates (condensation reaction) using the discontinuous TBA assay and activity was observed not only with GA but also with the phosphorylated substrate GAP, which contrast to previous reports on the *S. solfataricus* KDG aldolase [LAMBLE et al., 2003; HENDRY et al., 2000] (Fig 13).

These results were further confirmed by [^{14}C]-labelled pyruvate experiments, which revealed that both KD(P)G aldolase from *T. tenax* and *S. solfataricus* were able to form: KDG from GA and pyruvate and KDPG from GAP and pyruvate, while no product formation was observed in the controls (Fig 14). Therefore both the *T. tenax* and *S. solfataricus* enzyme are true 2-keto-3-deoxy-(6-phospho)-gluconate (KD(P)G) aldolases of low substrate specificity that are active on phosphorylated (GAP, KDPG) as well as non-phosphorylated (GA, KDG) substrates. The same labeling pattern was observed in the control reaction using the characterized KDPG aldolase (EDA) of the anaerobic, hyperthermophilic bacterium *T. maritima*, which was reported for activity on phosphorylated and non-phosphorylated substrates [GRIFFITHS et al., 2002]. Thus, the bifunctional KD(P)G aldolase is key enzyme in both the non- and the semi-phosphorylative ED pathway, which is also in line with the presence of the *kdgA* gene homolog in the haloarchaeal ED cluster.

The recombinant *S. solfataricus* KD(P)G aldolase was re-investigated in the group of Michael Danson (University of Bath, Bath, UK) and the activity on phosphorylated substrates was indeed confirmed [LAMBLE et al. 2003 THEODOSSIS et al., 2004; LAMBLE el al., 2005]. The kinetics of the *S. solfataricus* KD(P)G aldolase-catalyzed cleavage of KDPG and KGPGal was reported respectively [LAMBLE et al. 2005] and strongly provides the evidence that both compounds are natural substrates of the enzyme. These findings further indicate that the semi-phosphorylative ED pathway is promiscuous for the metabolism of both glucose and galactose in *S. solfataricus*. The comparison of the catalytic efficiency with the semi-phosphorylative substrates and the non-phosphorylative

substrates indicated that the semi-phosphorylative substrate is the preferred substrate for the *S. solfataricus* KD(P)G aldolase (K_{cat}/K_M values: 643 s^{-1} $mM^{-}1$ and 1.1 s^{-1} mM^{-1} for KDPG and KDG, respectively) [LAMBLE et al., 2005]. The crystal structure of the KD(P)G aldolase of *S. solfataricus* has been resolved and in addition the structure of the enzyme with the non-phosphorylative substrates (pyruvate, KDG and KDGal bound in the active site as Schiff-base intermediates) were determined [THEODOSSIS et al., 2004]. These structures provide the first insight in the lack of stereocontrol for this enzyme although data for the phosphorylative substrates are still missing.

The existence of a single central metabolic pathway for the metabolism of both glucose and galactose in *S. solfataricus* contrasts the situation observed in other organisms. In *Aspergillus* sp., glucose metabolism also proceeds via the non-phosphorylative ED pathway; however, separate enzymes exist for the metabolism of the two sugars glucose and galactose [ELZAINY et al., 1973; ELSHAFEI & ABDEL-FATAH, 2001]. Also many Gram-negative and Gram-positive Bacteria use the classical ED pathway for glucose metabolism, while the Delay-Doudoroff pathway often exist for the catabolism of galactose involving separate, inducible enzymes [DE LEY & DOUDOROFF, 1957]. Separate pathways for the utilization of sugars were also identified in Archaea, ^{13}C-NMR analysis and enzymatic studies of the aerobic halophilic *Haloarcula marismortis* revealed that glucose is degraded via the semi-phosphorylative ED pathway [JOHNSEN et al., 2001; TOMLINSON et al.1974], whereas fructose is almost completely metabolized via a modified EMP pathway [JOHNSEN et al., 2001].

Aldolases are divided into two main groups, Type I and Type II. Type I aldolases proceed via a Schiff-base intermediate formed between an active site lysine and the α-keto acid moiety of the substrate, whereas Type II aldolases are non Schiff-base forming and require a metal cofactor. Homologs of the *T. tenax* and *S. solfataricus* KDG aldolases (which displays high-level similarity; 43 % identities) were identified in many bacterial, archaeal and eukaryal species. However, they share no similarity to the classical ED aldolase (EDA) [BUCHANAN et al., 1999], but are members of the N-Acetylneuraminate lyase (NAL) superfamily [BABBITT & GERLT, 1997]. Members of the NAL superfamily catalyze substantially different overall reactions (e.g. dihydrodipicolinate synthases, N-

acetylneuraminate lyase, *trans-o*-hydroxybenzylidene-pyruvate aldolase/dehydratase) and their catalysis generally proceeds via the Schiff-base mechanism. Each of the enzymes of the NAL superfamily harbors a conserved lysine (Lys-165 in NAL) located in the sixth strand of β-sheet of the single β/α (TIM) barrel domain [BUCHANAN et al., 1999]. The corresponding active site lysine residue has indeed been identified in the crystal structure of the KD(P)G aldolase of *S. solfataricus* (Lys-155) [THEODOSSIS et al., 2004] therefore archaeal KD(P)G aldolases are type I aldolases. The involvement of a Schiff-base mechanism was confirmed experimentally by inactivation of the enzyme in the presence of $NaBH_4$ (Sodium Borohydride) [BUCHANAN et al., 1999]. In *E. coli* K12 two KD(P)G aldolase homologs in addition to the classical EDA were identified (*yjhH*, *yagE*). Both are organized in gene clusters encoding ED dehydratase orthologs (*yjhG, yagF*, [PEEKHAUS & CONWAY, 1998]), permeases (*yjhF, yagG*), regulators (*yjhI, yagI*) and a hypothetical protein (*yjhU*) or a putative β-xylosidase (*yagH*), respectively. This functional organization indicates that also in *E. coli* so far unknown ED modifications may exist.

4.3.3 Gluconate dehydratase of *T. tenax* and *S. solfataricus*

Gluconate dehydratase has been purified and characterized from different bacterial sources, although the encoding gene has never been identified and therefore representing a missing link in the central carbohydrate metabolism. Gluconate dehydratase (GAD) catalyzes the dehydration of gluconate. For the enzyme of *T. tenax,* the time dependent formation of KDG from gluconate and galactonate was demonstrated and the enzyme was shown to be specific for gluconate (Fig 15), whereas the enzyme of *S. solfataricus* is promiscuous for both gluconate and galactonate. The purification and characterization of the GAD from *S. solfataricus* was reported by two independent groups [KIM & LEE, 2005; LAMBLE et al., 2004]. Surprisingly, these studies revealed some contradicting results about molecular size and catalytic activity with galactonate; our analysis in *S. solfataricus* crude extract (see 3.6) supports the proposed substrate promiscuity of the *S. solfataricus* enzyme [LAMBLE et al., 2004].

Gluconate dehydratase (EC 4.2.1.39) activities have been reported in members of all three domains of life, Archaea (*Thermoplasma* sp. [BUDGEN & DANSON, 1986] and

Halobaterium sp. [CONWAY, 1992]), Bacteria (*Achromobacter* sp. and *Clostridium pasteurianum* [KERSTERS et al., 1971; KERSTERS & DE LEY, 1975; BENDER & GOTTSCHALK, 1973; GOTTSCHALK & BENDER, 1982]) and Eukarya (*Aspergillus* sp. [ELZAINY et al., 1973]).

The GAD of *T. tenax* and *S. solfataricus* are members of the mandelate racemase (MR) subgroup of the enolase superfamily, and thus represent the first reported GAD in this superfamily [BABBITT et al., 1996]. The enolase superfamily harbors a diverse set of enzymes, which at first sight catalyze markedly different overall reactions (e.g. enolase, mandelate racemase, galactonate dehydratase, muconate-lactonizing enzyme I, β-methylaspartate ammonia lyase, o-succinylbenzoate synthase). A common feature of all family members concerns the first step of their catalytic action, i.e. the abstraction of the α-proton of a carboxylic acid to form an enolic intermediate. The enolase superfamily is divided in the MR, muconate-lactonizing enzyme I (MLE I) and enolase subgroup. In the MR subgroup so far only glucarate dehydratase from *Pseudomonas putida*, *Bacillus subtilis* and *E. coli* as well as galactonate dehydratase from *E. coli* have been biochemically characterized [BABBITT et al., 1996; HUBBARD et al., 1998]. Homologs of the *T. tenax* and *S. solfataricus* GAD have been identified in many archaeal, bacterial and eukaryal species.

For example the GAD sequence of *T. tenax* and *S. solfataricus* show high similarities to homologs identified in other thermoacidophilic Archaea (e.g. sequence identities for the two *dgo*A proteins (*dgo*A1 and *dgo*A2) of *Sulfolobus tokodaii* (59 % and 52 % *T. tenax* and 79 % and 61 % *S. solfataricus* identity), mandelate racemase/muconate lactonizing enzyme of *Ferroplasma acidarmanus* (40 % *T. tenax* and 42 % *S. solfataricus* identity), GalD (Galactonate dehydratase) of *Thermoplasma acidophilum* (40 % *T. tenax* and 42 % *S. solfataricus* identity) and GalD1 (Galactonate dehydratase) of *Thermoplasma volcanium* (39 % *T. tenax* and 41 % *S. solfataricus* identity)). However, functional annotation of these proteins remains difficult due to the broad substrate specificity within the enolase superfamily.

4.3.4 KDG kinase of *T. tenax* and *S. solfataricus*

KDG kinase catalyzes the phosphorylation of KDG yielding KDPG and thus represents the key enzyme for the semi-phosphorylative ED pathway. However, so far little is known

about the biochemical properties of KDG kinases and only the bacterial enzymes of *E. coli* [CYNKIN & ASHWELL, 1960] and *Thermus thermophilus* [OHSHIMA et al., 2004] have been characterized in detail.

Activity of the KDG kinase from *T. tenax* was measured in a continuous assay by coupling the formation of KDPG to the reduction of NAD^+ via KD(P)G aldolase and GAPN of *T. tenax*. The KDG kinase activity was followed in response to different substrate concentrations, and the enzyme was shown to follow Michaelis Menten kinetics for KDG (K_m of 0.178 ±0.011 mM, V_{max} of 43.260 ±0.007 U/mg protein) (Fig 16). The coupled KDG kinase assay is not optimal, since KD(P)G aldolase is also active on the substrate KDG, resulting in an unknown effective KDG concentration in the assay. Furthermore, the *S. solfataricus* KD(P)G aldolase was reported to form the diastereomeric products KDG and KDGal by condensation of glyceraldehyde and pyruvate and so far we have no information about the stereoselectivity of the *T. tenax* enzyme, which was used for the generation of KDG. The S. *solfataricus* enzyme showed a relative lower specific activity rather than the enzyme from *T. tenax* and the time-dependent formation of ADP was only observed in the presence of gluconate, GAD and the KDG kinase of *S. solfataricus* (Fig 17)

The KDG kinases from the Euryarchaeota belong to the BadF/BadG/BcrA/BcrD ATPase family (pfam01869; COG2971). Recently the KDG kinase of *Thermoplasma acidophilum* has been purified and characterized [JUNG & LEE, 2005] which showed that the enzyme shares no similarity with known KDG kinases, and therefore belongs to a novel class of sugar kinases. KDG kinases from *T. tenax* and *S. solfataricus* are members of the ribokinase (PfkB) enzyme family, which is composed of prokaryotic sequences related to ribokinase, including enzymes such as fructokinases, the minor 6-phosphofructokinase of *E. coli*, 1-phosphofructokinase and archaeal ADP-dependent glucokinases and phosphofructokinases [BORK et al., 1993; ITO et al., 2001]. So far the KDG kinase purified from *E. coli* was characterized [CYNKIN et al., 1960] and activity was demonstrated for the gene product of *Erwinia chrysanthemi* ([HUGOUVIEUX-COTTE-PATTAT et al., 1994], accession number X75047, 25% identity to the *T. tenax* enzyme). The latter enzyme is involved in pectin and hexuronate (glucuronate and galacturonate) catabolism, routes that

converge through the common intermediate KDG. KDG kinase activity has also been proposed for the *kdgK* gene of *Bacillus stearothermophilus* T6 [SHULAMI et al., 1999] due to its high similarity to the *Erwinia* enzyme and the organization in the xylan and glucuronic acid utilization gene cluster.

Homologs of the *T. tenax* and *S. solfataricus* KDG kinase were identified in many archaeal genomes (e.g. *A. pernix* (28% identity), *P. furiosus* (30% identity), and *P. aerophilum* (31% identity)) and bacterial genomes (*Pseudomonas putida* (34% identity), *Bacillus halodurans* (30% identity), and *Streptomyces coelicolor* (33% identity)). In addition, we failed to identify KDG kinase orthologs in the Eukarya and thus, the KDG kinase seems to be a key player in glucose catabolism (semi-phosphorylative ED pathway) and sugar acid (extracellular polymer) degradation in prokaryotes. Interestingly, KDG kinase orthologs were not detected in the genomes of *T. volcanium* and *Picrophilus torridus*. However, the purification and the characterization of the KDG kinase from *Thermoplasma acidophilum* [JUNG & LEE, 2005] strongly suggests that glucose is also metabolized via the branched ED pathway in thermoacidophiles, the enzyme is a member of a novel class of a sugar kinases and share no homology to the KDG kinase of the ribokinase family.

4.3.5 Non-phosphorylating glyceraldehyde-3-phosphate dehydrogenase (GAPN) of *S. solfataricus*

The *S. solfataricus* GAPN activity was determined in a continuous assay monitoring the formation of NADPH or NADH. The enzyme was shown to follow Michaelis Menten kinetics for $NADP^+$ and DL-GAP (Fig 18).

The *T. tenax* GAPN has been studied in detail previously BRUNNER et al., 1998; LORENTZEN et al., 2004; POHL et al., 2002]. The GAPN of *S. solfataricus* shows high similarity (56% identity) to the enzyme of *T. tenax*. The clustering of *gapN* with ED genes in *S. solfataricus* and *S. tokodaii* underlines the role of GAPN in the semi-phosphorylative ED pathway and more general in the common shunt of the EMP pathway. Like the *T. tenax* GAPN, the enzyme of *S. solfataricus* represents a non-phosphorylating, allosteric GAPDH that catalyzes the irreversible oxidation of glyceraldehydes 3-phosphate yielding

3-phosphoglycerate. However, in contrast to the *T. tenax* GAPN, which uses both NAD^+ and in presence of activators even more efficiently $NADP^+$ as co-substrate (higher catalytic rates, [LORENTZEN et al., 2004]), the *S. solfataricus* enzyme clearly requires $NADP^+$ as co-substrate, thus resembling most GAPNs analyzed so far [LORENTZEN et al., 2004; HABENICHT, 1997; PEROZICH et al., 2000]. Thus, both enzymes –the GAPN of *T. tenax* and *S. solfataricus*– differ significantly in their enzymatic and allosteric properties. GAPN is a member of the aldehyde dehydrogenase superfamily, which comprises numerous enzymes with different substrate specificities (e.g. lactaldehyde, succinate semialdehyde, betaine aldehyde) [BRUNNER et al., 1998] (Table 4).

TABLE 4: COMPARATIVE KINETIC, MACROMOLECULAR, STRUCTURAL AND EFFECTOR PROPERTIES OF THE GAPN FROM *T. TENAX* AND *S. SOLFATARICUS*.

	S. solfataricus GAPN	*T. tenax* GAPN[1]
$NADP^+$		
without G1P		
V_{max} (U mg^{-1})	4.6 ±0.1	14
K_m (mM)	0.086 ±0.006	20
in presence of G1P		
V_{max} (U mg^{-1})	18.8 ±0.65	43
K_m (mM)	0.09 ±0.01	0.1
NAD^+		
without G1P		
V_{max} (U mg^{-1})	~0.61 [a]	36
K_m (mM)	17.38 [a]	3.1
in presence of G1P		
V_{max} (U mg^{-1})	~1.5 [a]	35
K_m (mM)	21.1 [a]	0.4
Molecular mass		
Subunit (kDa)	56.9	55.0 [b]
Native (kDa)	189 ±23	220 [b]

[1] [LORENTZEN et al., 2004]

[a] Saturation of the *S. solfataricus* GAPN could not be observed for NAD^+ concentrations up to 50 mM.

[b] Molecular mass as determined by[BRUNNER et al., 1998]

Further more effector studies revealed that the affinities of the *S. solfataricus* enzyme for NAD^+ and $NADP^+$ were unaffected upon addition of G1P. This finding contrasts with the 200-fold increase in affinity of the previously studied NAD^+-dependent GAPN from *T. tenax* [LORENTZEN et al., 2004] upon addition of G1P when $NADP^+$ was

used as co-factor (Table 2). Addition of G1P in the NAD^+-dependent reaction by *T. tenax* GAPN was less dramatic, but still significant, as an 8-fold increase in affinity was observed [LORENTZEN et al., 2004].

A general feature of all hyperthermophilic Archaea analyzed so far is the lack of a control point at the beginning of the EMP pathway. In Archaea ATP-dependent hexokinases, ADP-dependent glucokinases, ATP-, ADP-, and PP_i-dependent phophofructokinases all lack allosteric properties thus omitting the central control point of the classical EMP pathway as found in Bacteria and Eucarya. As shown for *T. tenax* and *S. solfataricus*, the GAPN takes over the central role in the regulation of the common lower shunt of the EMP and semi-phosphorylative ED pathway. The unidirectional catabolic enzyme substitutes for glyceraldehyde-3-phosphate (GAP) dehydrogenase (GAPDH) and 3-phosphoglycerate kinase (PGK), features allosteric properties and omits the extremely thermolabile intermediate 1,3-diphosphoglycerate and thus, allows metabolic thermoadaptation [AHMED et al., 2004]. Genome and biochemical data indicate that GAPN is active in addition to the classical GAPDH (e.g. Sulfolobales, *A. pernix*) and sometimes even to a third GAP converting enzyme the ferredoxin-dependent GAPOR (e.g. *T. tenax*, *P. furiosus*, *M. jannaschii*) [VERHEES et al., 2004; VERHEES et al., 2003; SIEBERS et al., 2004]. The coexistence of GAPN and GAPOR might reflect the presence of two different pools of reduction equivalents (pyridine nucleotides and ferredoxin), which may be used for energy generation. For *P. furiosus* it was recently shown that the electrons from reduced ferredoxin are transferred to protons via a membrane-bound hydrogenase to generate hydrogen and ATP synthesis by the means of proton motive force [SAPRA et al., 2003]. As such, GAPOR contributes to the net ATP production of the EMP variant in *P. furiosus*.

The distribution of GAP converting enzymes in archaeal genomes suggests a functioning GAPDH in gluconeogenesis (with exception of the halophiles), whereas GAPOR/GAPN are predicted to be solely active in catabolic direction. This theory is supported by the presence of a GAPOR encoding gene in the starch degrading *A. fulgidus* strain 7324 [SIEBERS & SCHÖNHEIT, 2005] and the apparent absence of such a gene in the genome of *A. fulgidus* DSM4304, which is lacking glycolytic capacity. Furthermore,

transcription analysis, as well as extensive enzyme characterization in *P. furiosus* and *T. tenax*, [SCHAFER et al 1993; BRUNNER et al. 1998; VAN DER OOST et al., 1998; BRUNNER et al. 2001; SCHUT et al., 2003; LORENTZEN et al. 2004] whose genomes encode all three GAP converting enzymes, are supportive of a catabolic role for GAPN and GAPOR and an anabolic role for the GAPDH/PGK couple. However, that the situation can be considerably less straightforward is exemplified by the situation in *Bacillus subtilus*, which contains two distinct GAPDHs, one acting in gluconeogenic direction and the other acting in glycolytic direction [FILLINGER et al. 2000]. Interestingly, two GAPDH encoding genes were identified in the genomes of *Methanosarcina* species suggesting different metabolic functions.

To date, *T. tenax* GAPN and *S solfataricus* GAPN are the only aldehyde dehydrogenases that are shown to display allosteric regulatory properties. The observed differences in fine tuning of regulation between *T. tenax* GAPN and *S solfataricus* GAPN might be a result of the different physiological background in these organisms. Possibly, *T. tenax* requires a more strictly regulated GAPN, as a consequence of the presence of an additional glycolytic pathway (EMP), whereas in *S. solfataricus*, the ED pathway appears to be the only glycolytic pathway.

4.4 THE BRANCHED ED PATHWAY IN *T. TENAX* AND *S. SOLFATARICUS*

The activity of the different recombinant ED enzymes from both *T. tenax* and *S. solfataricus* was confirmed by their incubation in different combination with [U-^{14}C]glucose and the identification of labelled intermediates by TLC and autoradiography (Fig 21). The step-wise addition of GDH, GAD and KD(P)G aldolase to labelled glucose (I-IV, Fig 21) revealed the characteristic intermediates of the non-phosphorylative ED pathway: gluconate, KDG, pyruvate and glyceraldehyde. However, after the addition of KDG kinase and co-substrates (ATP, Mg^{2+}) KDPG formation was observed in the presence or the absence of KD(P)G aldolase (V, VI; Fig 21) while KDG has disappeared. In addition, in the presence of KD(P)G aldolase formation of GAP was observed, as characteristic intermediate of the semi-phosphorylative ED pathway, in addition to formation of gluconate, pyruvate and some glyceraldehyde. The identification of GA and GAP in this

sample suggested that, at least *in vitro*, both the non-phosphorylative and the semi-phosphorylative versions of the ED pathway are active in parallel. Identical labelling patterns were observed using the KD(P)G aldolase and KDG kinase of *S. solfataricus* instead of the two *T. tenax* enzymes. These results are in agreement with both, a functional non- and semi-phosphorylative modification of the ED pathway in *T. tenax* and *S. solfataricus*. However, the disappearance of KDG in the presence of KDG kinase might indicate that the semi-phosphorylative pathway is preferred.

In addition, the *in vitro* reconstruction experiments indicate that no gluconolactonase (EC 3.1.1.17) is needed for a functional pathway. Whereas a gluconolactonase gene homolog seems to be absent in the *T. tenax* genome, a potential candidate (SSO3041) was identified adjacent to the glucose dehydrogenase gene (SSO3042) in *S. solfataricus* most likely indicating a functional link. Possibly, the presence of gluconolactonase allows an accelerated glucose turnover in *S. solfataricus*, where the ED pathway seems to be the only route for glucose catabolism.

A possible role of the ED pathway in gluconeogenesis was analyzed using a similar approach with ^{14}C-labelled pyruvate. However, in the presence of KD(P)G aldolase, GAD and GDH and the respective substrates and co-substrate (GA, pyruvate, NADPH) only the formation of KDG was observed, indicating that the pathway is at least partly irreversible, or it is catalyzed by a distinct set of enzymes.

The aforementioned *in vitro* results strongly demonstrates the presence of the semi-phosphorylative ED pathway in *T. tenax* and *S. solfataricus* in particular, and in hyperthermophilic Archaea in general, and indicates the presence of both ED modifications in one organism (pathway dualism). The conserved functional organization of ED genes encoding enzymes of the semi-phosphorylative modification (KDG kinase, GAPN) and for the common ”core” modified ED shunt (GAD; KD(P)G aldolase) raises questions about their regulation as well as the utilization of both ED branches *in vivo*. Enzyme assays performed on crude extract of *T. tenax* and *S. solfataricus* cells grown on glucose further confirmed the operation of a semi-phosphorylative ED pathway in these organisms (Table 3).

In the light of the results presented here, it is not evident that the lower shunt of the non-phosphorylative ED is active *in vivo* in *T. tenax* and *S. solfataricus*. Labelling studies with *T. tenax* and *S. solfataricus* crude extracts and ^{14}C glucose were performed in the absence of ATP presuming a conversion via the semi-phosphorylative ED pathway [DE ROSA et al., 1984; SIEBERS & HENSEl, 1993]. Additional information about characteristic enzymes of the non-phosphorylative ED pathway comes from the characterization of aldehyde:ferredoxin oxidoreductases (AOR) form *P. furiosus* [MUKUND & ADAMS, 1991] and *S. acidocaldarius* [KARDINAHL et al., 1999]. Both enzymes exhibit broad substrate specificity and are active on different aliphatic aldehydes in a strong pH-dependent manner. They were proposed to function as glyceraldehyde oxidoreductase due to their high cellular concentration and increased AOR activity in *P. furiosus* cells grown with tungsten and maltose [SCHICHO et al., 1993] and the strict molybdate-dependence of growth on glucose in *S. acidocaldarius* [KARDINAHL et al., 1999]. However, convincing evidence for the utilization of the non-phosphorylative ED pathway *in vivo* comes from the work of Budgen and Danson [BUDGEN & DANSON, 1986] who detected glyceraldehyde dehydrogenase, glycerate kinase (2-phosphoglycerate forming), enolase, and pyruvate kinase in dialyzed crude extracts of *T. acidophilum*. More recently the glyceraldehyde dehydrogenase of *T. acidophilum* and *Picrophilus torridus* [REHER & SCHÖNHEIT, 2006] and glycerate kinase (2-phosphoglycerate forming) in *Picrophilus torridus* [REHER & SCHÖNHEIT, 2006; REHER et al., 2006] was characterized. Also the recombinant glycerate kinase —the key enzyme of the non-phosphorylative ED branch— from *T. tenax* has been characterized further demonstrating the existence of the branched ED pathway [KEHRER et al., ready for submission]. In summary, biochemical data as well as genomic data (Table 5) suggest the coexistence of both ED modifications and thus the branched ED pathway in thermophilic and hyperthermophilic Archaea. This pathway dualism rises questions about the utilization and regulation of the carbon flux through the branched pathway, which seems to proceed at the level of KDG and KDPG by KDG kinase and KD(P)G aldolase.

4.5 PHYSIOLOGICAL IMPLICATIONS

The presence of various pathways for carbon metabolism in one organism raises questions about their physiological significance. With the anaerobe *T. tenax* and the aerobe *S. solfataricus* two hyperthermophiles are studied, which exhibit significant differences in the central carbon metabolism and thus allow to gain new insights into the flexibility of carbon metabolism.

Genome data and biochemical studies indicate that the anaerobe *T. tenax* uses at least two different pathways for glucose metabolism, a modification of the reversible EMP pathway and the branched ED pathway (semi-phosphorylative and non-phosphorylative) (Fig 22A). The clustering of the *gaa* gene, encoding a glucan-1,4-α-glucosidase, with the ED genes indicates a central role of the ED modifications in the hydrolytic degradation of polysaccharides (e.g. glycogen). In contrast, the modified EMP pathway seems to have a central function in the phosphorolytic glycogen degradation by glycogen phosphorylase, which was characterized recently [SIEBERS et al., 2004; AHMED et al., 2004]. The selection of the different pathways *in vivo* seems to be strongly influenced by the energy demand of the cell. Whereas no ATP is generated by the ED modifications, one (glucose degradation) or two ATP (phosphorolytic glycogen degradation) are generated using the EMP variant, taking into account that: (i) PP_i, the phosphoryl donor of phosphofructokinase, is a waste product of the cell [SIEBERS et al., 1998], and (ii) GAPN is used for glucose catabolism, which omits the formation of 1,3-diphosphoglycerate and as such does not couple the oxidation of GAP to the generation of ATP.

Additionally, the presence of the branched ED pathway might play an important role in metabolic thermoadaptation. The half-lives of intermediates (GAP, 14.5 min; dihydroxyacetone phosphate, 79.4 min; 1,3-diphosphoglycerate, 1.6 min; all at 60◦C) suggest that the stability of intermediates plays a critical role in thermoadaptation [DÖRR et al., 2003]. Whereas the EMP and the semi-phosphorylative ED pathways avoid the formation of the extremely heat-labile 1,3-diphosphoglycerate by the one-step conversion of GAP to 3-phosphoglycerate via GAPN or GAPOR, the non-phosphorylative ED variant would additionally circumvent the formation of the two other heat-labile intermediates GAP and dihydroxyacetone phosphate. Therefore, the non-phosphorylative ED pathway

might be appropriate for growth at the upper temperature range, indicating that the various pathways for carbohydrate metabolism do not reflect metabolic parallelism but represent a measure for 'metabolic thermoadaptation'.

In the aerobe *S. solfataricus* the modifications of the ED pathway seem to represent the only pathway for glucose and galactose degradation [LAMBLE et al., 2003] (Fig 22B). Analysis of genome data indicate an incomplete EMP pathway, and it is suggested that the enzymes that are present may be involved in fructose degradation or in the anabolic gluconeogenetic direction for glycogen synthesis [VERHEES et al., 2004; VERHEES et al., 2003; SHE et al., 2001].

The identification and characterization of the enzymes that constitute the modified ED pathway sheds new light in the functional role of this glycolytic pathway in hyperthermophilic Archaea and suggests a much broader distribution of ED-like pathways in other Archaea, Bacteria and Eukarya than it was previously assumed. This finding supports the important role of the ED pathway and its variants in glucose degradation and as a funnel for sugar acid (polymer) degradation and again underlines the variability and flexibility of central carbon metabolizing pathways.

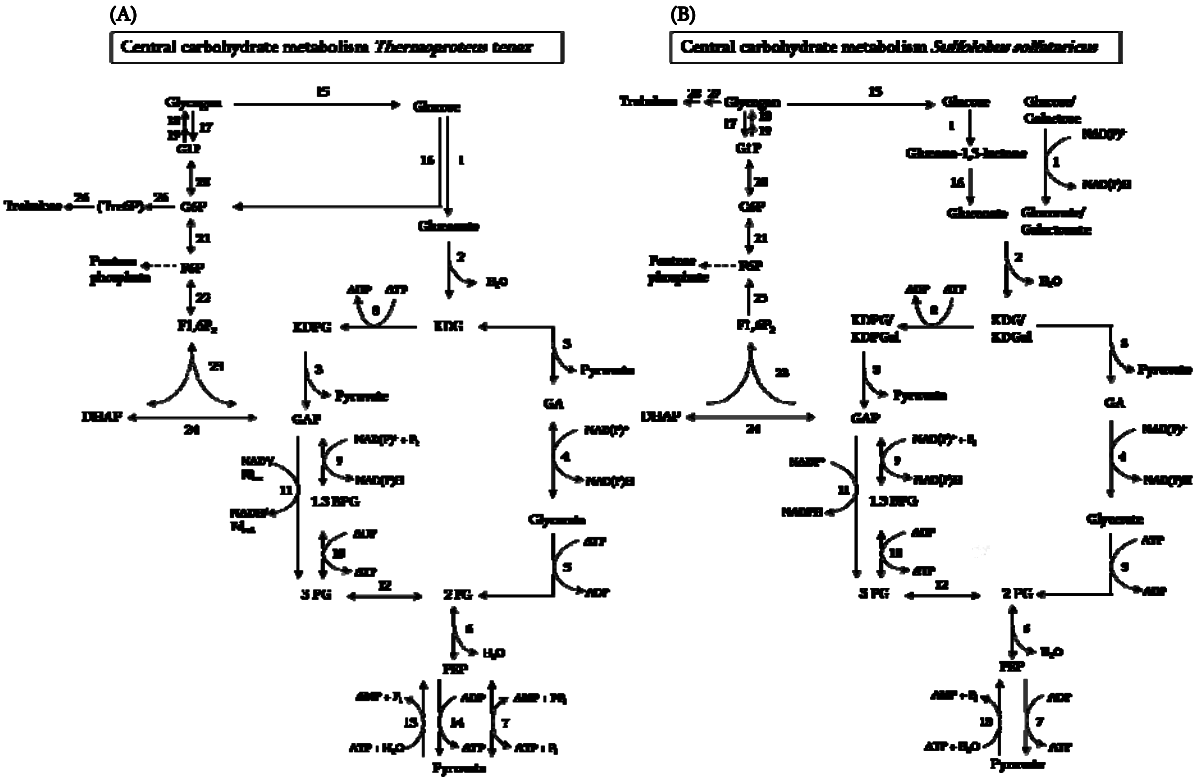

FIGURE 22: THE CENTRAL CARBOHYDRATE METABOLISM IN *T. TENAX* AND *S. SOLFATARICUS*.
Pathways and enzymes involved in the degradation of glycogen and glucose in the hyperthermophilic Archaea *T. tenax* (A) and S. *solfataricus* (B). Enzyme key: (1/1A) glucose dehydrogenase; (2) gluconate dehydratase; (3) KD(P)G aldolase; (4) glyceraldehyde dehydrogenase; (5) glycerate kinase; (6). Enolase; (7) pyruvate, phosphate dikinase; (8) KDG kinase; (9) glyceraldehyde-3-phosphate dehydrogenase (GAPDH); (10) phosphoglycerate kinase; (11) GAPN/GAP oxidoreductase; (12) phosphoglycerate mutase; (13) phosphoenolpyruvate synthetase; (14) pyruvate kinase; (15) glucan-1,4-α-glucosidase; (16) glucokinase; (17) glycogen phosphorylase; (18) glycogen synthase; (19) ADP/UDP-glucose pyrophosphorylase; (20) phosphoglucomutase; (21) glucose-6-phosphate isomerase; (22) phosphofructo kinase; (23) fructose-1,6-bisphosphate aldolase; (24) triosephosphate isomerase; (25) fructose-1,6-bisphosphatase; (26) trehalose-6-phosphate synthase/phosphatase (TPSP); (27) maltooligosyltrehalose synthase (TreY); (28) trehalose hydrolase (TreZ)

TABLE 5: BRANCHED ED PATHWAY IN ARCHAEA.

The branched ED pathway thermophilic and hyperthermophilic Archaea which harbor the branched ED pathway are shown. The identified ED gene homologs are indicated and the charachterized enzymes are underlined. For *T. tenax* genes numbers as well as the respective accession numbers are given [SIEBERS et al., 2004]. TTX, *Thermoproteus tenax*; SACI, *Sulfolobus acidocaldarius*; SSO, *Sulfolobus solfataricus*; STO, *Sulfolobus tokodaii*; PTO, *Picrophilus torridus* DSM 9790; TA, *Thermoplasma acidophilum*; TVN, *Thermoplasma volcanium* GSS1; FAC, *Ferroplasma acidarmanus* Fer1. Enzyme abbreviations: Glc DH, glucose dehydrogenase; Glc-lac, gluconolactonase; G-hydr, gluconate dehydratase; KD(P)G ald, 2-keto-3-deoxy-(6-phospho-)gluconate aldolase; Ald DH, glyceraldehyde dehydrogenase; Gly kin, glycerate kinase; KDG kin, 2-keto-3-deoxygluconate kinase. EC, Enzyme Commission; COG, Clusters of Orthologous Groups. For the KDG kin, two families are represented: PfkB ribokinase family and BadF/BadG/BcrA/BcrD ATPase family.

			Glc DH	Glc-lac	G-hydr	KD(P)G ald	Ald DH	Gly kin	KDG kin	
									PfkB	BadF/BadG /BcrA/BcrD
		EC	1.1.1.47	3.1.1.17	4.2.1.39	4.1.2.-	1.2.1.3	2.7.1.31	2.7.1.45	2.7.1.59
		COG	1063	3386	4948	0329	1012	2379	0524	2971
Crenarchaea	Thermoproteales	TTX	0329 (AJ621346)		1156 (AJ621281)	1156a (AJ621282)	1101 1787 (AJ621321) (AJ621277)	0788 (AJ621345)	1157 (AJ621283)	
	Sulfolobales	SACI	1079	1674	1967 2196	0225	1099 1858	0113	0226 0553	
		SSO	3003 3042 3204	3041	3198	3197	1629 3117	0666	3195	
		STO	1704	1108	2479	2479		2037	2478 0574	
Euryarchaea	Thermoplasmatales	PTO	0639 1070	0907 1226	0485	1026	0225 0332	1442		0011 1094
		TA	0897			0619	0809	0453		0122
		TVN	1019	0929	0168 1194	0669	0397 0653 1021 1045	0783		0199
		FAC	0085 0912 1194	1071 1513	0084 1545	1067 1133	0465 1113 1341	0418	1518	

5. SUMMARY

Vergleichende Studien der Glykolyse in hyperthermophilen Archaeen haben eine Vielzahl an Variationen der klassischen bakteriellen und eukaryontischen Wege offen gelegt, namentlich des Entner-Doudoroff (ED) Weg und des Embden-Meyerhof-Parnas (EMP) Weg. Während im aeroben *Sulfolobus solfataricus* der ED Weg die einzige Option für den Glukose Katabolismus darstellt, nutzt der anaerobe *Thermoproteus tenax* neben diesem zusätzlich einen reversiblen EMP Weg. Es wurden bislang zwei Modifikationen des ED Weg identifiziert, (i) der semi-phosphorylative (sp) ED Weg für halophile Archaea und (ii) der nicht-phosphorylative (np) ED Weg in thermophilen und hyperthermophilen Archaea. Durch einen Ansatz, basierend auf vergleichender Genomanalyse wurde ein ED Gencluster in den Genomen von *T. tenax* und *S. solfataricus* ausgemacht, was die Präsenz des sp ED Weg in diesen Organismen nahe legt.

Das ED Gencluster umfasst Gene (i) einer putativen Glukonat Dehydratase (*gad*), (ii) einer 2-Keto-3-deoxy-glukonat Aldolase (*kdgA*), welche zuvor in *S. solfataricus* charakterisiert wurde [BUCHANAN et al., 1999], (iii) einer Zucker (KDG) Kinase, (iv) in *T. tenax* einer Glukan-1,4-α-Glukosidase (*gaa* gene) und (v) in *S. solfataricus* einer nicht phosphorylierenden Glycerinaldehyd-3-phosphat Dehydrogenase (GAPN, *gapN*). Northern Blot und Primer Extension zeigten eine koordinierte Transkription der für die Synthese und Degradation von 2-Keto-3-deoxy-glukonat (KDG) und 2-Keto-3-deoxy-6-phosphoglukonat (KDPG) kodierenden ED Gene. In *T. tenax* verfügt das ED Gencluster über ein *gad* Gen und das *kdgA-kdgK-gaa* Operon und in *S. solfataricus* findet sich ein *gad-kdgA-kdgK* Operon und das *gapN* Gen.

Um die vorhergesagten Enzymaktivitäten zu bestätigen, wurden die entsprechenden Gene kloniert (für *S. solfataricus* geschah die Klonierung in Zusammenarbeit mit Prof. Dr. John van der Oost, Universität Wageningen, Niederlande), rekombinant exprimiert und für die Bestimmung der Enzymaktivitäten gereinigt bzw. angereichert. Zusammenfassend offenbart diese Arbeit (i) einen neuen Typ der Glukonat Dehydratase, (ii) eine bifunktionale 2-Keto-3-deoxy-(6-phospho)-glukonat Aldolase, (iii)

eine 2-Keto-3-deoxy-glukonat Kinase und (iv) in *S. solfataricus* eine nicht phosphorylierende Glycerinaldehyd-3-phosphat Dehydrogenase (GAPN).

Die Glukonat Dehydratase (GAD) katalysiert die Dehydratation von Glukonat zu KDG. Obwohl die GAD aus verschiedenen bakteriellen Quellen gereinigt und charakterisiert wurde, war das kodierende Gen nie zuvor identifiziert worden und stellt damit ein fehlendes Schlüsselelement im zentralen Kohlenhydratmetabolismus dar. Für *T. tenax* wurde die entsprechende Enzymspezifität mit Glukonat nachgewiesen, wohingegen für das Enzym aus *S. solfataricus* zusätzliche Aktivität mit Galaktonat nachgewiesen werden konnte [LAMBLE et al., 2004]

Entgegen vorangehenden Studien der KDG Aldolase aus *S. solfataricus* [LAMBLE et al., 2003; HENDRY, et al., 2000], wurde sowohl für dieses Enzym, als auch für das Enzym aus *T. tenax,* Aktivität nicht nur mit den nicht-phosphorylierten Substraten, sondern auch mit den phosphorylierten Substraten, nachgewisen. Demnach ist das Enzym eine echte bifunktionale KD(P)G Aldolase und katalysiert die reversible Spaltung von KDG und KDPG. Für das Enzym aus *S. solfataricus* konnte gezeigt werden, dass es unspezifisch für KDG/KDPG und 2-Keto-3-Desoxygalaktonat/2-Keto-3-Desoxy-6-Phosphogalaktonat (KDGal/KDPGal) ist [LAMBLE et al., 2005; THEODOSSIS et al., 2004; LAMBLE et al., 2003]. Bislang gibt es noch keine Information über die Stereoselektivität für das Enzym aus *T. tenax*.

KDG Kinase vermittelt die ATP abhängige Phosphorylierung von KDG zu KDPG und stellt somit ein Schlüsselenzym für den sp ED Weg dar. Für das Substrat KDG folgt das Enzym der Michaelis-Menten Kinetik. Das Enzym aus *T. tenax* ist damit die erste identifizierte und charakterisierte archaeale KDG kinase.

Die Aktivität der nicht phosphorylierenden Glycerinaldehyd-3-phosphat Dehydrogenase (GAPN) aus *S. solfataricus* wurde mittels eines kontinuierlichen Tests bestimmt, indem die Bildung von NADPH oder NADH gemessen wurde. Das Enzym folgt der Michaelis Menten Kinetik für $NADP^+$ und DL-GAP. In Gegenwart von NAD^+ zeigte sich lediglich eine geringe Aktivität. Außerdem weist das Enzym allosterische Eigenschaften auf, wobei für Glukose 1-phosphat der größte Effekt beobachtet wurde.

Zusammenfassend kann festgehalten werden, dass sowohl die enzymatischen Studien, als auch die *in vivo* Identifizierung von Enzymaktivitäten in Rohextrakten, sowie Experimente zur *in vitro* Rekonstruktion, die Präsenz des semi-phosphorylativen ED Weg und des nicht-phosphorylativen ED Weg und damit eines verzweigten ED Weg in *T. tenax* und *S. solfataricus* belegen. Verfügbare Genomdaten, ebenso wie biochemische Daten zeigen darüber hinaus die Anwesenheit des verzweigten ED Wege in thermophilen Mitgliedern der Thermoproteales (*T. acidophilum, T. volcanium, P. torridus und F. acidiphilum*). Folglich stellt der verzweigte ED Weg die ED Modifikation in thermophilen und hyperthermophilen Archaea dar. Darüber hinaus legen BLAST Analysen eine noch weit größere Verbreitung dieses archaealen Typs der ED-ähnlichen Pfade auch bei den Bacteria und Eukarya nahe und helfen daher Komplexität und Flexibilität des zentralen Kohlenhydratmetabolismus in allen drei Domänen des Lebens zu entschlüsseln.

6. LITERATURE

AHMED H ETTEMA TJ TJADEN B GEERLING AC VAN DER OJ & SIEBERS B (2005)
The semi-phosphorylative Entner-Doudoroff pathway in hyperthermophilic Archaea: a re-evaluation
Biochem J 390, 529-540

AHMED H TJADEN B HENSEL R & SIEBERS B (2004)
Embden-Meyerhof-Parnas and Entner-Doudoroff pathways in *Thermoproteus tenax*: metabolic parallelism or specific adaptation?
Biochem Soc Trans 32, 2-4

ALTSCHUL SF GISH W MILLER W MYERS EW & LIPMAN DJ (1990)
Basic local alignment search tool
J Mol Biol 215, 403-410

ALTSCHUL SF MADDEN TL SCHAFFER AA ZHANG J ZHANG Z MILLER W & LIPMAN DJ (1997)
Gapped BLAST and PSI-BLAST: a new generation of protein database search programs
Nucleic Acids Res 25, 3389-3402

ANDREESEN JR & GOTTSCHALK G (1969)
The occurence of the modified Entner-Doudoroff pathway in *Clostridium aceticum*
Arch Microbiol 69, 160-170

BABBITT PC & GERLT JA (1997)
Understanding enzyme superfamilies - Chemistry as the fundamental determinant in the evolution of new catalytic activities
J Biol Chem 272, 30591-30594

BABBITT PC HASSON MS WEDEKIND JE PALMER DRJ BARRETT WC REED GH RAYMENT I RINGE D KENYON GL & GERLT JA (1996)
The enolase superfamily: A general strategy for enzyme-catalyzed abstraction of the alpha-protons of carboxylic acids
Biochem 35, 16489-16501

BANKIER AT WESTON KM & BARRELL BG (1987)
Random cloning and sequencing by the M13/dideoxynucleotide chain termination method
Methods Enzymol 155, 51-93

BAUMEISTER W & LUPAS A (1997)
The proteasome
Curr Opin Struct Biol 7, 273-278

BELLY RT & BROCK TD (1972)
Cellular stability of a thermophilic, acidophilic mycoplasma
J Gen Microbiol 73, 465-469

BENDER R & GOTTSCHALK G (1973)
Purification and properties of D-gluconate dehydratase from *Clostridium pasteurianum*
Eur J Biochem 40, 309-321

BOEHRINGER MANNHEIM MANUAL (1995)
The DIG system user's guide for filter hybridization
J Bacteriol

BORK P SANDER C & VALENCIA A (1993)
Convergent Evolution of Similar Enzymatic Function on Different Protein Folds - the Hexokinase, Ribokinase, and Galactokinase Families of Sugar Kinases
Protein Science 2, 31-40

BRADFORD MM (1976)
A rapid and sensitive method for the quantitation of microgram quantities of protein utilizing the principle of protein-dye binding
Anal Biochem 72, 248-254

BIRNBOIM H C & DOLY J. (1979)
A rapid alkaline extraction procedure for screening recombinant plasmid DNA
Nucl Acids Res 7, 1513-1523

BROCK TD BROCK KM BELLY RT & WEISS RL (1972)
Sulfolobus: a new genus of sulfur-oxidizing bacteria living at low pH and high temperature
Arch Mikrobiol 84, 54-68

BRUNNER NA BRINKMANN H SIEBERS B & HENSEL R (1998)
NAD^+-dependent glyceraldehyde-3-phosphate dehydrogenase from *Thermoproteus tenax*. The first identified archaeal member of the aldehyde dehydrogenase superfamily is a glycolytic enzyme with unusual regulatory properties
J Biol Chem 273, 6149-6156

BRUNNER NA & HENSEL R (2001)
Nonphosphorylating glyceraldehyde-3-phosphate dehydrogenase from *Thermoproteus tenax*
Methods Enzymol 331, 117-131

BUCHANAN CL CONNARIS H DANSON MJ REEVE CD & HOUGH DW (1999)
An extremely thermostable aldolase from *Sulfolobus solfataricus* with specificity for non-phosphorylated substrates
Biochem J 343, 563-570

BUCKLEY DH GRABER JR & SCHMIDT TM (1998)
Phylogenetic analysis of nonthermophilic members of the kingdom Crenarchaeota and their diversity and abundance in soils
Appl Environ Microbiol 64, 4333-4339

BUDGEN N & DANSON MJ (1986)
Metabolism of glucose via a modified Entner-Doudoroff pathway in the thermoacidophilic archaebacterium *Thermoplasma acidophilum*
FEBS Lett 196, 207-210

CARSTENS CP & WAESCHE A (1999)
Codon bias-adjusted BL21 derivatives for protein expresion
Strategies Newsletter 12,

CHOMCZYNSKI P MACKEY K DREWS R & WILFINGER W (1993)
A reagent for the rapid isolation of genomic DNA
Biotechniques 22, 550-553

CONDO I CIAMMARUCONI A BENELLI D RUGGERO D & LONDEI P (1999)
Cis-acting signals controlling translational initiation in the thermophilic archaeon *Sulfolobus solfataricus*
Mol Microbiol 34, 377-384

CONWAY T (1992)
The Entner-Doudoroff pathway: history, physiology and molecular biology
FEMS Microbiol Rev 9, 1-27

CYNKIN MA & ASHWELL G (1960)
Uronic acid metabolism in bacteria. IV. Purification and properties of 2-keto-3-deoxy-D-gluconokinase in *Escherichia coli*
J Biol Chem 235, 1576-1579

DE ROSA M GAMBACORTA A NICOLAUS B GIARDINA P POERIO E & BUONOCORE V (1984)
Glucose metabolism in the extreme thermoacidophilic archaebacterium *Sulfolobus solfataricus*
Biochem J 224, 407-414

DE LJ & DOUDOROFF M (1957)
The metabolism of D-galactose in *Pseudomonas saccharophila*
J Biol Chem 227, 745-757

DÖRR C ZAPARTY M TJADEN B BRINKMANN H & SIEBERS B (2003)
The hexokinase of the hyperthermophile *Thermoproteus tenax* - ATP-dependent hexokinases and ADP-dependent glucokinases, two alternatives for glucose phosphorylation in Archaea
J Biol Chem 278, 18744-18753

DUNN JJ & STUDIER FW (1983)
Complete nucleotide sequence of bacteriophage T7 DNA and the locations of T7 genetic elements
J Mol Biol 166, 477-535

ELSHAFEI AM & BDEL-FATAH OM (2001)
Evidence for a non-phosphorylated route of galactose breakdown in cell-free extracts of *Aspergillus niger*
Enzyme Microb Technol 29, 76-83

ELZAINY TA HASSAN MM & ALLAM AM (1973)
New pathway for nonphosphorylated degradation of gluconate by *Aspergillus niger*
J Bacteriol 114, 457-459

ENTNER N & DOUDOROFF M (1952)
Glucose and gluconic acid oxidation of *Pseudomonas saccharophila*
J Biol Chem 196, 853-862

EVGUENIEVA-HACKENBERG E WALTER P HOCHLEITNER E LOTTSPEICH F & KLUG G (2003)
An exosome-like complex in *Sulfolobus solfataricus*
EMBO Rep 4, 889-893

FABRY S & HENSEL R (1987)
Purification and characterization of D-glyceraldehyde-3-phosphate dehydrogenase from the thermophilic archaebacterium *Methanothermus fervidus*
Eur J Biochem 165, 147-155

FILLINGER S BOSCHI-MULLER S AZZA S DERVYN E BRANLANT G & AYMERICH S (2000)
Two glyceraldehyde-3-phosphate dehydrogenases with opposite physiological roles in a nonphotosynthetic bacterium
J Biol Chem 275, 14031-14037

FORTERRE P & ELIE C (1993)
Chromosome structure, DNA polymerases and topoisomerases in Archaebacteria (Archaea)
New Comprehensive Biochemistry 26, 325-366

FOX GE MAGRUM LJ BALCH WE WOLFE RS & WOESE CR (1977)
Classification of methanogenic bacteria by 16S ribosomal RNA characterization
Proc Natl Acad Sci U S A 74, 4537-4541

GAVIN AC BOSCHE M KRAUSE R GRANDI P MARZIOCH M BAUER A SCHULTZ J RICK JM MICHON AM CRUCIAT CM REMOR M HOFERT C SCHELDER M BRAJENOVIC M RUFFNER H MERINO A KLEIN K HUDAK M DICKSON D RUDI T GNAU V BAUCH A BASTUCK S HUHSE B LEUTWEIN C HEURTIER MA COPLEY RR EDELMANN A QUERFURTH E RYBIN V DREWES G RAIDA M BOUWMEESTER T BORK P SERAPHIN B KUSTER B NEUBAUER G & SUPERTI-FURGA G (2002)
Functional organization of the yeast proteome by systematic analysis of protein complexes
Nature 415, 141-147

GOTTSCHALK G & BENDER R (1982)
D-Gluconate dehydratase from *Clostridium pasteurianum*
Methods in enzymology 90, 283-287

GRIFFITHS JS WYMER NJ NJOLITO E NIRANJANAKUMARI S FIERKE CA & TOONE EJ (2002)
Cloning, isolation and characterization of the *Thermotoga maritima* KDPG aldolase
Bioorg Med Chem 10, 545-550

GROGAN DW (1989)
Phenotypic characterization of the archaebacterial genus Sulfolobus: comparison of five wild-type strains
J Bacteriol 171, 6710-6719

HABENICHT A (1997)
The non-phosphorylating glyceraldehyde-3-phosphate dehydrogenase: Biochemistry, structure, occurrence and evolution
Biol Chem 378, 1413-1419

HANAHAN D (1983)
Studies on transformation of Escherichia coli with plasmids
J Mol Biol 166, 557-580

HANES CS (1932)
Studies on plant amylases: The effect of starch concentration upon the velocity of hydrolysis by the amylase of germinated barley
Biochem J 26, 1406-1421

HENDRY EJ BUCHANAN CL RUSSELL RJM HOUGH DW REEVE CD DANSON MJ & TAYLOR GL (2000)
Preliminary crystallographic studies of an extremely thermostable KDG aldolase from *Sulfolobus solfataricus*
Acta Crystallographica Section D-Biological Crystallography 56, 1437-1439

HUBBARD BK KOCH M PALMER DRJ BABBITT PC & GERLT JA (1998)
Evolution of enzymatic activities in the enolase superfamily: Characterization of the (D)-glucarate/galactarate catabolic pathway in *Escherichia coli*
Biochemistry 37, 14369-14375

HUBER H HOHN MJ RACHEL R FUCHS T WIMMER VC & STETTER KO (2002)
A new phylum of Archaea represented by a nanosized hyperthermophilic symbiont
Nature 417, 63-67

ITO S FUSHINOBU S YOSHIOKA I KOGA S MATSUZAWA H & WAKAGI T (2001)
Structural basis for the ADP-specificity of a novel glucokinase from a hyperthermophilic archaeon
Structure 9, 205-214

JOHNSEN U SELIG M XAVIER KB SANTOS H & SCHONHEIT P (2001)
Different glycolytic pathways for glucose and fructose in the halophilic archaeon *Halococcus saccharolyticus*
Arch Microbiol 175, 52-61

JUNG JJ & LEE SB (2005)
Identification and characterization of Thermoplasma acidophilum 2-keto-3-deoxy-d-gluconate kinase: a new class of sugar kinases
Biotecnol Bioprocess Eng 10, 535-539

KARDINAHL S SCHMIDT CL HANSEN T ANEMULLER S PETERSEN A & SCHAFER G (1999)
The strict molybdate-dependence of glucose-degradation by the thermoacidophile *Sulfolobus acidocaldarius* reveals the first crenarchaeotic molybdenum containing enzyme - an aldehyde oxidoreductase
Eur J Biochem 260, 540-548

KASSAVETIS GA BUTLER ET ROULLAND D & CHAMBERLIN MJ (1982)
Bacteriophage SP6-specific RNA polymerase. II. Mapping of SP6 DNA and selective *in vitro* transcription
J Biol Chem 257, 5779-5788

KERSTERS K & DE LEY J (1975)
D-Glucose drhydratase from Alcaligenes
Methods in enzymol 42, 301-304

KERSTERS K KHAN-MATSUBARA J NELEN L & DE LJ (1971)
Purification and properties of D-gluconate dehydratase from Achromobacter
Antonie Van Leeuwenhoek 37, 233-246

KIM S & LEE SB (2005)
Identification and characterization of *Sulfolobus solfataricus* D-gluconate dehydratase: a key enzyme in the non-phosphorylated Entner-Doudoroff pathway
Biochem J 387, 271-280

KOONIN EV WOLF YI & ARAVIND L (2001)
Prediction of the archaeal exosome and its connections with the proteasome and the translation and transcription machineries by a comparative-genomic approach
Genome Res 11, 240-252

LAEMMLI UK (1970)
Cleavage of structural proteins during the assembly of the head of bacteriophage T4
Nature 227, 680-685

LAMBLE HJ HEYER NI BULL SD HOUGH DW & DANSON MJ (2003)
Metabolic pathway promiscuity in the Archaeon *Sulfolobus solfataricus* revealed by studies on glucose dehydrogenase and 2-keto-3-deoxygluconate aldolase
J Biol Chem 278, 34066-34072

LAMBLE HJ MILBURN CC TAYLOR GL HOUGH DW & DANSON MJ (2004)
Gluconate dehydratase from the promiscuous Entner-Doudoroff pathway in *Sulfolobus solfataricus*
FEBS Letters 576, 133-136

LAMBLE HJ THEODOSSIS A MILBURN CC TAYLOR GL BULL SD HOUGH DW & DANSON MJ (2005)
Promiscuity in the part-phosphorylative Entner-Doudoroff pathway of the archaeon *Sulfolobus solfataricus*
FEBS Lett 579, 6865-6869

LORENTZEN E HENSEL R KNURA T AHMED H & POHL E (2004)
Structural basis of allosteric regulation and substrate specificity of the non-phosphorylating glyceraldehyde 3-phosphate dehydrogenase from *Thermoproteus tenax*
J Mol Biol 341, 815-828

MACKEY K WILLIAMS P SEIM S & CHOMCZYNSKI P (1996)
The use of DNAzol® for the rapid isolation of genomic DNA from whole blood
Biomedical Products Supplement 263, 13-15

MILBURN CC LAMBLE HJ THEODOSSIS A BULL SD HOUGH DW DANSON MJ & TAYLOR GL (2006)
The structural basis of substrate promiscuity in glucose dehydrogenase from the hyperthermophilic archaeon *Sulfolobus solfataricus*
J Biol Chem 281, 14796-14804

MUKUND S & ADAMS MW (1991)
The novel tungsten-iron-sulfur protein of the hyperthermophilic archaebacterium, *Pyrococcus furiosus*, is an aldehyde ferredoxin oxidoreductase. Evidence for its participation in a unique glycolytic pathway
J Biol Chem 266, 14208-14216

MULLIS KB FALOONA S SCHARF R SAIKI RK HORN G & EHRLICH H (1986)
Specific enzymatic amplification of DNA *in vitro*: the polymerase chain reaction
Cold Spring Harbor Symposium of Quantitative Biology 51, 263-273

OHSHIMA N INAGAKI E YASUIKE K TAKIO K & TAHIROV TH (2004)
Structure of *Thermus thermophilus* 2-Keto-3-deoxygluconate kinase: evidence for recognition of an open chain substrate
J Mol Biol 340, 477-489

PACE NR (1997)
A molecular view of microbial diversity and the biosphere
Science 276, 734-740

PAN HQ WANG YP CHISSOE SL BODENTEICH A WANG Z IYER K CLIFTON SW CRABTREE JS & ROE BA (1994)
The complete nucleotide sequences of the SacBII Kan domain of the P1 pAD10-SacBII cloning vector and three cosmid cloning vectors: pTCF, svPHEP, and LAWRIST16
Genet Anal Tech Appl 11, 181-186

PEEKHAUS N & CONWAY T (1998)
What's for dinner?: Entner-Doudoroff metabolism in *Escherichia coli*
J Bacteriol 180, 3495-3502

PEROZICH J KUO I WANG BC BOESCH JS LINDAHL R & HEMPEL J (2000)
Shifting the NAD/NADP preference in class 3 aldehyde dehydrogenase
European Journal of Biochemistry 267, 6197-6203

POHL E BRUNNER N WILMANNS M & HENSEL R (2002)
The crystal structure of the allosteric non-phosphorylating glyceraldehyde-3-phosphate dehydrogenase from the hyperthermophilic archaeum *Thermoproteus tenax*
J Biol Chem 277, 19938-19945

PROMEGA TECHNICAL MANUAL (1994)
The spectrum of beta-thalassaemia in Burma
Alteres sites II in vitro mitagenesis systems 316B, 161-169

REHER M BOTT M & SCHONHEIT P (2006)
Characterization of glycerate kinase (2-phosphoglycerate forming), a key enzyme of the nonphosphorylative Entner-Doudoroff pathway, from the thermoacidophilic euryarchaeon *Picrophilus torridus*
FEMS Microbiol Lett 259, 113-119

REHER M & SCHONHEIT P (2006)
Glyceraldehyde dehydrogenases from the thermoacidophilic euryarchaeota *Picrophilus torridus* and *Thermoplasma acidophilum*, key enzymes of the non-phosphorylative Entner-Doudoroff pathway, constitute a novel enzyme family within the aldehyde dehydrogenase superfamily
FEBS Lett 580, 1198-1204

RONIMUS RS & MORGAN HW (2002)
Distribution and phylogenies of enzymes of the Embden-Meyerhof-Parnas pathway from Archaea and hyperthermophilic bacteria support a gluconeogenic origin of metabolism
Archaea 1, 199-221

SAMBROOK J FRITSCH EF & MANIATIS T (1989)
Molecular Cloning - A Laboratory Manual, 2nd Ed.

SANGER F NICKLEN S & COULSON AR (1977)
DNA sequencing with chain-terminating inhibitors
Proc Natl Acad Sci U S A 74, 5463-5467

SAPRA R BAGRAMYAN K & ADAMS MWW (2003)
A simple energy-conserving system: Proton reduction coupled to proton translocation
Proc Natl Acad Sci U S A 100, 7545-7550

SCHAFER T SELIG M & SCHONHEIT P (1993)
Acetyl-Coa Synthetase (Adp Forming) in Archaea, A Novel Enzyme Involved in Acetate Formation and Atp Synthesis
Arch Microbiol 159, 72-83

SCHICHO RN SNOWDEN LJ MUKUND S PARK JB ADAMS MWW & KELLY RM (1993)
Influence of Tungsten on Metabolic Patterns in *Pyrococcus furiosus*, A Hyperthermophilic Archaeon
Arch Microbiol 159, 380-385

SCHLEPER C PUHLER G KUHLMORGEN B & ZILLIG W (1995)
Life at extremely low pH
Nature 375, 741-742

SCHRAMM A SIEBERS B TJADEN B BRINKMANN H & HENSEL R (2000)
Pyruvate kinase of the hyperthermophilic crenarchaeote *Thermoproteus tenax*: physiological role and phylogenetic aspects
J Bacteriol 182, 2001-2009

SCHUT GJ BREHM SD DATTA S & ADAMS MWW (2003)
Whole-genome DNA microarray analysis of a hyperthermophile and an archaeon: *Pyrococcus furiosus* grown on carbohydrates or peptides
J Bacteriol 185, 3935-3947

SELIG M & SCHÖNHEIT P (1994)
Oxidation of Organic-Compounds to Co2 with Sulfur Or Thiosulfate As Electron-Acceptor in the Anaerobic Hyperthermophilic Archaea *Thermoproteus tenax* and *Pyrobaculumislandicum* Proceeds Via the Citric-Acid Cycle
Arch Microbiol 162, 286-294

SELIG M XAVIER KB SANTOS H & SCHÖNHEIT P (1997)
Comparative analysis of Embden-Meyerhof and Entner-Doudoroff glycolytic pathways in hyperthermophilic archaea and the bacterium Thermotoga
Arch Microbiol 167, 217-232

SHE Q SINGH RK CONFALONIERI F ZIVANOVIC Y ALLARD G AWAYEZ MJ CHAN-WEIHER CCY CLAUSEN IG CURTIS BA DE MOORS A ERAUSO G FLETCHER C GORDON PMK HEIKAMP-DE JONG I JEFFRIES AC KOZERA CJ MEDINA N PENG X THI-NGOC HP REDDER P SCHENK ME THERIAULT C TOLSTRUP N CHARLEBOIS RL DOOLITTLE WF DUGUET M GAASTERLAND T GARRETT RA RAGAN MA SENSEN CW & VAN DER OOST J (2001)
The complete genome of the crenarchaeon *Sulfolobus solfataricus* P2
Proc Natl Acad Sci U S A 98, 7835-7840

SHULAMI S GAT G SONENSHEIN AL & SHOHAM Y (1999)
The glucuronic acid utilization gene cluster from *Bacillus stearothermophilus* T-6
J Bacteriol 181, 3695-3704

SIEBERS B & HENSEL R (1993)
Glucose Catabolism of the Hyperthermophilic Archaeum *Thermoproteus Tenax*
FEMS Lett 111, 1-8

SIEBERS B & HENSEL R (2001)
Pyrophosphate-dependent phosphofructokinase from *Thermoproteus tenax*
Methods Enzymol 331, 54-62

SIEBERS B KLENK HP & HENSEL R (1998)
PPi-dependent phosphofructokinase from *Thermoproteus tenax*, an archaeal descendant of an ancient line in phosphofructokinase evolution
J Bacteriol 180, 2137-2143

SIEBERS B & SCHONHEIT P (2005)
Unusual pathways and enzymes of central carbohydrate metabolism in Archaea
Curr Opin Microbiol 8, 695-705

SIEBERS B TJADEN B MICHALKE K DÖRR C AHMED H ZAPARTY M GORDON P SENSEN CW ZIBAT A KLENK HP SCHUSTER SC & HENSEL R (2004)
Reconstruction of the central carbohydrate metabolism of *Thermoproteus tenax* by use of genomic and biochemical data
J Bacteriol 186, 2179-2194

SIEBERS B WENDISCH VF & HENSEL R (1997)
Carbohydrate metabolism in *Thermoproteus tenax*: *in vivo* utilization of the non-phosphorylative Entner-Doudoroff pathway and characterization of its first enzyme, glucose dehydrogenase
Arch Microbiol 168, 120-127

SIMON HM JAHN CE BERGERUD LT SLIWINSKI MK WEIMER PJ WILLIS DK & GOODMAN RM (2005)
Cultivation of mesophilic soil crenarchaeotes in enrichment cultures from plant roots
Appl Environ Microbiol 71, 4751-4760

SKOZA L & MOHOS S (1976)
Stable thiobarbituric acid chromophore with dimethyl sulphoxide. Application to sialic acid assay in analytical de-O-acetylation
Biochem J 159, 457-462

SLUPSKA MM KING AG FITZ-GIBBON S BESEMER J BORODOVSKY M & MILLER JH (2001)
Leaderless transcripts of the crenarchaeal hyperthermophile *Pyrobaculum aerophilum*
J Molec Biol 309, 347-360

STANIER RY VNC (1941)
The Main Outlines of Bacterial Classification
J Bacteriol 42, 437-466

STANIER RY VNC (1962)
The concept of a bacterium
Arch Microbiol 42, 17-35

STANIER RY (1970)
Some aspects of the biology of cells and their possible evolutionary significance
Symp Soc Gen Microbiol 20, 1-38

STAYNOV DZ PINDER JC & GRATZER WB (1972)
Molecular weight determination of nucleic acids by gel electrophoresis in non-aqueous solution
Nat New Biol 235, 108-110

STUDIER FW & MOFFATT BA (1986)
Use of bacteriophage T7 RNA polymerase to direct selective high-level expression of cloned genes
J Mol Biol 189, 113-130

SZYMONA M & DOUDOROFF M (1958)
Carbohydrate metabolism in *Rhodopseudomonas spheroides*
J Gen Microbiol 22, 167-183

THEIN SL & WALLACE RB (1986)
The use of synthetic oligonucleotides as specific hybridization probes in the diagnosis of genetic disorders
In: Davis (editor), Human genetic diseases, a practical approach, IRL Press

THEODOSSIS A WALDEN H WESTWICK EJ CONNARIS H LAMBLE HJ HOUGH DW DANSON MJ & TAYLOR GL (2004)
The structural basis for substrate promiscuity in 2-keto-3-deoxygluconate aldolase from the Entner-Doudoroff pathway in *Sulfolobus solfataricus*
J Biol Chem 279, 43886-43892

THOMPSON JD HIGGINS DG & GIBSON TJ (1994)
CLUSTAL W: improving the sensitivity of progressive multiple sequence alignment through sequence weighting, position-specific gap penalties and weight matrix choice
Nucleic Acids Res 22, 4673-4680

TOLSTRUP N SENSEN CW GARRETT RA & CLAUSEN IG (2000)
Two different and highly organized mechanisms of translation initiation in the archaeon *Sulfolobus solfataricus*
Extremophiles 4, 175-179

TOMLINSON GA KOCH TK & HOCHSTEIN LI (1974)
The metabolism of carbohydrates by extremely halophilic bacteria: glucose metabolism via a modified Entner-Doudoroff pathway
Can J Microbiol 20, 1085-1091

VAN DER OOST J SCHUT G KENGEN SWM HAGEN WR THOMM M & DE VOS WM (1998)
The ferredoxin-dependent conversion of glyceraldehyde-3-phosphate in the hyperthermophilic archaeon *Pyrococcus furiosus* represents a novel site of glycolytic regulation
J Biol Chem 273, 28149-28154

VERHEES CH KENGEN SWM TUININGA JE SCHUT GJ ADAMS MWW DE VOS WM & VAN DER OOST J (2003)
The unique features of glycolytic pathways in Archaea
Biochem J 375, 231-246

VERHEES CH KENGEN SWM TUININGA JE SCHUT GJ ADAMS MWW DE VOS WM & VAN DER OOST J (2004)
The unique features of glycolytic pathways in Archaea
Biochem J 377, 819-822

WEBER K & OSBORN M (1969)
The reliability of molecular weight determinations by dodecyl sulfate-polyacrylamide gel electrophoresis
J Biol Chem 244, 4406-4412

WHITE MF (2003)
Archaeal DNA repair: paradigms and puzzles
Biochem Soc Trans 31, 690-693

WOESE CR & FOX GE (1977)
Phylogenetic structure of the prokaryotic domain: the primary kingdoms
Proc Natl Acad Sci U S A 74, 5088-5090

WOESE CR KANDLER O & WHEELIS ML (1990)
Towards a natural system of organisms: proposal for the domains Archaea, Bacteria, and Eucarya
Proc Natl Acad Sci U S A 87, 4576-4579

WOESE CR MAGRUM LJ & FOX GE (1978)
Archaebacteria
J Mol Evol 11, 245-251

YANISCH-PERRON C VIEIRA J & MESSING J (1985)
Improved M13 phage cloning vectors and host strains: nucleotide sequences of the M13mp18 and pUC19 vectors
Gene 33, 103-119

ZILLIG W STETTER KO SCHÄFER W JANEKOVIC D WUNDERL S HOLZ I & PALM P (1981)
Thermoproteales: a novel type of extremely thermoacidophilic anaerobic archaebacteria isolated from Icelandic solfatares
Zentbl Bakteriol Hyg 1 Abt Org C 2, 205-227

ZILLIG W STETTER KO WUNDERL S WUNDERL S PRIESS H & SCHOLZ J (1980)
The Sulfolobus-"*Caldariella*" group: taxonomy on the basis of the structure of DNA-dependent RNA polymerases.
Arch Microbiol 125, 259-269

ABBREVIATIONS LIST

A. bidest	Aqua bidestillata = two times distilled water
aa	Amino acid
APS	Ammonium persulfate
bp	Base pair
BSA	Bovine serum albumin
ca.	circa = about, around
CE	Crude extract fraction
CIP	Calf intestinal phosphatase
DMSO	Dimethyl sulfoxide
DNA	Deoxyribonucleic acid
dNTP	Desoxy-nucleotide triphosphate
DSMZ	Deutsche Sammlung von Mikroorganismen und Zellkulturen= German Collection of Microorganisms and Cell Cultures
DTT	dithiothreitol; Cleland's reagent
ε	Extension coefficient
e.g.	For example
ED	Entner-Doudoroff pathway
EDTA	Ethylene diamine tetraacetic acid
EMP	Embden-Meyerhof-Parnas pathway
et al.	et alii = and the others
etc.	et = cetera and so on
F1,6P	Fructose-1,6-bisphosphate
F6P	Fructose-6-phosphat
Fig	Figure
g	Gram
G1P	Glucose-1-phosphate
G6P	Glucose-6-phosphate
GA	Glyceraldehyde
GAA	Glucan-1,4-α-glucosidase
GAD	Gluconate dehydratase
GAP	Glyceraldehyde 3-phosphate
GAPN	Non-phosphorylating glyceraldehyde-3-phosphate dehydrogenase
GAPOR	Glyceraldehyde-3-phosphate oxidoreductase
GDH	Glucose dehydrogenase
GF	Gel filtration fraction
hr	Hour
HP	Heat precipitation fraction
i.e.	id est = that is, that is to say
IPTG	Isopropyl-ß-D-thiogalactopyranoside
Kb	Kilobase
kDa	Kilodalton

KDG	2-keto-3-deoxygluconate
KDGA	KDG aldolase
KDGal	2-keto-3-deoxygalactonate
KDGK	KDG kinase
KDPG	2-keto-3-deoxy-6-phosphogluconate
KD(P)GA	KD(P)G aldolase
KDPGal	2-keto-3-deoxy-6-phosphogalactonate
K_M	Michaelis constant
L	Liter
LB	Luria-Bertani
LDH	Lactate dehydrogenase
m	milli (10^{-3})
M	molar (mol/l)
mA	Milliampere
Min	Minute
MW	Molecular weight
NAD^+	Nicotinamid-adenin-dinucleotid (oxidized)
NADH	Nicotinamid-adenin-dinucleotid (reduced)
NCBI	National Center for Biotechnology Information
OD	Optical density
PAGE	Polyacrylamide gel electrophoresis
PCR	polymerase chain reaction
PEP	Phosphoenolpyruvate
PEPS	Phosphoenolpyruvate Synthetase
pH	Negative logarithm of the hydrogen ion (H^+) concentration
Pi	Inorganic Phosphate
PK	Pyruvate Kinase
PPDK	Pyruvate, Phosphate Dikinase
PPi	Inorganic Pyrophosphate
Psi	Pounds per square inch
Pwo-Polymerase	DNA-Polymerase from *P. woesei*
RNA	ribonucleic acid
Rnase	Ribonuclease
rRNA	ribosomal RNA
RT	Room temperature
S_0	Elementary sulfur
SDS	sodiumdodecylsulfate
Sec	Seconds
Sp.	Species
SSC	Standard saline citrate
Tab	Table
TAE	Tris-Acetat-EDTA-buffer
Taq-Polymerase	DNA-Polymerase from *Thermus aquaticus*
TEMED	N,N,N',N'-Tetramethylethylenediamine
TLC	Thin layer chromatography

Tris	Tris-(hydroxymethyl)-aminomethane
U	Unit = Enzyme activity
UV	Ultraviolet
v	Velocity
V	Volt
V_{max}	Maximal velocity
Vol	Volume
W	Watt
www	world wide web
x *g*	Gravitational acceleration
µ	micro (10^{-6})

ACKNOWLEDGMENT

At the end of my thesis, I would like to thank all those people who made this thesis possible and an enjoyable experience for me.

I am deeply indebted to my supervisor PD Dr. Bettina Siebers, without her help, this work would not be possible. I am deeply thankful for her constant support, for enriching my knowledge with her exceptional insights, for encouraging me and for her proofreading of hundreds of thesis drafts which reflects an endless care.

I wish to express my sincere gratitude to Prof. Dr. Rheinhard Hensel, who guided and supported me since I started this work. Thank him for his fruitful advices and for helping me whenever I was in need.

I would also like to thank the members of the x-men lab. Many thanks for Thomas Knura for teaching me all of the lab techniques, for his invaluable advice and for his incredible patience with me. Thanks for Jörg Meyer "Mr. President" for his interesting conversations and for making the work enjoyable. Thanks to Dr. Klaus Michalke for his encouragement and many helpful discussions. Thanks for Patrick Moritz for his comradeship. Thanks for Annette Schmidt, Bianca Rheichstein, Britta Huber, Frank Thomas, Dr. Sonja Koning, Theresa Kouril and thanks for Sabine Effenberger for her wonderful SDS-PAGE gels.

Special thanks for Daniel Kehrer for sharing me the working place, for his patience and permanent good mood and for always being there in when I needed him.

Many thanks for the members of the Ladies lab. Thanks for Dr. Britta Tjaden for always being there and for her critical corrections "The too many the-s". Thanks for Melanie Zaparty for her useful guides. Thanks for Hidegard Eling, André Plagens, Fabian Blombach and for Christine Dörr for teaching me my first German words "Ich hätte gerne Eis".

I am grateful to the office staff members, Karin Bendt for her great and unbelievable care and for her open heart and Veronika Schneider, for her help, support and for keeping always smiling.

Finally, I wish to thank my parents, my sisters and my brother for their continuous support and encouragement, for teaching me how to love and how to give. I would like also to express my deepest gratitude for the constant support, for standing by my side all the time, for understanding and for the love I received from my Anne and her lovely family during the whole last time.

LEBENSLAUF

PERSÖNLICHE DATEN

NAME:	Ahmed	
VORNAME:	Hatim	
GEBOREN AM:	28. Juni 1976	
GEBOREN IN:	Hannover	
STAATSANGEHÖRIGKEIT:	ägyptisch	
ELTERN:	Ragab Ahmed Khalil	
	Tahani Hanafi Al-Abassery	
GESCHWISTER:	BRUDER	Hossam
	SCHWESTERN	Hassna
		Israa

SCHULISCHER WERDEGANG

1981-1987	"Al-Marefa Primary School", Dubai, Vereinigte Arabische Emirate
1987-1990	"Al-Khalig Al-Arabi Elementary School", Dubai, Vereinigte Arabische Emirate
1990-1993	"Al-Oroubeh Secondary School", Dubai, Vereinigte Arabische Emirate
ABSCHLUSS:	"General Secondary Education Certificate"

WISSENSCHAFTLICHER WERDEGANG

1993-1998	Studium der Mikrobiologie an der "Faculty of Science", Suez Kanal Universität, Ägypten
ABSCHLUSS:	"B. Sc. of Microbiology"

1999-2000	"Research Student, Pre-Master"
2000-2001	"Lecturer" in der "Biological and Geological Sciences Dept., Faculty of Education", Suez Kanal Universität, Ägypten
Jul. 2001-Okt. 2002	Einarbeitung in biochemische und molekularbiologische Methoden in der Mikrobiologie I (ehemals Fachbereich 9/ Mikrobiologie) an der Universität Duisburg-Essen
seit Okt. 2002	Promotion in der Arbeitsgruppe von HD Dr. Bettina Siebers in der Mikrobiologie I (ehemals Fachbereich 9/ Mikrobiologie) an der Universität Duisburg-Essen

ESSEN 26. Juni 2006

ERKLÄRUNGEN

Hiermit erkläre ich gem. § 6 Abs. 2 Nr. 7 der weiterhin geltenden Promotionsordnung der Fachbereiche 6 bis 9 zur Erlangung des Dr. rer. nat., dass ich das Arbeitsgebiet, dem das Thema „The Branched Entner-Doudoroff Pathway in Hyperthermophilic Archaea " zuzuordnen ist, in Forschung und Lehre vertrete und den Antrag von Herrn Hatim Ahmed befürworte.

Essen, den HD Dr. Bettina Siebers

Hiermit erkläre ich gem. § 6 Abs. 2 Nr. 6 der weiterhin geltenden Promotionsordnung der Fachbereiche 6 bis 9 zur Erlangung des Dr. rer. nat., dass ich die vorliegende Dissertation selbstständig verfasst und mich keiner anderen als der angegebenen Hilfsmittel bedient habe.

Essen, den Hatim Ahmed

Hiermit erkläre ich gem. § 6 Abs. 2 Nr. 8 der weiterhin geltenden Promotionsordnung der Fachbereiche 6 bis 9 zur Erlangung des Dr. rer. nat., dass ich keine anderen Promotionen bzw. Promotionsversuche in der Vergangenheit durchgeführt habe und dass diese Arbeit von keiner anderen Fakultät abgelehnt worden ist.

Essen, den Hatim Ahmed